Review

NMR as a "Gold Standard" Method in Drug Design and Discovery

Abdul-Hamid Emwas [1],*, Kacper Szczepski [2], Benjamin Gabriel Poulson [2], Kousik Chandra [2], Ryan T. McKay [3], Manel Dhahri [4], Fatimah Alahmari [5], Lukasz Jaremko [2], Joanna Izabela Lachowicz [6],* and Mariusz Jaremko [2],*

[1] Core Labs, King Abdullah University of Science and Technology, Thuwal 23955-6900, Saudi Arabia
[2] Biological and Environmental Sciences & Engineering Division (BESE), King Abdullah University of Science and Technology (KAUST), Thuwal 23955-6900, Saudi Arabia; kacper.szczepski@kaust.edu.sa (K.S.); benjamingabriel.poulson@kaust.edu.sa (B.G.P.); kousik.chandra@kaust.edu.sa (K.C.); lukasz.jaremko@kaust.edu.sa (L.J.)
[3] Department of Chemistry, University of Alberta, Edmonton, AB T6G 2W2, Canada; ryan.mckay@ualberta.ca
[4] Biology Department, Faculty of Science, Taibah University, Yanbu El-Bahr 46423, Saudi Arabia; Manel.dhahri@gmail.com
[5] Nanomedicine Department, Institute for Research and Medical, Consultations (IRMC), Imam Abdulrahman Bin Faisal University (IAU), Dammam 31441, Saudi Arabia; fsalahmari@iau.edu.sa
[6] Department of Medical Sciences and Public Health, Università di Cagliari, Cittadella Universitaria, 09042 Monserrato, Italy
* Correspondence: abdelhamid.emwas@kaust.edu.sa (A.-H.E.); lachowicz@unica.it (J.I.L.); Mariusz.jaremko@kaust.edu.sa (M.J.); Tel.: +966-2-8084313 (A.-H.E.)

check for updates

Abstract: Studying disease models at the molecular level is vital for drug development in order to improve treatment and prevent a wide range of human pathologies. Microbial infections are still a major challenge because pathogens rapidly and continually evolve developing drug resistance. Cancer cells also change genetically, and current therapeutic techniques may be (or may become) ineffective in many cases. The pathology of many neurological diseases remains an enigma, and the exact etiology and underlying mechanisms are still largely unknown. Viral infections spread and develop much more quickly than does the corresponding research needed to prevent and combat these infections; the present and most relevant outbreak of SARS-CoV-2, which originated in Wuhan, China, illustrates the critical and immediate need to improve drug design and development techniques. Modern day drug discovery is a time-consuming, expensive process. Each new drug takes in excess of 10 years to develop and costs on average more than a billion US dollars. This demonstrates the need of a complete redesign or novel strategies. Nuclear Magnetic Resonance (NMR) has played a critical role in drug discovery ever since its introduction several decades ago. In just three decades, NMR has become a "gold standard" platform technology in medical and pharmacology studies. In this review, we present the major applications of NMR spectroscopy in medical drug discovery and development. The basic concepts, theories, and applications of the most commonly used NMR techniques are presented. We also summarize the advantages and limitations of the primary NMR methods in drug development.

Keywords: NMR; drug design; drug development; drug discovery; therapeutics

1. Introduction

The unexpected SARS-CoV-2/COVID-19 outbreak, with over 34 million confirmed cases globally (Oct. 2020) and the struggle for survival in the absence of a proven and efficient treatments, emphasizes

the critical need to develop effective, novel, and rapid drug discovery methodologies. Even though the pharmaceutical industry works constantly to discover and develop novel drugs, the process is still slow and expensive. The cost of introducing a new drug has increased steadily, with current cost estimates predicting that a future drug will cost in excess of $2.6 billion. The typical development cost is usually spread out over the course of 14 years [1–3], making investment even more difficult (i.e., cost recovery delay). This high investment barrier for drug development is a result of numerous testing phases (Scheme 1), with each phase requiring a statistically significant number of cases. Although there are several other substantial costs to drug development, that discussion of experimental methods to reduce costs is beyond the scope of this review.
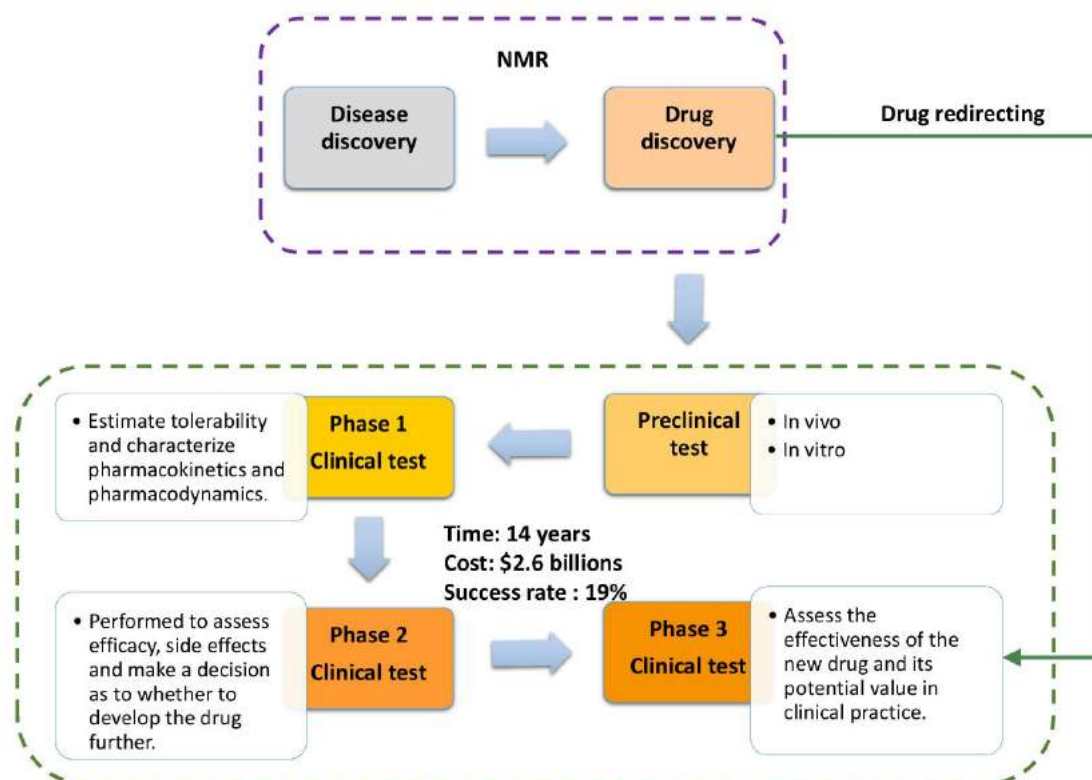

Scheme 1. Schematic representation of drug discovery [4]. Numerical data were reported from Meigs et al. [3].

The emergence of a pandemic and the emergencies it creates worldwide understandably drive and motivate the rapid development and/or optimization of drugs. However, patient safety and subsequent earned public trust is a primary requirement. Drug redirecting/repurposing (Scheme 1) is an efficient short-cut method in disease treatment that utilizes existing tools, and combines artificial intelligence, machine learning algorithms, and experimental NMR techniques (i.e., "*from Bench to Bedside*"). This process must be relatively rapid and efficient to have any benefit to patients and the health-care system.

Compared to mass spectrometry and high-performance liquid chromatography (HPLC), nuclear magnetic resonance (NMR) is another powerful technique with several unique advantages [5–8]. NMR is intrinsically quantitative, and it provides several different approaches that are routinely utilized to identify and structurally elucidate molecules of interest [9–18]. In contrast to mass spectrometry, NMR is non-destructive, non-invasive, has extremely high reproducibility permitting researchers to acquire measurements under different experimental conditions (e.g., temperature, time points, and concentrations) often while the same sample is inside the magnet [19–23]. NMR can be used in reaction kinetic studies while several consecutive measurements are taken, and while spectral changes (function

of the reaction time) are analyzed [24–28]. Moreover, molecules are studied at the atomic level [29–31]. Unlike other analytical tools, NMR provides dynamic information, and NMR experiments can be carried out under physiological conditions (e.g., atmospheric pressure, temperature, and different pH values) [32,33]. This is especially important in medical drug design since one must understand the interactions between an enzyme of interest and the ligand(s). NMR provides information on the binding affinity of such ligands, details/location of the binding site, and associated structural changes following binding [32–35]. These biophysical details are essential when evaluating the potential efficacy of a drug, and during any subsequent optimization. The available literature [32–34,36] highlights the practicality of NMR in drug design studies. For these reasons, NMR spectroscopy is highly sought after in drug development [37–41], for both molecule identification [11,13,14,18,42–46] and structural elucidation [15–17,45,47–51]. NMR has been successfully applied in stereochemistry [52–56] and isomer determination [57–61], in drug-protein interactions studies [62–64], and in the evaluation of drug toxicity [65–68].

The use of NMR in drug design is not restricted to academic laboratories and gained interest from those in development industries. The use of NMR in drug development increased in the late '80s, as seen in both scientific and patent literature (Figure 1). While scientific interest in NMR is still growing, the number of patents has been decreasing since the early 2000s. The top applicants of NMR in pharmaceutical patents are Bristol Myers, AstraZeneca, and Wyeth, with 146, 104, and 67 patent families, respectively.
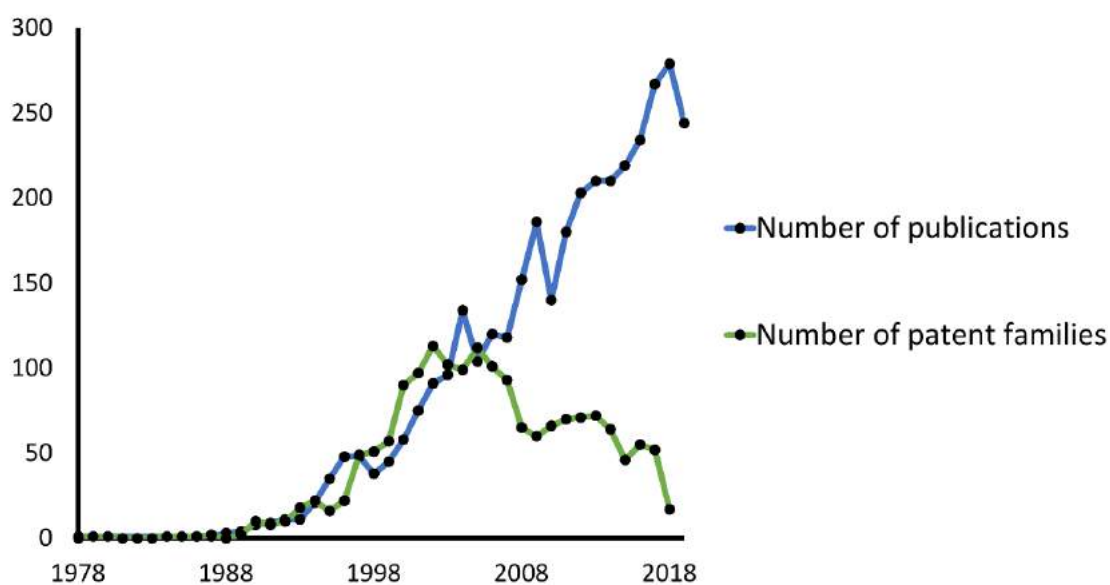

Figure 1. Data search results for: "NMR" and "Drug design" in Scopus (blue) (www.scopus.com) and Orbit patent (orange) (www.orbit.com) databases.

In addition to the advantages provided by NMR, it is often used with complementary methods such as X-ray crystallography, HPLC, and mass spectrometry [69]. An example of this is found in work by Wyss et al. [36], where they combined X-ray crystallography with NMR fragment-based screening to create the first inhibitor candidate for BACE-1 in Alzheimer's disease. BACE-1 is a membrane-anchored aspartic acid protease and is responsible for the production of amyloid beta peptides in neurons related to the progression of Alzheimer's disease [36,70]. Using NMR fragment-based screening, Wyss et al. identified isothiourea as binding to BACE-1 and confirmed this observation with the X-ray crystal structure of the complex of a ligand-efficient isothiourea fragment. Information obtained from these experiments aided in design optimization, resulting in the selection of iminopyrimidinones as BACE-1 inhibitors [36]. This is a perfect example of using different complementary methods to maximize scientific outcome. However, in order to be efficient, one must know the advantages and disadvantages

of each method. One of the major issues regarding NMR is the effective size restriction when measuring targets such as proteins above 40kDa. Recent progress has extended this mass limit; an example of this is the resolved structure of chaperone SecB in complex with unstructured proPhoA (PDB ID 5JTL) with a total mass of 119kDa using NMR [71]. In this review, we present practical guideline to use NMR techniques in drug design studies and provide examples of the successful use of NMR in drug-design.

2. An Introduction to NMR Spectroscopy

NMR is a versatile tool for studying biomolecules of all kinds and is a unique regarding the biophysical analysis of drugs [72–75]. The basic feature of NMR lies in the fact that it inductively detects the Larmor precession of individual nuclei (i.e., spins) which vary because of different atomic, electronic, and chemical environments (i.e., structural atomic relationships). Initially, the sample is placed in a strong, static, and homogeneous magnetic field. Because spins contain angular momentum, they exhibit Larmor precessions around this static magnetic field. A net magnetization builds up over time as the spin population (represented by different energy levels) is minutely differential in the presence of the magnetic field. These levels are dictated by the spin quantum number and can be roughly thought of as different orientations with respect to the static field. Subsequently, induced electromagnetic fields at radiofrequencies (called RF pulses) are applied transverse to the plane of the static magnetic field, and the net or bulk magnetization undergoes an effective rotation. The bulk coherence moves into the transverse plane and the subsequent coherently precessing magnetization vectors induce a detectable alternating voltage in the NMR receiver coil. This tiny alternating voltage is amplified and converted from an analog time domain signal to a frequency reading via Fourier transformation. These signals are recorded in response to the induced radio-wave pulses (Figure 2) and are representative of the Larmor frequencies that are converted into normalized values termed chemical shifts in order to be field independent.
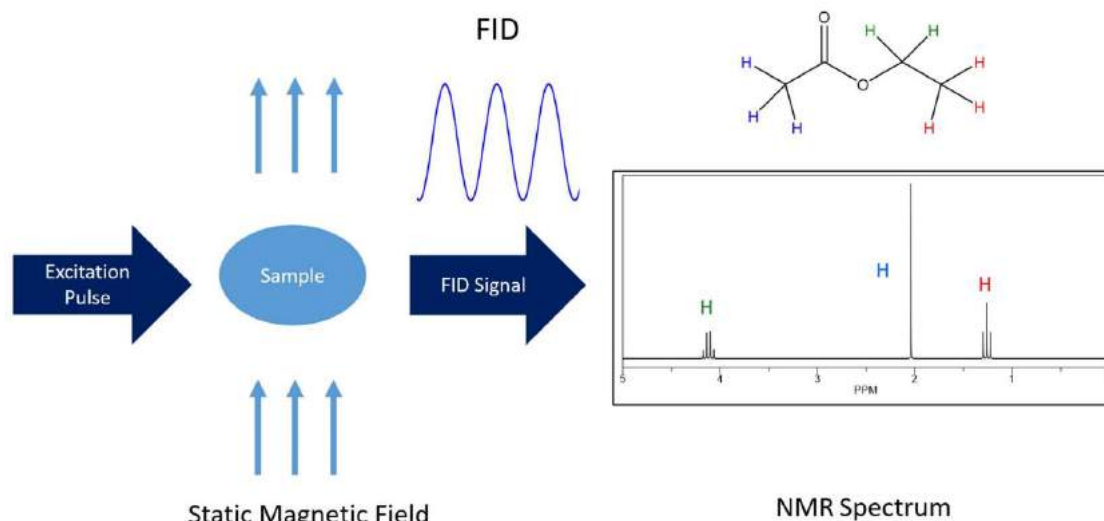
Figure 2. The most simplified layout of an NMR experiment. The NMR spectrum of ethyl acetate Table 1. H chemical shift assignments is shown as an example. The chemical structure and simulated ^{1}H-NMR spectrum were created using ChemDraw 18.1.

This is the final, representative spectroscopic signature of the chemical and magnetic environment of the atom, and it provides detailed atomic resolution information about the molecular structure [76–79]. A wealth of information can be derived from the NMR signal made up components such as the chemical shift position, signal linewidth, and observed couplings/multiplet structure. The signal contains precise details about the chemical environment of the involved and interacting spins in the structure of the molecule, dynamics of the spins in various timescales, conformational exchange, etc. [80–82]. Any change in the environment of the associated spin can be observed. These changes include

molecular binding, interactions, and/or exchange between different conformations [20,83–85]. Thus, NMR has been used to study a wide range of functional molecules such as natural products [86–88], saccharides [89,90], metabolites [91,92], DNA [93,94], and proteins [95], and its use as an analytical tool in drug design research has increased immensely in recent years (see Figure 1).

As NMR is non-destructive in nature, the same sample can be analyzed repeatedly. NMR can be performed first and then submitted to mass spectrometry (MS); however, the addition of common deuterated NMR solvents (such as D_2O) can perturb MS results and should be avoided (e.g., tube-in-tube or by using non-deuterated solvent and running the NMR unlocked). In fact, high-performance liquid chromatography (HPLC), ion-trap MS and NMR have been combined to detect the effects of drugs demonstration in urine and blood serum samples [69,96,97]. Corcoran and Spraul [98] emphasize that liquid chromatography (LC), MS, and NMR utilized in parallel give comprehensive structural data on molecules of novel drugs in development.

In the following subsections we briefly describe NMR methods that have been used in drug design, and then discuss how NMR principles are used in drug discovery research.

2.1. One Dimensional NMR Spectroscopy

The one-dimensional (1D) experiment is by far the most common NMR experiment used for drug studies. The 1D acquisition takes the least amount of time, has one of the simplest hardware requirements, and therefore, in most cases, 1D-NMR is more attractive for high throughput studies. One dimensional NMR spectroscopy normally incorporates a preparation period, some form of induced excitation to form coherence, and lastly, a signal "read" detection period. The preparation period can be modified according to the needs of the experiment or the specifics of the sample. Simple 1D NMR is capable of rapidly producing high-quality spectra of drugs and their targets while revealing how the drugs and targets may interact at the atomic level. 1D ^{1}H-NMR is extremely effective in drug design studies because it has a (relatively) high sensitivity, it is non-destructive, and because hydrogen atoms are extremely abundant in most molecules of interest. Therefore the resulting spectra usually contains a large amount of relevant information and this wealth of data can be acquired in a relatively short period of time. The basic 1D ^{1}H-NMR, along with 1D ^{13}C-NMR, 1D ^{15}N-NMR, and 1D ^{31}P-NMR, and their respective uses in drug design/discovery are briefly discussed below.

2.1.1. 1D ^{1}H-NMR

The ^{1}H hydrogen isotope is NMR visible, has the highest gyromagnetic ratio (apart from tritium) of all of NMR active nuclei, and is combined with a vast natural abundance in organic chemical compounds. This makes the 1D-^{1}H-NMR experiment the most commonly applied NMR approach. Moreover, many software databases [99–102] are well established for ^{1}H-NMR spectra therefore assisting with processing, analyzing, and identifying the detected molecules automatically. Since almost all drug discovery and drug development studies are performed on samples dissolved in water, many different solvent suppression methods have been applied. The most common is presaturation [103,104]. The key point of this method is to use a low power induced field at the specific frequency of water. This effectively averages out any coherence of the water resonance. The experiment is simple for common hardware to perform and easy to set up; however, presaturation has a substantial disadvantage in that signals resonating close to the solvent signal will show decreased intensity [103,104] or may be lost entirely. This is due to the fact the even selective pulses or very low power pulses also excite some area around the water signal. Also suppressed hydrogen from H_2O in solution can exchange with atoms of interest in the molecule and effectively bleed the suppressive spin state to any neighboring atoms. The water signal itself is usually broad, so a wider area of suppression is not necessarily undesirable but affects more of the molecule(s) of interest. More recent water suppression techniques have been developed such as those based on a scheme known as excitation sculpting [105,106]. The basic pulse sequence consists of a double pulsed field gradient echo (DPFGE) in each of which a selective component pulse is flanked by two pulsed field gradients [107]. The particular elements differ for different applications. In the case of

water suppression known as WATER suppression by GrAdient Tailored Excitation (WATERGATE), this involves an initial encoding gradient along with the middle element; a combination of two selective 90° rotations on the water along with a central non-selective 180° excitation of all resonances [108]. This is predicated in that water experiences a 360° rotation (effectively nothing) while all other spins experience 180° rotation. The application of the second refocusing gradient does not rephase the water and therefore removes the signal. The reader is referred to the detailed literature [103,104,109] for further information. In principle, a water suppression element (or many elements combined) can be incorporated in any existing pulse sequence to enhance the performance, and it has been implemented in various 1D, 2D, and triple resonance 3D/4D experiments. Although ^{1}H is the most sensitive nucleus for NMR yielding strong, sharp signals within a few minutes [110], chemical shift dispersion of ^{1}H is quite narrow (only around 10 ppm). This has prompted the consideration of other nuclei such as ^{13}C, ^{15}N, or ^{31}P for resolution improvements.

2.1.2. 1D ^{13}C-NMR

Compared with ^{1}H, ^{13}C has a much higher chemical shift dispersion (~200 ppm), however the natural abundance of ^{13}C is low (1.1%). Additionally, the gyromagnetic ratio is ~4 times weaker than ^{1}H and therefore ^{13}C spectra are far more difficult to obtain especially for less concentrated samples. There are some polarization transfer techniques such as Distortionless Enhancement by Polarization Transfer (DEPT) or Insensitive Nuclei Enhanced by Polarization Transfer (INEPT), which can enhance signal intensity by starting the magnetization on a higher sensitivity and abundance proton and then transferring magnetization to the less sensitive carbon nuclei for subsequent direct detection [111], but this requires additional hardware and acquisition times. The use of 1D ^{13}C in drug design studies was illustrated by Tsujimoto et al. [112]. The goal of the study was to examine if a metabolomics approach based on ^{1}H and ^{13}C offers significant improvements when comparing potential drugs. The authors prepared a total of 40 samples with five different citrus-type crude drugs (kijitsu, tohi, chimpi, kippi and seihi) and measured 1D ^{1}H and 1D ^{13}C for each sample. While ^{1}H-NMR spectra allowed the identification of three compounds (naringin, sucrose, and β-glucose), using ^{13}C-NMR allowed unambiguous identification of eight additional compounds (naringin, neohesperidin, α- and β-glucose, sucrose, limonene, narirutin, and synephrine). The added signal resolution from ^{13}C-NMR spectra allowed researchers to obtain better structural information about the compounds than from ^{1}H-NMR spectra alone.

2.1.3. 1D ^{15}N-NMR

In comparison to the previous example, ^{15}N has a lower shift dispersion (~100ppm) than ^{13}C, but higher than that of [1]H. Here, the situation is unfortunately severely limited due to an even lower natural abundance (0.37%) and a gyromagnetic ratio ~10 times smaller than [1]H. This means that [15]N's combined sensitivity is around 260,000 times lower than [1]H. As a result, isotopic enrichment of ^{15}N combined with [1]H-mediated enhancement via indirect detection is often needed in order to obtain a satisfactory 1D ^{15}N spectra. Similar to ^{13}C, a few methods are available to overcome such low sensitivity. One of them focuses on tagging molecules with carboxyl groups using ^{15}N-ethanolamine and later detecting the signal using a 2D heteronuclear correlation NMR experiment [113]. Currently, novel approaches such as "smart isotope labeling" have been developed [114]. Also, the SOFAST (Band-Selective Optimized Flip Angle Short Transient) technique can help but results in substantial hardware considerations/drawbacks and often increased concentrations, and/or dramatically longer experiments are still required [115–117].

Promising methods are on the horizon. These methods include ^{15}N heteronuclear signal enhancement via Signal Amplification by Reversible Exchange in SHield Enables Alignment Transfer to Heteronuclei (SABRE-SHEATH); however, more work and research are required before such methods can be applied for biomedical purposes [118].

2.1.4. 1D ^{31}P-NMR

With a natural abundance of 100% and a gyromagnetic ratio of about 2.5 times smaller than ^{1}H, one may think that phosphorus could be broadly used for NMR experiments regarding the drug discovery and development. However, the application of ^{31}P is limited due to the fact that most of the molecules of interest simply do not contain a phosphorus atom. Therefore ^{31}P-NMR is usually applicable for studies related to energy, phospholipid metabolism (ATP, NADP), and/or characterization of changes in DNA [94,119,120]. For example, Overall et al. conducted an experiment in which they showed that ^{31}P solid-state NMR can be used for quantitative analysis of DNA dynamics within live bacteria [94]. For that, the researchers first prepared untreated cultures of *E. coli*, and measured them using a Hartmann-Hahn ^{1}H to ^{31}P cross-polarization (^{31}P CP) experiment. Afterwards, they measured *E. coli* treated with ampicillin and maculatin 1.1 (Mac1.1) in a similar manner. Spectra obtained from treated bacteria compared to those obtained from untreated bacteria showed alterations in the lineshape, reduced signal intensity at the spectrum's edges, and a shift in spectral density towards 0 ppm which indicated the increased dynamics of the phosphorus from nucleic acids [94].

Over time, several innovations have been applied to expand the usage of ^{31}P. Like in ^{13}C and ^{15}N labeling of specific biological compounds, incorporation of ^{31}P can also be used. In order to achieve that, 2-chloro-4,4,5,5-tetramethyldioxaphospholane (CTMDP) can be used for tagging lipids containing hydroxyl, aldehyde, and carboxyl groups that can later be detected with better resolution [121]. Another fairly recent method enables toxicological screening of ^{31}P in living cells for several hours without affecting cell viability [122]. This specific method can be used to observe the changes in energy metabolism in real-time while enabling the evaluation of the effects of administered drugs.

2.2. Multi-Dimensional NMR Spectroscopy

NMR experiments are not limited to one-dimensional direct acquisition; they can be extended to multidimensional methods including 2D, 3D, 4D, and even higher dimensionality. The focus of this section is common 2D NMR experiments that have been used in drug design and drug development. A brief description of Correlation Spectroscopy (COSY), Total Correlation Spectroscopy (TOCSY), and Heteronuclear Multiple Bond Correlation (HMBC), along with their uses in drug design and discovery will be presented.

2.2.1. 2D ^{1}H,^{1}H-COSY

COSY is one of the simplest and most frequently used 2D NMR experiment [123]. It shows the homonuclear coupling of nuclei (i.e., ^{1}H-^{1}H) separated by up to several covalent bonds. The pulse sequence consists of a 90° excitation pulse followed by a specific evolution time (t_1), a second pulse, and finally a measurement period (t_2, not to be confused with relaxation rates or times). The second pulse can be 90° or 45° or 135°, depending upon the specific requirements, and respectively yield COSY [124], COSY-45 or COSY-135 functionality (see [125–127]). A two-dimensional Fourier Transform (FT) yields the final spectra and shows the frequencies for proton (^{1}H) or carbon (in the case of carbon detection) along both axes. There are two types of peaks; (I) Diagonal peaks, which represent the peaks of the conventional 1D spectra, and (II) cross-peaks, which have different values in the two frequency axes and are therefore off the diagonal. These off diagonal cross-peaks are the most important pieces of information as they mark correlations between pairs of nuclei due to through bond magnetization transfer. This helps in identifying which atoms are connected [128], critical for structural elucidation of both known molecules and unknown molecules in solution [129]. By implementing phase-cycling [130,131], it is also possible to distinguish different types of coupling and yields further helpful information about the chemical structure of a molecule [132]. As an example, the use of the COSY experiment was presented in the work of Zheng et al. [88]. The main goal of their work was to investigate potential biological differences and compare the pharmacological effects between Danggui (an herbal drug used in traditional Chinese medicine) and European Danggui.

For that, Zheng et al. treated blood deficiency rats with Danggui and European Danggui and collected samples of their serum and urine. The samples were later measured using ^{1}H-CPMG-NMR, [1]H-NOESYPRESAT-1D, ^{1}H,^{1}H-COSY, and ^{1}H,^{13}C-HSQC, and then compared to equivalent spectra from untreated rats. The results showed that exposure to Danggui and European Danggui altered the levels of 18 different metabolites, such as lactate, nicotinamide, glycerol and formate, which were involved in a total of seven different metabolism pathways. Additionally, it was proven that Danggui and European Danggui have different chemical compositions, with Danggui having better blood-enriching effects than European Danggui.

2.2.2. 2D ^{1}H,[1]H-TOCSY

Total Correlation Spectroscopy (TOCSY) also originally known as the Homonuclear Hartmann Hahn (HOHAHA) experiment can be considered an extension of the 2D ^{1}H,^{1}H-COSY experiment. The difference between the two experiments is that a TOCSY experiment will show multiple cross-peaks including indirectly coupled nuclei (i.e., longer range via scalar coupling) throughout the J-coupled spin system of a chemical compound. The basic pulse sequence of the TOCSY consists of excitation by a 90° pulse, followed by a free variable evolution period which encodes the indirect dimension. This is normally followed by an isotropic mixing sequence to transfer magnetization between spins via the strong scalar coupling. The mixing generates in-phase magnetization throughout a spin coupled network of the associated nuclei during the mixing time. Lastly, a direct detection is performed. A major advantage of the TOCSY experiment is that it detects in-phase magnetization (i.e., pure absorptive line-shape) which is far easier to analyze compared to the anti-phase information in the phase sensitivity COSY-type experiment. The isotropic mixing is usually performed using a composite pulse scheme such as WALTZ, MLEV or DIPSI [133,134] pulse train, and can be sandwiched between two z-filters [135] where isotropic mixing is performed on the longitudinal magnetization. The most obvious advantage of TOCSY is that all cross-peaks of the same spin system can be observed for whole spin system at once. This is useful for identifying the complete network of spins and reducing the ambiguity of any spectral overlap. The TOCSY experiment can be produced as 1D with a relatively shorter time and easier analysis compared to 2D but lacks the benefit of multi-dimensional resolution. The 2D TOCSY is usually done to resolve spectra overlap [50] when first identifying molecules [136–138]. For example, Jiang et al. used this to predict the response to gemcitabine-carboplatin (GC) chemotherapy in patients with metastatic breast cancer who were previously exposed to treatment with both anthracyclines and taxanes [137]. For that, researchers collected serum samples from 29 patients prior to treatment and measured them using 1D ^{1}H-NMR. Additionally, they conducted 2D NMR experiments such as the ^{1}H,^{1}H-COSY, [1],^{1}H-TOCSY, ^{1}H,^{13}C-HSQC, and ^{1}H,^{13}C-HMBC to help assign serum metabolites. After receiving the treatment with gemcitabine-carboplatin, patients were divided into four groups based on the results from the computed tomography: complete response (CR), partial response (PR), stable disease (SD), or progressive disease (PD). After comparing NMR results prior to the treatment with the outcome of chemotherapy, the researchers observed lower baseline levels of serum format and acetate in breast cancer patients who progressed with the disease than in those who achieved a clinical benefit from therapy, indicating that those two biomarkers could be used to distinguish between patients who will benefit from GC treatment from those who do not [137].

2.2.3. 2D ^{1}H,^{13}C-HSQC

2D- Heteronuclear Single Quantum Coherence (HSQC) experiments are commonly used to help resolve spectral overlap [139] while providing ^{13}C information without the inherent sensitivity losses involved in ^{13}C direct detection (see below). HSQC shows the correlations between directly coupled nuclei [140], e.g., [1]H-^{13}C or [1]H-[15]N [140]. As such, an HSQC spectrum will show clean peaks for each unique proton directly connected to the heteronuclear nuclear atom of interest [140,141]. In ^{1}H,^{13}C/^{15}N HSQC experiments, the magnetization is transferred from the more sensitive nucleus (I:[1]H) to the less sensitive nucleus (S:[13]C/^{15}N) [142–144] (Figure 3). This is especially useful when applying NMR

spectroscopy to drug design, as most drugs are organic (i.e., contain carbon atoms), and the relative abundance of ^{13}C (1.1%) is quite low [143]. By transferring sensitivity from ^{1}H to ^{13}C, one can circumvent the long experimental time required for 1D ^{13}C experiments [143].
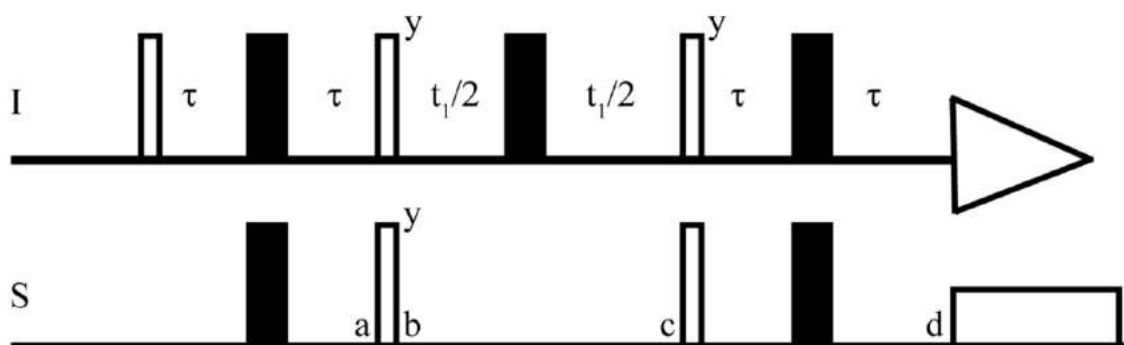
Figure 3. The pulse sequence of HSQC. I and S represent two heteronuclear spins. The τ is (1/4J) where J is the coupling constant. The thick and thin bars represent the 180° and 90° pulse respectively [142].

For example, De Castro et al. [145] studied Ptac2S and its related cytotoxicity to the cisplatin-resistant epithelial ovarian carcinoma (EOC), Skov-3 cells. In the study, they used NMR spectroscopy and multi-variate statistical analysis to observe how Skov-3 cells reacted to treatment with Ptac2S. In particular, they used ^{1}H,^{13}C-HSQC along with ^{1}H-COSY and Heteronuclear Multiple Bond Correlation (HMBC), and the Human Metabolome Database to assign the chemical shifts of the lipid metabolites present in the studied samples. Interestingly, Skov-3 cells treated with Ptac2S produced more pyruvate than Skov-3 cells treated with cisplatin. The authors also noticed an unexpected difference in lipid metabolite expression levels between the cells treated with Ptac2S and those treated with cisplatin. These results provide a possible explanation for how Ptac2S is able to overcome cisplatin resistance in Skov-3 cells [145].

2.2.4. 2D ^{1}H, 13C-HMBC

Heteronuclear 2D experiments are useful for transferring magnetization from sensitive nuclei (i.e., ^{1}H) to less sensitive nuclei (i.e., ^{13}C) [146] thereby reducing the time needed for the acquisition of spectra [147]. Heteronuclear Single Quantum Coherence (HSQC) will only show one cross peak for each coupled pair [92,128] of nuclei. This makes HSQCs useful for assigning the backbone of proteins [148] and in metabolites of complex biofluids [149], whose 1D ^{1}H-NMR spectra can suffer from severe spectral overlap.

The HMBC technique, while similar to HSQC, is an example of a heteronuclear 2D experiment that reveals correlations between nuclei separated by two or more chemical bonds while also suppressing one-bond correlations at the same time. This experiment combined with HSQC is often used to assign NMR spectra for studied molecules in drug design experiments [65,66,137,145].

As an example, HMBC was used in a recent study by Xu et al. [66] to investigate the changes in the metabolic profiles of rats treated with different dosages of the "RenqingMangjue" pill, a traditional Tibetan medicine. In this study, the rats were divided into four groups based on the amount of "RenqingMangjue" administered: low dose group (LD)-83.33 mg/kg/day, middle dose group (MD)-333.33 mg/kg/day, high dose group (HD)-1333.33 mg/kg/day and a control group (NC). After 15 days of consecutive administration, half of the rat population was used to collect samples such as serum, kidney, and liver tissue, while the other half underwent an additional 15 days of recovery before the same samples were acquired. The samples were measured using ^{1}H-NMR CPMG (an experiment used to suppress signals from larger molecules, see below) [150–152] along with ^{1}H,^{1}H-COSY, ^{1}H,^{13}C-HSQC, and ^{1}H,^{13}C-HMBC used for molecules assignment. The obtained spectra showed that the "RenqingMangjue" pill alters many metabolites, which are related to a variety of

metabolic pathways including energy metabolism, amino acid metabolism, and lipid metabolism indicating potentially harmful effects on kidneys and liver.

2.2.5. Relaxation-Edited NMR Spectroscopy

Relaxation in NMR is a phenomenon describing the time dependence involved in signal intensity after an induced RF (radiofrequency) pulse is applied [153]. After application of a 90° RF pulse, the bulk magnetization will move to the transverse (xy) plane and will gradually return to its original equilibrium position along the longitudinal (z) axis [154]. This process is described in Figure 4, and is termed T_1 relaxation. The details are beyond the scope of the manuscript and interested readers are directed to [155] and references therein. Relaxation times for NMR are even more complicated and exist in two categories: T_1 and T_2. T_1 refers to the rate of longitudinal (or spin-lattice) Z-axis relaxation as the system returns to equilibrium. A second component also contributes, i.e., T_2 relaxation and refers to the rate of transverse (or spin-spin) relaxation [154] which occurs in the XY plane. T_2 is independent of the longitudinal relaxation (T_1) and represents the loss of coherence in the precessing spins. Therefore NMR relaxation spectroscopy can be based on T_1 and/or T_2 [156], and is collectively referred to as "relaxation edited NMR" [157].
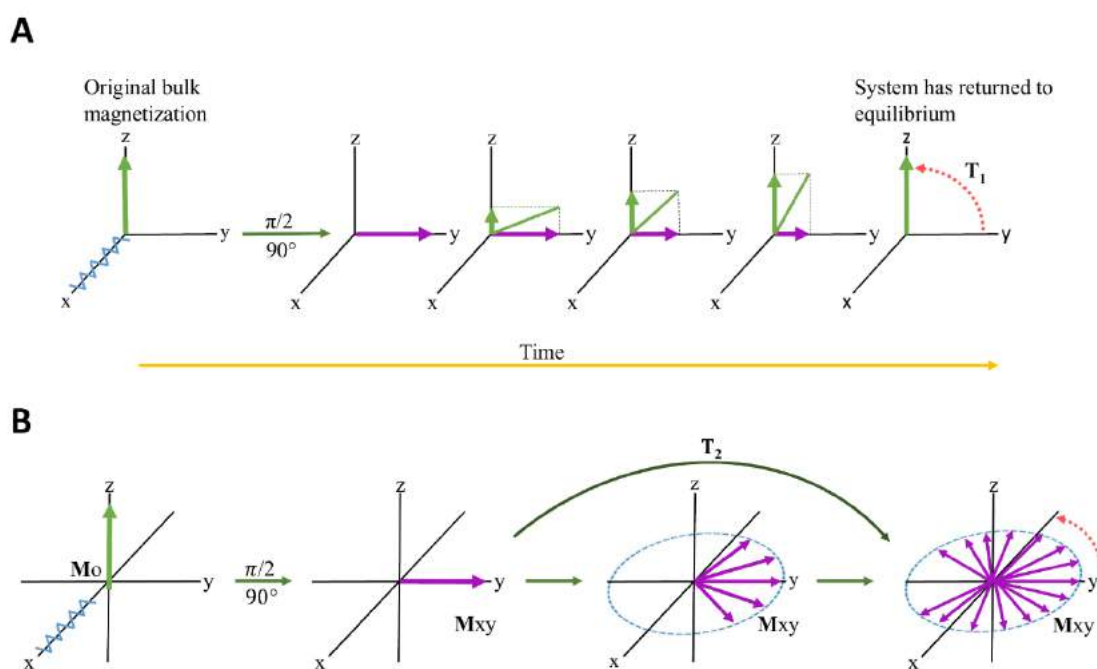
Figure 4. RF (radiofrequency) pulse causes the bulk magnetization to move to the transverse plane. Over time (ms to seconds, and in extreme cases, minutes [155]), the bulk magnetization will decrease in the transverse plane, and increase in the longitudinal axis, returning to its original, equilibrium value. (**A**) represents T_1 relaxation and (**B**) represents T_2 relaxation.

T_1-based methods typically measure and compare the T_1 times of the free and bound ligands. A common way to measure the T_1 value of a small molecule is the inversion recovery experiment [158, 159], although other experiments are also available such as ultrafast NMR T_1 [160] and saturation inversion recovery [161]. In general, the shorter T_1 the relaxation time the less intense the peak signal will be and the broader the signal linewidth [162]. The T_1 values of free and bound ligand will differ depending on how strongly the ligand binds because molecular interactions with the target will influence the ligand's molecular motion, and hence, its longitudinal relaxation [156]. Bound ligands will have smaller T_1 values than in their free form because, overall, they will experience slower molecular motion upon interacting with a target [163] therefore behaving like a much larger molecule. They can (depending on molecule size) also display a negative NOE difference spectrum (transferred

NOE) [164], whereas non-binding ligands normally show small-positive NOEs [156]. For binding ligands to display negative NOEs, their T_1 values must be comparatively longer than the $1/k_{off}$ value of the target [156].

T_1 relaxation times can be easily used to screen small molecules as ligands for DNA [165] and serve as a basis for HTS experiments [166]. An experiment related to drug design that utilized 1D and 2D relaxation edited NMR was done by Hajduk et al. [167] in which he and others used 1D and 2D relaxation edited NMR techniques to detect ligands that bind to FK506 binding protein and stromelysin. One year earlier, Liu et al. [157] used relaxation edited one-and two-dimensional ^{1}H-NMR spectroscopy to characterize biological fluids. Tang et al. [168] extended this by applying relaxation edited NMR Spectroscopy to improve the detection of metabolites in blood plasma. More recently, Jaremko et al. commented on available models used to interpret ^{15}N protein relaxation data [169], and even used deficient ^{15}N relaxation data to rapidly calculate the dynamics of proteins [170].

The T_2 relaxation experiment relies on so-called Carr–Purcell–Meiboom–Gill (CPMG) building blocks (Figure 5).
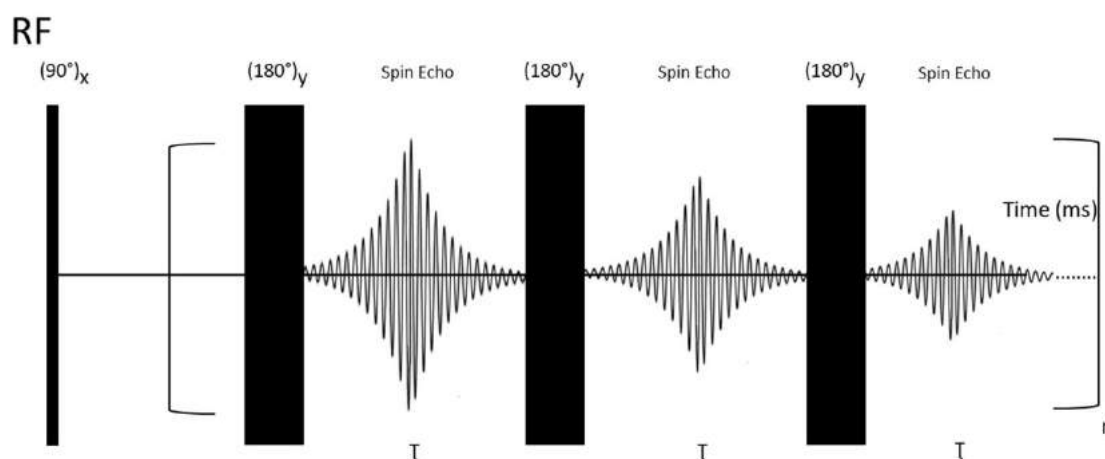
Figure 5. CPMG pulse sequence. First, a 90° RF pulse is applied and results in transverse magnetization in the xy plane. Then a $180°_y$ pulse is applied to re-phase the magnetization vectors. After $180°_y$, the vectors who were faster during the dephasing are overtaken by the slower vectors, which results in re-phasing and generation of a spin-echo signal. This process is repeated several times.

This pulse sequence is explained with the following steps: First, application of a 90° RF pulse creates a transverse (xy plane) magnetization. Second, a spin-echo period (delay-180°-delay block) is responsible for Mx/y magnetization decay. This period is repeated "n" times (CPMG building blocks). It is essential to point out that every NMR experiment involving a large number of pulses (e. g. due to the repeating building blocks) is likely to be sensitive to hardware restrictions and small miscalibrations of the duration of the applied pulses. To attenuate the unwanted effects of miscalibrations, Meiboom and Gill modified the previously used Carr–Purcell sequence [171] by changing the phase of the applied 180° pulses from x to y [172]. This procedure can be used to measure T_2 relaxation times of any type of nuclei. For instance, in the case of ^{13}C, all pulses and acquisitions are applied on ^{13}C channel, while broadband proton decoupling is applied during all pulse sequences. It works analogically for different NMR-active nuclei [173].

In a typical CPMG experiment, the effective transverse relaxation rate, $R_{2,eff}$, is typically measured by fitting the signal decay as a function of a variable number of CPMG blocks [174]. The experimental half-height linewidth (d) of a given resonance signal is directly related to T_2^* (also called as 'effective' or "observed") by the following equation:

$$d = \frac{1}{\pi\, T_2^*} \tag{1}$$

T_2 represents the transverse relaxation times, and additional broadening comes from the magnetic field inhomogeneities (T_2^{inh}), which must be taken into account.

$$\frac{1}{T_2^*} = \frac{1}{T_2} + \frac{1}{T_2^{inh}} \tag{2}$$

T_2 measurements of ligands are also useful for determining the binding nature of a small molecule. The T_2 values of small molecules are quite large compared to those of bigger molecules (i.e., proteins) mostly because macromolecules have more spin-spin diffusion [175]. Bound ligands will, therefore, display shorter T_2 values than non-binding ligands because they interact with the target (i.e., protein), adopting similar vibrational and rotational energies to the target [176]. This interaction is represented by the resonance line broadening in the binding ligand's spectrum when a receptor is introduced into the sample [156]. Given the sizable difference of T_2 values of binding and non-binding ligands, one can utilize 1D relaxation-edited experiments to distinguish the binding ligands from the non-binding ligands efficiently and effectively based on the differences in the T_2 values [167]. These and other related relaxation edited experiments prove useful in drug design.

Relaxation edited NMR spectroscopy takes advantage of an inherent atomic property (i.e., the return of bulk magnetization back to equilibrium [177]), so no molecular enrichment (e.g., ^{15}N isotopic enrichment of protein targets) is required [167]. Furthermore, the slow time scale of NMR relaxation allows the user to manipulate the external conditions (i.e., length and power of pulse) to increase the resolution of targets and potential drugs [155] in NMR drug design experiments. However, this slow timescale also sets the lower limit at which NMR drug design experiments can be performed [155], meaning that any external manipulations cannot decrease experimental time below a certain threshold. This varies based on the drugs and targets used in the experiment. Low drug solubility is also a challenge, as the ligands must be at a sufficiently high concentration to allow detection via NMR, although the use of organic solvents has helped to attenuate this effect in relaxation edited NMR spectroscopy [156]. For examples of experiments that use different NMR techniques mentioned above, see Table 1.

Table 1. Recent pharmacological studies complemented with NMR approaches for evaluating the efficacy/safety of new or existing drugs.

Tested Substance	Evaluated Effect	NMR Experiments Used in the Study	Ref.
Isoniazid (INH)	INH induces oxidative stress, disturbs energy metabolism, and causes disorders in neurotransmission and neuromodulation processes in Sprague Dawley rats.	^{1}H-NMR CPMG ^{1}H,^{1}H-TOCSY ^{1}H,^{13}C-HSQC	[178]
Naproxen	Naproxen induces a disturbance in energy and choline metabolism, and promotes catabolism of tryptophan in Sprague Dawley rats.	^{1}H-NOESYPRESAT-1D	[179]
Cisplatin (CP)	Identification of six serum (alanine, betaine, glucose, glutamine, lactate, and leucine) and eight urinary (alanine, acetate, citrate, glucose, glycine, guanidinoacetate, hippurate, and lactate) metabolites that can be used as biomarkers for cisplatin nephrotoxicity.	^{1}H-NMR	[180]
Shell of *Herpetospermum caudigerum* Wall (SHCW)	A high dosage of SHCW causes the disturbance of energy and amino acid metabolism and induces oxidative stress in Sprague-Dawley rats.	^{1}H-NMR CPMG ^{1}H,^{13}C-HSQC ^{1}H,^{13}C-TOCSY	[86]
Ampicillin, Maculatin 1.1	Both antibiotics cause destabilization of membrane integrity and increase breakdown of nucleic acids in *E. coli*.	^{1}H-^{31}P CP	[94]
Emodin	Emodin can affect the immune response and interrupt energy metabolism (citric acid cycle) along with glutathione synthesis, which can lead to oxidative stress.	^{1}H-NMR CPMG ^{1}H,^{1}H-COSY ^{1}H,^{13}C-HMBC ^{1}H,^{13}C-HSQC	[65]

Table 1. *Cont.*

Tested Substance	Evaluated Effect	NMR Experiments Used in the Study	Ref.
"RenqingMangjue" pill (RMP)	RMP can disturb the citric acid cycle in cells, and decreases levels of glutamate, glutamine and BCAAs in the plasma of Wistar rats.	^{1}H-NMR CPMG ^{1}H,^{1}H-COSY ^{1}H,^{13}C-HSQC ^{1}H-^{13}C HMBC	[66]
Ptac2S	Ptac2S limits cancer cell (Skov-3) proliferation by reducing the efficiency of the citric acid cycle and induces changes in cell membranes in a shorter period of time (6h) compared to cisplatin (24h). Additionally, Ptac2S may inhibit lactate dehydrogenase.	^{1}H-NMR CPMG ^{1}H,^{1}H-COSY ^{1}H,^{13}C-HSQC ^{1}H,^{13}C-HMBC	[145]
Gemcitabine-carboplatin (GC)	Identification of two biomarkers (formate and acetate) that can predict a positive response in MBC (metastatic breast cancer) patients treated with GC chemotherapy.	^{1}H-NMR CPMG ^{1}H JRES ^{1}H,^{1}H-COSY ^{1}H,^{1}H-TOCSY ^{1}H,^{13}C-HSQC ^{1}H,^{13}C-HMBC	[137]
Doxorubicin (DOX)/dexrazoxane (DEX)	DOX decreases ATP production and induces oxidative stress in H9C2 cells. DEX counteracts those changes, having a cardioprotective effect on H9C2 cell lines.	^{1}H-NOESYPRESAT-1D	[67]
Curcumin	Curcumin shows antihyperlipidemic effects on C57BL/6Slac mice by partially restoring metabolic defects induced by a high-fat diet. Affected metabolic pathways include the citric acid cycle, glycolysis and gluconeogenesis, ketogenesis of BCAA, synthesis of ketone bodies and cholesterol, and choline and fatty acid metabolism.	^{1}H-NOESYPRESAT-1D ^{1}H-^{1}H TOCSY ^{1}H,^{13}C-HSQC	[136]
Formosanin C (FC)	Formosanin C shows the ability to inhibit synthesis and methylation of DNA as well as reducing the activity of the citric acid cycle and energy metabolism in the mitochondria of HepG2 cells.	^{1}H-NMR	[181]
Melamine	Melamine disrupts metabolism of glucose, nitrogen, and protein in the liver of Wistar rat.	^{1}H-NMR CPMG	[182]
Aristolochic acid (AA)	Aristolochic acid causes renal lesions and a disorder in tubular reabsorption in Wistar rats.	^{1}H-NMR	[68]
Rituximab	Evaluating response outcome for patients with rheumatoid arthritis, treated with rituximab. Identification of metabolites changes between responders and non-responders such as succinate, taurine, lactate, pyruvate and aspartate.	^{1}H-NMR	[183]
Levetiracetam, Lamotrigine, Topiramate	No distinction between metabolite profiles of serum from patients treated with levetiracetam, lamotrigine and topiramate. Could not evaluate response of initial treatment of epilepsy.	^{1}H-NOESYPRESAT-1D	[184]
Hexacationic Ruthenium Metallaprism	Metallaprism mainly affects lipid metabolism in A2780 (human ovarian cancer) and HEK-293 (human embryonic kidney) cells, and increases GSH levels in all cell lines. In A2780cisR (cisplatin resistant A2780) cells, lipid biogenesis and glycosylation are affected by treatment with metallaprism.	HR-MAS: a)1D -^{1}H NOESY -^{1}H CPMG b)2D -^{1}H,^{1}H-TOCSY -^{1}H J-resolved	[138]
Centella asiatica extract	Extract from *Centella asiatica* promotes glycolysis, boosts the citric acid cycle and decreases gluconeogenesis and lipid metabolism in T2DM Sprague–Dawley rats.	^{1}H-NMR CPMG	[185]
VR24, VR27 (1,3,4-thiadiazoles)	VR24 and VR27 improve glycerol metabolism, decrease betaine levels, and normalize the altered level of myoinositol in serum of DMH-induced CRC (colorectal cancer) Wistar rats.	^{1}H-NMR CPMG	[186]
Xiaoyaosan	Xiaoyaosan regulates energy metabolism, can play an important role in the regulation of the nervous system, and might restore the balance in gut microbiota of depressed patients.	^{1}H-NMR CPMG ^{1}H,^{1}H-COSY ^{1}H,^{13}C-HMQC	[187]
Sini decoction (SND)	SND may restore balance in myocardial energy metabolism, and regulate the citric acid cycle and amino acid metabolism. Identification of 10 biomarkers showing potential efficiency of SND administration in Sprague-Dawley rats.	^{1}H-NMR	[188]
Fu Fang Jin Jing Oral Liquid (FJJOL) with Herba Rhodiol	FJJOL regulates energy metabolism of brain tissue, can affect the function of neurons abundant in GABA and glycine receptors, and may help to maintain the membrane integrity of the cells in Kunming-strain mice exposed to hypobaric hypoxia.	^{1}H-NOESYPRESAT-1D ^{1}H,^{1}H-gCOSY ^{1}H,^{1}H-TOCSY	[87]

Table 1. *Cont.*

Tested Substance	Evaluated Effect	NMR Experiments Used in the Study	Ref.
Acyclovir, Pyrazinamide, Isoniazid, Sulfamethoxazole	Evaluating the efficacy (determined by the concentration of a drug able to reach the therapeutic site) of four drugs in cerebrospinal fluid of tuberculous meningitis patients.	^{1}H-NOESYPRESAT-1D ^{1}H,^{1}H-COSY	[189]
Genipin	Genipin can recover energy metabolism to normal levels, and regulate methylamine and amino acid metabolisms of diabetic Sprague Dawley rats.	[1]H-NOESY-1D	[190]
Adriamycin (ADR)	Identification of seven biomarkers: trimethylamine oxide (TMAO), taurine, trimethylamine (TMA), hippurate, trigonelline, citrate and 2-oxoglutarate that can predict tumor's (gastric adenocarcinoma) response to ADR treatment in BALB/c-nu/nu mice.	[1]H-NOESYPRESAT-1D	[191]
Danggui/European Danggui	Comparison between Danggui and European Danggui showed that Danggui has a different chemical composition and provides a better enriching effect on blood than European Danggui. Identification of 18 metabolites affected by Danggui treatment.	^{1}H-NMR CPMG ^{1}H-NOESYPRESAT-1D ^{1}H,^{1}H-COSY ^{1}H,^{13}C-HSQC	[88]
Erythromycin	Erythromycin decreases citric acid cycle activity, enhances fatty acid oxidation, causes dysfunction in amino acid metabolism, and creates oxidative stress in livers of Wistar rats.	^{1}H-NMR CPMG ^{1}H-NMR BPPLED	[192]
Fuzi/Gancao	Fuzi causes a shift in energy metabolism (from aerobic respiration to anaerobic), induces membrane toxicity, and disrupts the balance of gut microbiota of Wistar rats. Administrating Fuzi with Gancao diminishes the toxic effects of Fuzi.	[1]H-NOESY-1D	[193]
Kijitsu, Tohi, Chimpi, Kippi, Seihi	^{1}H-NMR spectra enabled the identification of three compounds (naringin, sucrose, and β-glucose), and ^{13}C-NMR enabled the identification of eight compounds (naringin, neohesperidin, α- and β-glucose, sucrose, limonene, narirutin, and synephrine).	^{1}H-NMR ^{13}C-NMR	[112]

## 3. NMR Methods for Drug Discovery and Drug Development

As stated, NMR spectroscopy can be fundamental in studying how drugs interact with their targets. This has been done mainly via the Fragment Based Drug Design (FBDD) approach, which has two sub-approaches: target- (i.e., protein) based, or ligand- (drug) based. Target based screening monitors how the target responds to binding molecules in a method called Structure Activity Relationship ("SAR") by NMR. Ligand (drug)-based screening methods provide ways to observe the binding/non-binding behavior of the drug in approaches such as Saturation Transfer Difference (STD) and other Nuclear Overhauser Effect (NOE) type methods, diffusion-based methods, relaxation-based methods (i.e., T_1 and T_2). Target based screening, ligand (drug) based screening, and their respective methods, are discussed in detail below.

3.1. NMR in Fragment Based Drug Design (FBDD)

NMR-based drug discovery can be broadly classified into two groups: chemical and biological (in-cell) categories. One of the principal methods of drug discovery using NMR spectroscopy is called fragment-based drug design (FBDD) [194]. In-cell NMR (biological) based drug discovery techniques will be discussed later in this review.

FBDD was first reported in 1996 [195] and used throughout the late 1990s as evidenced by the use of keywords related to FBDD in papers published during this time [196]. The use of FBDD as a viable drug screening technique began to be widely adopted in the mid-2000s [197]. High Throughput Screening (HTS) is another technique widely used in drug discovery [198]. HTS analyzes molecules from a chemical library to see which ones are suitable leads [198–201] (see Figure 6). FBDD techniques will screen against a carefully designed fragment library composed of a few thousand molecules (for details on the choice of compounds and design of fragment libraries, see [202,203]) and identified hits are

further developed via fragment growing, fragment merging, or fragment linking [194]. For examples of drugs derived from the FBDD approach that are currently in clinical trials, refer to Table 2.
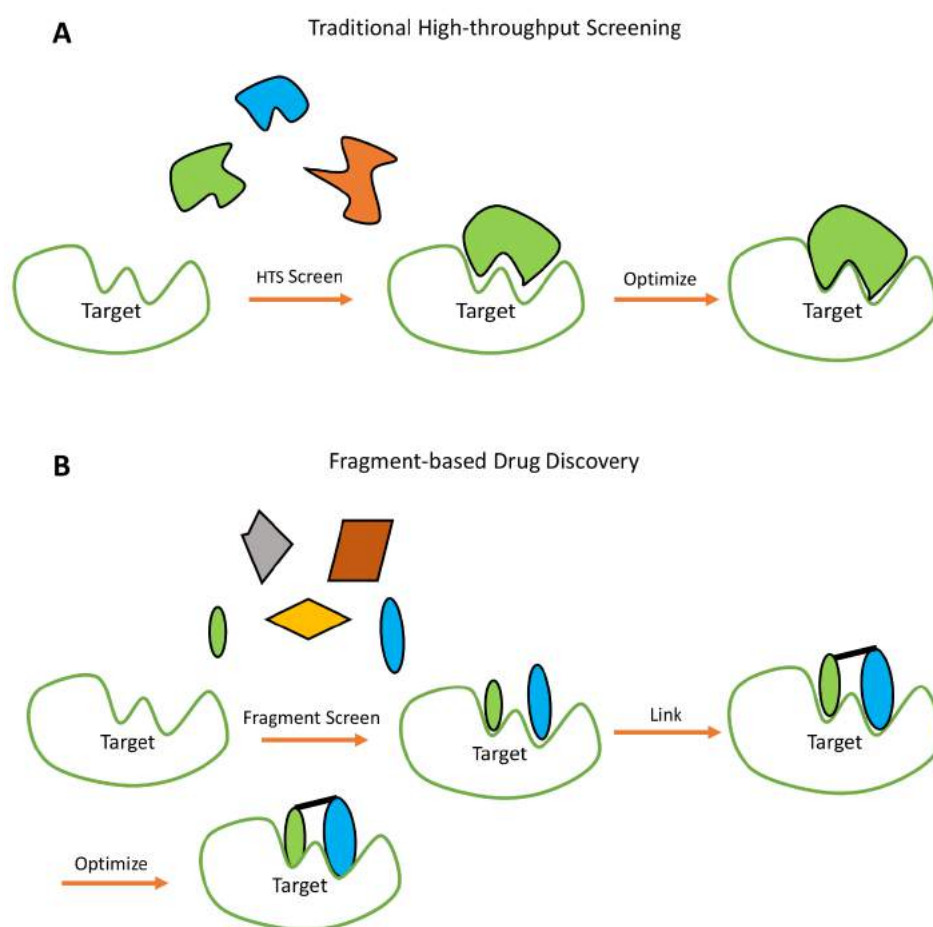
Figure 6. Underlying mechanisms of (**A**) Traditional High-throughput Screening, and (**B**) Fragment Based Drug Discovery.

HTS has been productive in drug design [204,205], but the method is time and resource intensive [206] and expensive [206] because of the numerous molecules to be examined (~100 million) [207]. Furthermore, the success rate is only estimated to be at ~50% [204,208]. Unlike traditional HTS, which can survey a large number of molecules ranging from a few hundred thousand to a few million [209], FBDD usually surveys a few thousand molecules (~1000–15000) from libraries with greater chemical diversity [209,210]. FBDD is a main-stream screening technique for drug discovery [207,209,211–216] and NMR is standard for many FBDD studies [209]. Additional methods and techniques such as SPR, X-ray crystallography [209,217–220] etc. have also been used in FBDD studies, accompanied or unaccompanied by NMR experiments. For examples of FBDD derived drugs using methods besides NMR, refer to Table 2.

At the time of writing, and to the best of our knowledge, there are three Food and Drug Administration (FDA)-approved drugs derived from the FBDD approach [221], and over 30 are in clinical trials [222]. The first marketed drug derived via the FBDD approach is vemurafenib [223]. Vemurafenib is also the first drug approved for treatment of *BRAF*-mutant cancer [224], and is reported to exhibit significant clinical benefit for patients with metastatic melanoma [224]. Venetoclax, a common drug used to treat patients with chronic lymphocytic leukemia [225], is considered the second drug to be discovered using the FBDD approach [221], and ribociclib, a CDK4 inhibitor, the third [221]. The names, structures, targets/applications, and clinical status of vemurafenib, venetoclax, ribociclib, and other drugs are listed in Table 2.

Table 2. The names, structures, targets, FBDD optimization strategy used, biophysical techniques used, and status in clinical trials of select drugs derived from the FBDD approach.
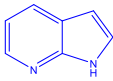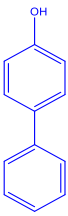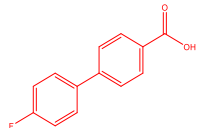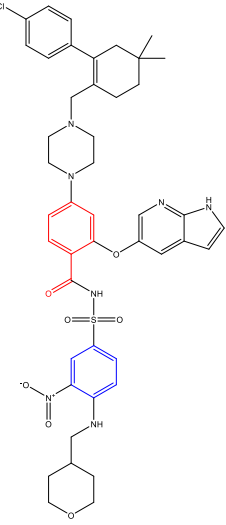
Drug (Company)	Target	Original Fragment(s) *	Advanced Molecule and Progress in Clinical Trials	Techniques Used
Vemurafenib (Plexxikon) [224,226]	BRAF-V600E		Approved	high-concentration biochemical fragment screening, X-ray crystallography
Venetoclax (AbbVie, Genetech) [227–230]	BCL-2		Approved	NMR, X-ray crystallography

Table 2. *Cont.*
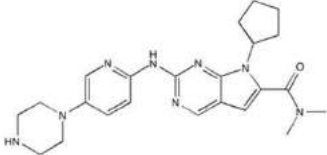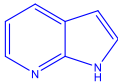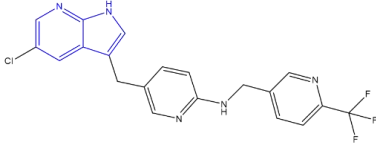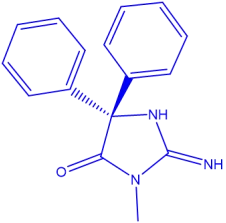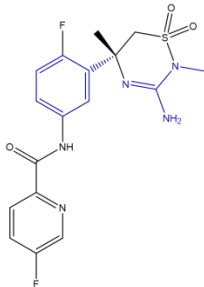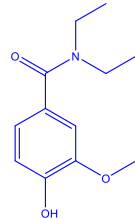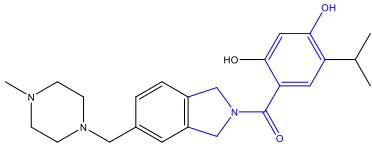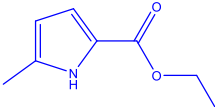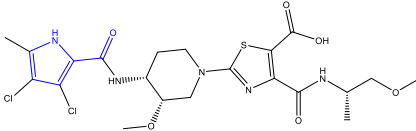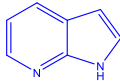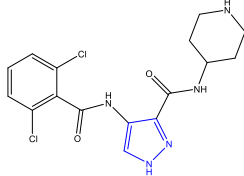
Drug (Company)	Target	Original Fragment(s) *	Advanced Molecule and Progress in Clinical Trials	Techniques Used
Ribociclib (Novartis Europharm Limited) [231]	CDK4 and 6	Information Not Available	Approved	Information not Available
PLX3397 (Plexxikon) [232–234]	FMS, KIT, and FLT3-ITD		Phase 3	X-ray crystallography, Structure Confirmed by NMR, MS, and HPLC
Verubecestat (Merck) [235,236]	BACE1		Phase 3	NMR, X-ray crystallography, inhibition of cathepsin D

Table 2. *Cont.*

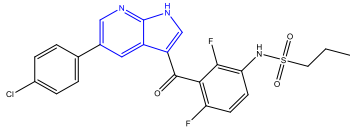| Drug (Company)	Target	Original Fragment(s) *	Advanced Molecule and Progress in Clinical Trials	Techniques Used
Onalespib (Astex) [237,238]	HSP90		Phase 2	X-ray crystallography, isothermal titration calorimetry, NMR
AZD5099 [239,240]	Topoisomerase II		Phase 1	NMR, Surface Plasmon Resonance, isothermal calorimetry, X-ray cystallography
AT7519 [241–244]	CDK 1, 2, 4, and 5		Phase 2	NMR, MS, X-ray crystallography

* Structures for some of the fragments are taken directly from Dan Erlanson's blog at [245].

As mentioned, NMR spectroscopy can be used in FBDD in two different ways: (1) target (or receptor) based screening, and (2) ligand-based screening. With the stated advantages and disadvantages, researchers must select based on their available compounds.

3.1.1. Target Based Screening

Target based screening typically utilizes the "SAR by NMR" (structure-activity-relationship by nuclear magnetic resonance) approach [246]. SAR is primarily used to identify and develop extremely tight-binding ligands [247]. The ligand to target binding is traditionally monitored via chemical shift changes [247] using a correlation spectroscopy such as ^{1}H-^{15}N HSQC starting with the target and no ligand present [248]. Multiple spectra for the target are recorded in the presence and absence of ligands. The binding ligand will cause chemical shift perturbations in the target, and these perturbations are often easily visualized by overlaying the two spectra [247]. For example Hajduk et al. investigated the binding interactions of 2-phenylimidazole with the FKBP protein as shown in Figure 7 [249].
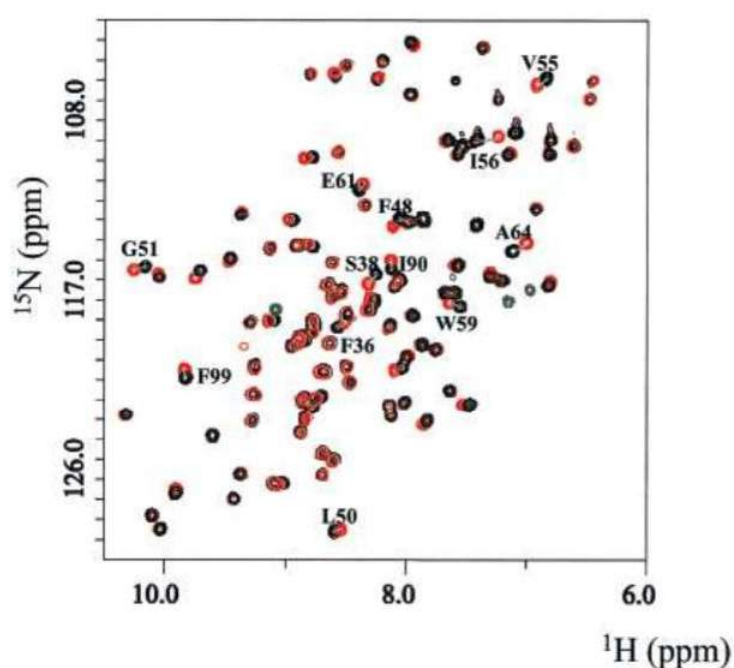
Figure 7. Overlaid 1H-15N-HSQC for FKBP in the absence (black contours) and presence (red contours) of 2-phenylimidazole. Adapted with permission from Hajduk et al. [249].

From the overlaid spectra, chemical shift changes are measured, and from the molecular location, extent, and rate of the chemical shift changes, the binding site and affinity of the ligand is calculated [250]. Then, by following a procedure completely analogous to that of FBDD (see Figure 6), a ligand developed from multiple fragments can be optimized for the binding site of interest, again by monitoring the changes in chemical shifts of the target. Several examples of the successful applications of SAR by NMR in drug design research are replete in the scientific literature [204,251,252].

SAR by NMR spectroscopy allows researchers to observe directly ligand binding [247] in both solution state and solid-state spectra [253], increasing the method's versatility [254]. It works particularly well for targeting proteins with adjacent "subpocket" binding sites [248]. Furthermore, SAR by NMR is cost-effective when combined with HTS (High Throughput Screening) [255]. SAR by NMR can also be used even when atomic peak assignments in spectra are unknown, though it is much more powerful when the resonance frequency of each atom is known [254]. The main limitation of SAR by NMR, however, is its inability to distinguish between multiple binding modes (i.e., cleavage of covalent bonds or allosteric changes), and if multiple binding modes are present, it can be difficult to pinpoint the "true" binding site of the ligand solely using data obtained using SAR by NMR [254].

3.1.2. NMR Ligand-Based Screening

Ligand-based screening, the second approach of NMR in FBDD, has three main categories: 1) Saturation Transfer Difference (STD) and Nuclear Overhauser Effect (NOE) type methods, based on 2) diffusion methods, or 3) relaxation-based methods (i.e., T_1 and T_2).

3.1.3. Saturation Transfer Difference (STD)

Saturation Transfer Difference (STD) NMR depends on the Nuclear Overhauser Effect (NOE), which is often used to enhance the sensitivity of less sensitive nuclei such as ^{13}C and ^{15}N [256,257]. This increase in sensitivity is possible because of dipolar coupling (i.e., through space interactions of separate nuclei) [257]. The increase in sensitivity is actually brought about by applying a long, low power radiofrequency pulse that selectively saturates the magnetization [256] of a specific chemical group (i.e., the methyl groups on a protein), which is then given time to transfer to another chemical group via the NOE dipolar coupling within a few angstroms [258]. The transfer in magnetization is easily visualized on a NMR spectrum that takes the differences in the signal intensities from before and after the irradiation. This new spectrum is called a "difference spectrum", and it reveals what chemical groups interact with the irradiated signal [259] (see Figure 8).
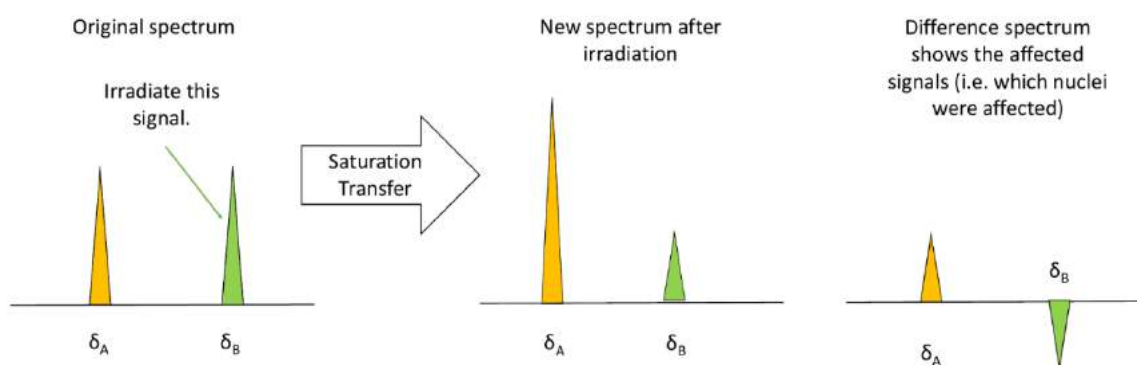
Figure 8. Basic layout of the different NOE effect on NMR signals.

STD NMR is an application of NOE used to probe the binding of ligands to a specific site within the targeted proteins [256]. A generic example of detecting ligand binding via STD is presented in Figure 9a. The STD NMR method follows the same concepts as a normal NOE experiment: a spectrum of the ligand in the free, non-binding form is recorded, the ligand is allowed to bind to the protein, which has a functional group of interest (i.e., methyls) with a saturated signal from a previous selective radiofrequency pulse. The saturated signal travels to the ligand, increasing the intensity of a signal on the ligand spectrum and finally a difference spectrum is used to determine precisely which sections of the ligands bind. The difference in peak intensities proves the presence of ligand binding [260].

Water-Ligand Observed through Gradient Spectroscopy (WaterLOGSY) is a second type of STD (see Figure 9b). The main difference with normal STD NMR is that water is the saturated signal [261], and instead of observing lower peak intensities, peak *inversions* indicate the presence of ligand binding [209].

For STD NMR to work properly, the ligand concentration must be in large excess (often 100–1000 fold) over the receptor so that effective saturation transfer can take place [260]. This means that for STD NMR, and WaterLOGSY, only small amounts (μg) of protein are required to get results [261–263]. This is advantageous for researchers, as they can perform STD NMR on a protein of interest, and preserve the rest of the unused sample for future/other experiments. Also, the same sample can be used for multiple NMR measurements. STD NMR facilitates the differentiation of binding ligands from non-binding ligands because the change in signal (as determined by the difference spectrum) is easy to measure and observe, as shown in Figure 9. WaterLOGSY has been extended to study ligand interactions with DNA and RNA [261].
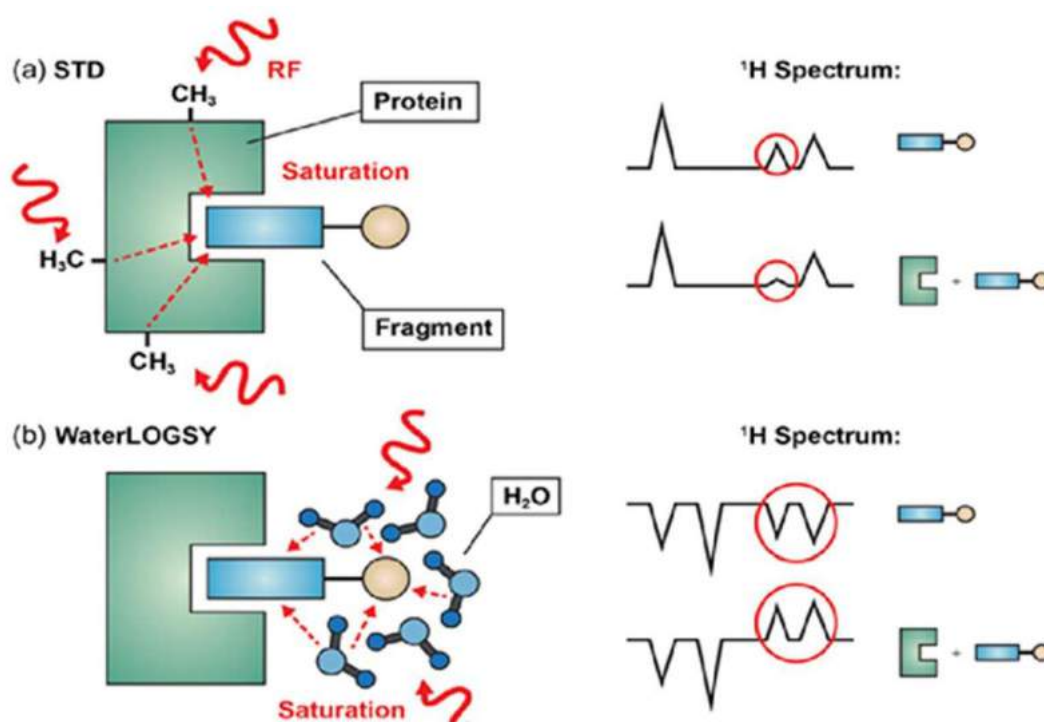
Figure 9. Illustration of STD NMR (**a**) and WaterLOGSY (**b**) in drug design. Copied with permission from Robson-Tull [209].

There are additional NOE-type experiments (trNOE, INPHARMA, SALMON, etc.) used for drug design, and specific details regarding individual methods are found in the scientific literature [264].

With the pressing search for new antiviral drugs, any techniques for identifying and characterizing novel leads has become increasingly important. Benie et al. [265] described the use of saturation transfer difference (STD) NMR spectroscopy [262,266–271] to identify and characterize the binding of an antiviral compound to native human rhinovirus serotype 2 (HRV2). The experiments demonstrated that it is possible to subject targets of the size and complexity of whole viruses (for a model of an HRV2 particle cut open, cf. the table of contents) to STD NMR experiments. The principles of STD NMR have been known for many years [267,268] but it was only recently that the potential of this technique for screening libraries for compounds with binding activity toward protein receptors has been realized [262,266]. The technique also permitted the analysis of epitopes of ligands bound to receptor proteins. Previous NMR studies of virus-ligand interactions used chemical shift titrations, which required very large quantities of the virus. This approach was unworkable when studying pathogenic viruses. Benie et al. [265] demonstrated that solution state STD methodology not only reduces the amount of virus required by approximately 2 orders of magnitude, but also allows for the identification and characterization of virus-ligand interactions with atomic resolution [272].

The very large size of viruses makes them particularly attractive for studies by STD NMR, as they inherently yield large line widths allowing for easy irradiation of the virus without affecting the ligand protons. Furthermore, because of the larger correlation time of a virus in comparison to an average-sized protein, spin diffusion, and thus saturation transfer, is very efficient. The large line width has additional benefits not just for STD-based NMR methods but also for transfer NOESY spectra, as protons from the virus capsid are invisible in the NMR spectra (for an example of a transfer NOESY spectrum, see [265]). Moreover, competitive STD titration experiments can be used to determine the K_d value of a ligand [271]. Analysis of the STD spectra using the group epitope mapping method [271] allows for the determination of the binding epitope. STD NMR methods can considerably speed up the determination of the binding epitope for potential antiviral lead compounds.

Simple STD NMR experiments provide substantial information on the binding of ligands to native viruses and require very small amounts of the virus with measurement times in the range of tens of minutes. This allows for a high throughput of ligand samples without significant consumption of viral material because it remains unaffected by the experiments and is easily separated from the low molecular weight ligands by ultra-filtration subsequently. In addition to the detection of binding, a complete mapping of the ligand-binding epitope can be achieved [265].

Noroviruses (NV) are non-enveloped, single-stranded, positive-sense RNA viruses that are the major cause of epidemic outbreaks of gastroenteritis worldwide [273–275]. The viral coat consists of a single protein, VP1, which assembles into a capsid with overall icosahedral symmetry [276–278]. Attachment of human noroviruses to histo-blood group antigens (HBGAs) is thought to be critical for the infection process [279]. The protruding domains of the VP1 proteins, called P-domains, harbor highly conserved binding sites for HBGAs. STD NMR-based epitope mapping was used [262,271] to identify structural features of different core types critical for the binding of synthetic A- and B-tetrasaccharides [280] to virus-like particles (VLPs) of a highly homologous GII.4 strain (Ast6139). STD NMR experiments provide a robust and straightforward technique for obtaining ligand binding epitopes at atomic resolution. Comparing binding epitopes of related ligands then delivers critical information about structural requirements for ligand recognition. Conversely, comparison of binding epitopes of a given ligand binding to wild type, and to mutant proteins reveals the importance of individual amino acids for binding. STD NMR experiments with L-Fuc and B-trisaccharide in the presence of wild type and mutant VLPs yield virtually identical binding epitopes and suggest that these two mutations do not significantly alter HBGA recognition. The STD NMR approach to characterize binding of HBGA ligands to noroviruses has employed VLPs as targets and thus taken advantage of the large size of VLPs yielding excellent signal-to-noise ratios of the corresponding STD NMR spectra, as demonstrated previously [281].

3.1.4. Transferred NOE (tr-NOE) in Ligand Based Screening

The application of the transferred NOE (Tr-NOE) effect was first demonstrated by Bothner-By [282]. The Tr-NOE is the nuclear Overhauser effect between ligand spins, which are in chemical exchange between the bound and unbound form with the protein or receptor. Ligands, which are a mixture of target molecules, are small in size (below 500–1000 Da). Since they are usually low molecular weight molecules, they exhibit much shorter correlation times when compared to the receptor and have slow NOE build-ups with no spin diffusion. This is the reason they show small positive NOEs in the free form. When binding to a protein receptor, the situation changes, where the ligand acquires large correlation times in the bound state with rapid NOE build-up. Then they show spin diffusion and a strong negative NOE, which is termed the transferred NOE. Signals arising from the protein are usually not observed for large proteins as they are generally kept low in concentration, with ligands in a high excess concentration. In addition, most of the time protein signals are suppressed by their very short T_2 period. It is worthwhile to mention that ligands that are in fast exchange between the bound and the free form (dissociation constants ranging from μM to mM) get enough bound time to transfer the negative NOE from the protein complex to the population of the free molecules, yet usually retain the chemical shift of the free molecule along with the relaxation characteristics. In order to observe tr-NOEs, the following condition have to be fulfilled:

$$\left|N_b\partial_b\right|\gg\left|N_f\partial_f\right| \tag{3}$$

where N and ∂ represent the number of molecules and the cross-relaxation rate, respectively. The subscript b and f represent the bound and free form, respectively. Therefore, to observe the tr-NOEs, a high excess concentration of ligands over protein is maintained. On the other hand, if the ligand concentration is kept too high, the excess free ligand in solution will exhibit positive NOE, which can result in a significant reduction of the tr-NOESY enhancements due to negative NOE developed

by the very small concentration of bound ligand. Hence, the preparation of the sample becomes tricky and an optimum ratio between 10–30 to 1 is maintained while considering the dissociation constant values. The binding of a ligand to a receptor protein can easily be identified by observing the sign and size of the NOEs. There are some distinct experimental features for the discrimination between tr-NOEs from the bound state and NOEs of the ligand in free states like the build-up rate. For tr-NOEs, this is in the range of 50 to 100 ms, whereas for small ligands it is much longer. There have been various instances of experimental implementations to quickly determine the binding activity of ligand libraries. One example was to find the ligand molecule among a library of 10 similar structure polysaccharides that is bioactive in binding with recombinant E-selectin [283]. This is a protein present in an IgG chimera with a molecular weight of about 220 kDa. In this case, two 2D NOESY spectra were recorded. The NOESY spectra for the ligand library was measured at several temperatures and it was found that most of the 10 compounds exhibited the weak positive NOEs at 310 K, which was then chosen to differentiate between trNOEs showing large negative values. The trNOESY spectra of the ligand library in the presence of protein was recorded at different ratios, such as 5:1, 8:1, 12:1, 15:1, and 20:1, at 310 K. In all the ratios, trNOEs were observed; however, the ratio of 15:1 represented the best-case scenario.

3.1.5. The INPHARMA Method for Pharmacophore Mapping

The INPHARMA method (see Figure 10) was designed to determine the relative orientation between two competitive ligands in the receptor-binding pocket through the observation of inter-ligand NOE between the two ligands. It is a tr-NOE in nature as it is mediated by the bound conformation of the competing ligands and in exchange with the receptor protein. The first example was competitive binding and observation of inter-ligand NOE between baccatin III and epothilone A in the presence of tubulin, which acts as a receptor [284]. Since the observation is on the ligand site, it provides unique advantages. The detailed conformation of a ligand-protein complex can be addressed by conventional NMR. However, it is time-consuming and demands full solving of the structure and there is also a size limitation. From that aspect, ligand-based methods are more useful. The only limiting fact is that it should fulfill all the conditions of tr-NOE explained previously in terms of dissociation constant (K_d), fast exchange regime, and proper ligand to protein ratio. Then, information on the ligand structure can be derived from tr-NOE build up as a function of mixing time. This can be readily explained using the originally proposed schematics [284]. The NOESY spectrum of a mixture of the two ligands A and B in the presence of the common receptor (T) is recorded. Under the situation that each of A and B exhibit competitive binding in a fast exchange regime with the receptor T, intermolecular tr-NOE peaks between the two ligands A and B can then be observed in the NOESY spectrum due to extensive spin diffusion. During the NOESY mixing time, the first proton of ligand A (H_A) binds to receptor T, which results in transfers of magnetization from H_A to H_T. Subsequently, the complex AT dissociates as they fulfill the dissociation constant range, which creates the opportunity for ligand B to bind to the receptor T at the same binding site. This results in the transfer of the magnetization of H_T, which had been originally coming from H_A, to H_B. As a result, an inter-molecular correlation H_A–H_B can be seen, and this inter-molecular NOE will be a function of mixing time as described above. The detailed analysis of such intermolecular NOE peaks helps in assessing the relative orientation of each ligand in the binding pocket.
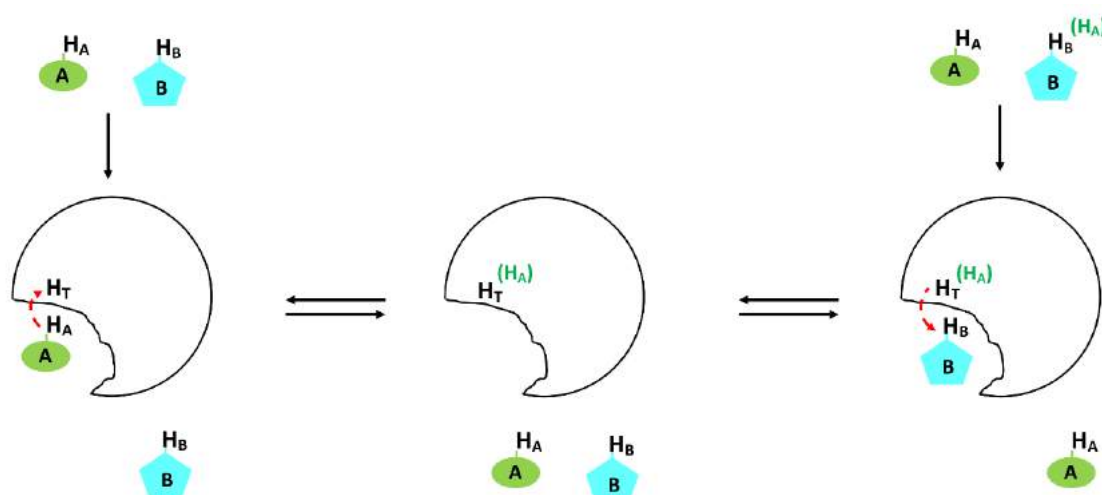
Figure 10. Schematic representation of the principle of the *INPHARMA*. The inter-ligand NOEs observed between two competitive ligands A (in green) and B (in blue), which bind consecutively to the same target receptor T. The figure is adapted from [284].

3.1.6. Diffusion Based Spectroscopy in Drug Design

Diffusion is the random, translational motion of molecules in solution as a consequence of their thermal energy [285]. This type of motion is often referred to as "Brownian motion", a motion that describes molecular movement induced by random collisions between the molecules [286]. In the presence of a concentration gradient, molecules will naturally move from places of higher concentration to places of lower concentration [287] after a period of time, t, as shown in Figure 11. Fick's Law can be used to model this type of movement [288]. The distribution of the diffusing molecules is accurately represented by a Gaussian curve, a normal distribution centered at a single point, which gradually "flattens" as t approaches infinity [213]. The extent to which a molecule diffuses is directly related to its shape, size, and mass [285]. In homogeneous isotropic solutions, the root mean square distance (z_{rms}) traveled by a molecule is given by following equation [289,290]:

$$z_{rms} = (2Dt)^{\frac{1}{2}}$$

where D is the diffusion coefficient of the molecule, and t is the diffusion time. Making the assumption that the molecules are solid rigid spheres, the value of D can be calculated according to the famous Einstein-Stokes equation (Equation (2)):

$$D = \frac{k_b T}{6\pi\eta r_s} \tag{4}$$

where k_b is the Boltzmann's constant (1.3807×10^{-23} J/K), T is the absolute temperature, η is the solution viscosity, and r_s is the hydrodynamic radius of the molecule [290]. Equation (1) and Equation (2), however, are not universally applicable; they only apply to molecules that are freely diffusing in isotropic, homogeneous solutions, and importantly that can be accurately described as hard, rigid spheres [285]. Different molecular geometries and additional modes of diffusion (i.e., restricted and anisotropic) require more advanced mathematics and theory [291,292], but the essential concepts of diffusion remain the same.
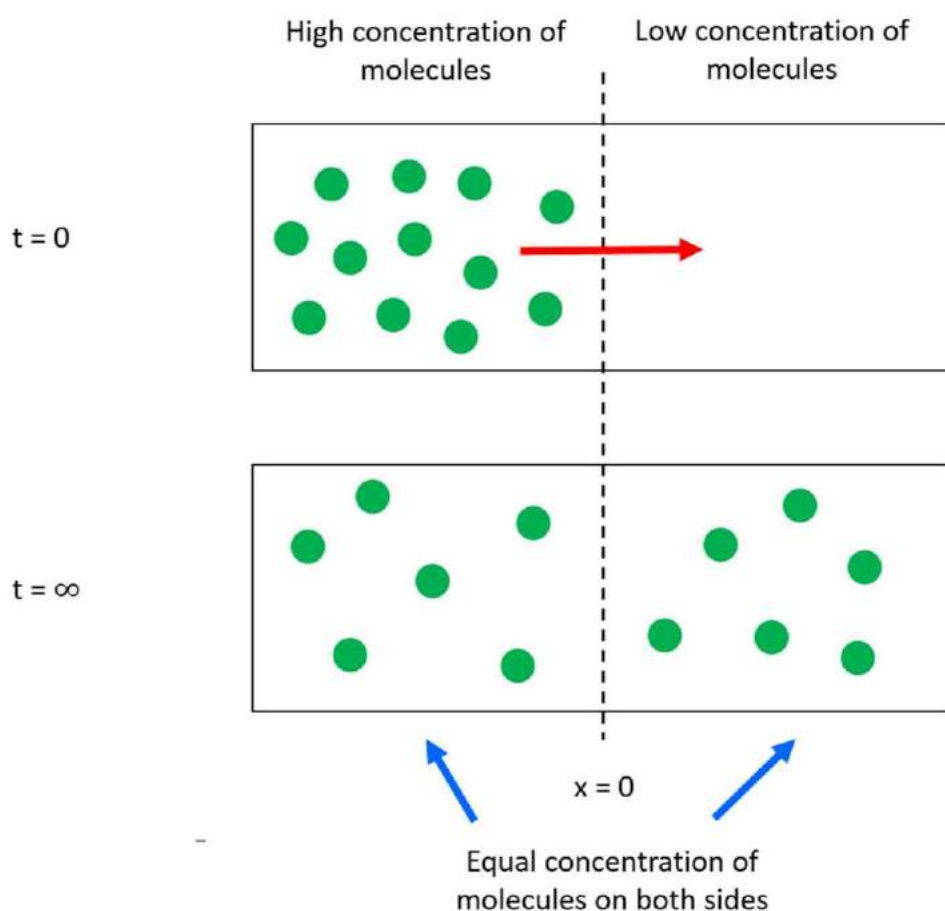
Figure 11. Visual representation of how molecules diffuse in solution from a high concentration to a low concentration across an arbitrarily defined point (x = 0) after some period of time (t = ∞) [289]. The red arrow indicates the direction of translational motion as the molecules (green) move from an area of higher concentration (left) to an area of lower concentration (right) [287].

The earliest pulse sequence used to measure diffusion in NMR spectroscopy is the gradient spin echo sequence (SE), developed by Stejskal et al. [293]. The SE pulse sequence is shown in Figure 12. The SE pulse sequence uses a gradient (G) of the externally applied magnetic field, (pulsed field gradient), the first after the 90° pulse, and the other after the 180° refocusing pulse. The first gradient pulse (G_1) labels or gradient-encodes the NMR-active nuclei based on their physical position in the sample tube. If the molecules diffuse during the time period they are not in the correct position to experience the second gradient which re-focuses the spins. This is detected via NMR as a signal intensity decrease. After a diffusion time (Δ), the second gradient pulse is applied to decode the spatial labeling of NMR-active nuclei, obtaining a well-defined spectra of diffusing molecules in solution [294]. Additional NMR sequences are available for diffusion experiments [295], and are detailed in more comprehensive reviews dealing with the subject [296,297].
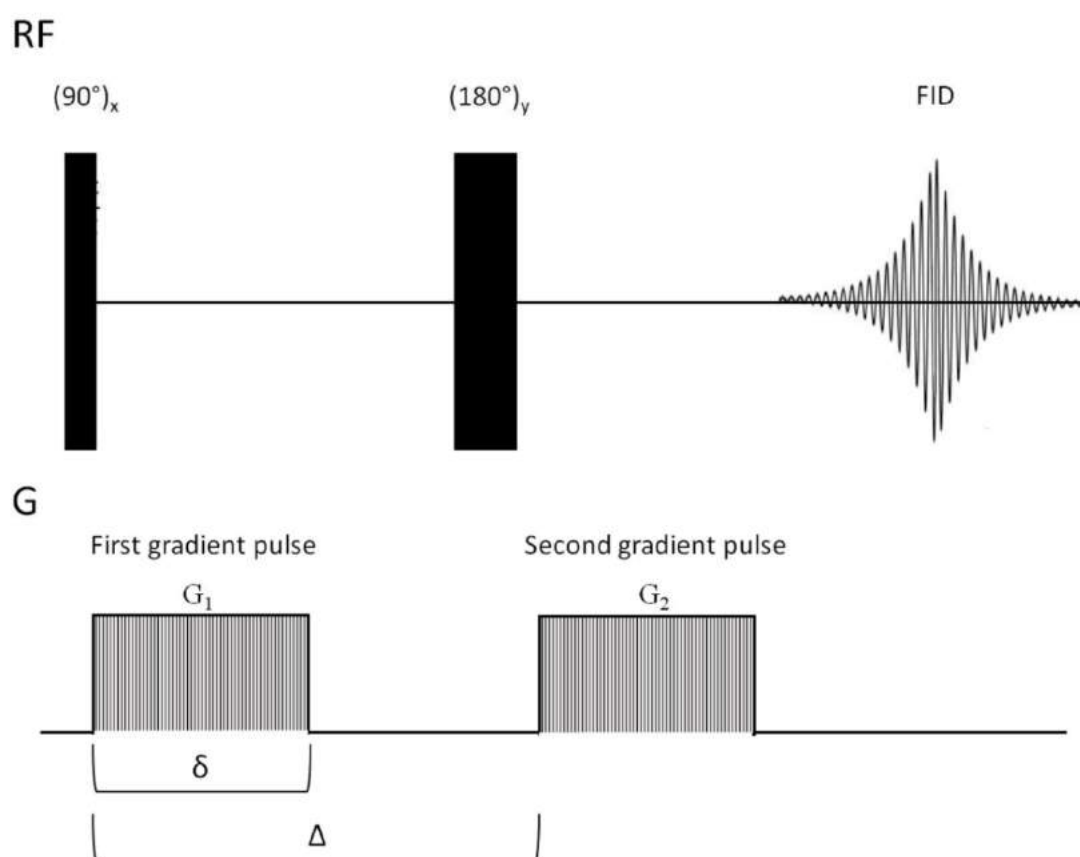
Figure 12. Spin echo (SE) sequence, as discovered by Stejskal et al. [293]. G_1 is the first gradient pulse applied after the first 90° pulse, and G_2 is the second gradient pulse applied after the first 180° pulse. δ and Δ are the gradient length, and diffusion time, respectively.

The signal intensity of the diffusing molecules depends on three factors, as described by Equation (3) [294]:

$$I = I_0 e^{-D\gamma^2 g^2 \delta^2} \tag{5}$$

where I is the observed intensity, I_0 the reference intensity (unattenuated signal intensity), D is, of course, the diffusion coefficient referred to earlier, γ is the gyromagnetic ratio of the observed nucleus, g is the strength of the gradient, δ the length of the gradient, and Δ the diffusion time [294]. From Equation (3), it is easy to see that the signal intensity decreases exponentially with time, so it is vital to optimize the values of g, δ, and Δ for diffusion NMR measurements [294].

The drug design approach based on diffusion NMR is basically a screening technique used to differentiate the binding ligands (drug) from non-binding components [264]. Ligands able to bind should have significantly different diffusion coefficients (D) compared to non-binding ligands [297], i.e., the diffusion coefficients of binding ligands will be smaller than those of non-binding ligands [264]. Thus, diffusion-based NMR is a way of effectively "filtering" and identifying which ligands are binding [264].

Diffusion-based NMR spectroscopy has advantages in ligand based screening applied to drug discovery. For example, Diffusion Ordered Spectroscopy (DOSY) does not require prior separation/purification of the ligand/target solution [298]. Diffusion based NMR allows simultaneous determination of diffusion coefficients in multicomponent systems containing large molecules (i.e., proteins) and possible binding partners (i.e., small drug compounds) [285], and no special labeling or contrasting agents are required, though their use is not exclusively inhibited (for an example of the use of labeled compounds in diffusion NMR spectroscopy, see [299]). A problem occurs when there is significant chemical shift overlap between the binding molecule signals and the target. This

situation makes it hard to distinguish the NMR signals [300], and the calculations typically assign an intermediate value to the diffusion rate (i.e., one gets a smear). Multidimensional diffusion NMR pulse sequences are available [301], which may help resolve spectral overlap in 1D experiments [300]. Another issue is that molecules in chemical databases may have generally low solubility [302,303]. Low solubility decreases the overall signal intensity and therefore makes accurately measuring diffusion experiments far more difficult [304].

There are many examples demonstrating the successful application of diffusion NMR in examining drugs of pharmaceutical interest [305], and ligand-target interactions [167]. Hajduk et al. [167] exploited the changes in diffusion rates to detect ligands that bind to the FK506 binding protein and the catalytic domain of stromelysin. Nishimura et al. [306] utilized DOSY, in combination with NOESY to determine the orientation of two guest molecules, *p*-ethoxyiodobenzene and 2-iodo-6-methoxynaphthalene, within a host composed of a tetrakis(4-hydroxyphenyl)-cavitand and a tetra(4-pyridyl)-cavitand.

Furthermore, Matthias et al. [307] used ^{1}H molecular diffusion and ^{19}F spin diffusion to probe the drug loading properties of the Rf-PEG hydrogel for 5-fluorouracil (FU) and 1,3-dimethyl-5-fluorouracil (DMFU), two anticancer drugs.

DOSY can be combined with Saturation Transfer Difference (STD, discussed earlier in this review) to yield new insights about ligand-target interactions. Kramer et al. [308] combined STD with DOSY to analyze a mixture composed of wheat germ agglutinin and two derivatives of N-acetyl glucosamine (ligands). Using this new technique they were able to obtain high quality spectra of the components in the mixture. Tanoli et al. [309] also combined STD and DOSY to explore the interactions of smaller molecules with bovine serum albumin.

These are just a few examples to show that diffusion NMR spectroscopy has played, and will continue to play, a prominent role in drug design.

3.2. NMR and In Silico Screening-Two Complementary Approaches

In silico (virtual) screening is now a standard technique in drug design and discovery [310] that has been in use since at least 1991 [311], though the exact origin of the phrase "in silico" is not clear [312]. The nearly ubiquitous use of virtual screening is due to its efficiency in searching massive chemical databases in order to generate lead molecules [313] that inhibit protein-protein interactions [314], and its ability to help identity ligand (drug) binding sites on the target of interest [310] to lend insight to the mechanisms of action for lead compounds [315,316]. Virtual screening is often accompanied by in vitro or in vivo techniques for pharmacology drug research [312], to increase drug throughput, helping to reduce the time and cost of developing novel drug candidates [317]. Virtual screening has also been used to identify candidates for anti-viral drugs [318] and anticancer drugs [319]. Several chemical databases are available both for public and academic use [320]. Virtual screening is properly identified as a high-throughput screening (HTS) technique [321], though using its full capacity as an HTS technique is not required for most purposes.

Virtual screening requires a minimum of two inputs, (1) a three-dimensional model of the ligand (drug), and (2) a three-dimensional model of the receptor (protein) [322], the latter generated from the atomic studies of proteins via X-ray crystallography or NMR spectroscopy [323]. Virtual screening is not a truly "stand-alone" technique and has often been combined with additional biophysical techniques besides NMR spectroscopy and/or X-ray crystallography [324], such as differential scanning fluorimetry [325], fluorescence polarization, and surface plasmon resonance [324]. In this section, we briefly introduce how virtual screening has been combined with NMR spectroscopy, and how they are complementary approaches to each other in drug design. The complete details of how virtual screening works, and how it applies to drug design outside of its combination with NMR is well documented in additional reviews [310,322,326–330].

A prime example of the complementarity between NMR screening and virtual docking is found in the work of Chen et al. [331], in which the authors sought to target the A_{2A} adenosine receptor (A_{2A}AR) protein, a drug target for the treatment of Parkinson's disease [332]. They used virtual screening and

an NMR-based screening method against the same 500 molecules in a fragment library so they could compare the results of both methods. The virtual screen successfully predicted (based on calculated binding affinities) four out of the five orthosteric ligands discovered by NMR that were within the top 5% of the fragment library, showing that the two separate methods can give similar and reliable results. Later on, Chen et al. discovered that virtual screening picked up three additional fragments that remained undetected by the NMR-based method, and were, in fact, $A_{2A}AR$ ligands; this shows that though neither method is flawless, they are still perfectly complementary approaches for drug design [322,331].

In another scientific work that integrated NMR with virtual screening, Di Lello et al. [333] found small molecular inhibitors of the enzyme ubiquitin specific protease 7 (USP7), a key regulator of the tumor suppressor protein, p53 [334]. A fragment screen by NMR revealed a series of small molecules that bind in the active site of USP7 near the catalytic cysteine (amino acid 223). A ligand-based virtual screen utilizing the fastROCS program identified ~30 hit molecules, several of which were further characterized by ^{1}H-^{15}N TROSY chemical shift perturbation and line broadening to probe the binding site of the active hits. Di Lello. also tested the active compounds against EOL-1 cells to verify the hits as identified by virtual screening and further characterized by NMR, showing that the active compounds do indeed inhibit USP7 activity. Through additional study of the active molecules and further optimization of their structures, they eventually discovered a series of ligands that bind in the "palm" region of the catalytic domain of USP7, inhibiting its catalytic activity [333]. This study clearly demonstrates that NMR screening-based techniques can be combined with virtual screening to find viable drugs for targets of interest.

Additional examples of the successful integration of NMR and virtual screening as applied to protein targets are also found in the literature, further demonstrating the practicality and complementarity of virtual screening and NMR [329,335–337]. For example, Li et al. [338] used virtual screening filtered by NMR to identify and characterize non-metal chelating metallo-β-lactamase (MBL) inhibitors, and in particular, Verona integron-encoded MBL (VIM)-2, when previously there were no clinically significant inhibitors of MBL, since MBL enzymes hydrolyse many, if not all, β-lactam antibacterials compounds specifically designed to inhibit their activity [339]. Furthermore, Shan et al. [340] and Bertini et al. [337] both used virtual screening and NMR, in their respective studies. Through the combined use of NMR and virtual screening, Shan et al. was able to identify, design, and synthesize novel PDZ domain inhibitors, which are proteins implicated in tumorigenesis [340]. Bertini et al. was able to combine NMR to study the interaction of ligands with metalloproteinases, using known inhibitors of metalloproteinases as a starting point [337]. While HSQC NOESY NMR data provided structural and spatial constraints for the proposed 3D models, virtual screening was used to refine the models, and to probe the ligand-protein interaction. In each case (i.e., ligand-protein interaction), Bertini et al. was able to obtain a well-defined ligand conformation in the protein binding site, thus offering a viable alternative to other approaches described in the literature [337]. Clearly, combining virtual screening with NMR-based methods is advantageous in studying how ligands (drugs) bind and interact with targets (proteins) of interest.

3.3. Paramagnetic Resonance in Drug Discovery

Paramagnetic NMR (PNMR) can also play a prominent role in drug discovery [341], as PNMR can provide key structural information in situations where crystal structures cannot due to the weak binding of ligands [341]. PNMR can be used to quantify the binding between ligands and large biomolecules such as proteins, DNA, and RNA [342].

PNMR depends on the presence of a group (called the paramagnetic center) with an unpaired electron [343], and since many naturally occurring biomolecules and organic compounds lack a paramagnetic center, one such as caged lanthanide (CLaNP) [344], must be introduced artificially [341]. Once the paramagnetic center (often a metal ion) is present, paramagnetic effects can be used to measure the distance and the relative orientation (i.e., angle) between molecules [345]. This information

is crucial when it comes to determining how ligands and substrates bind. Thus, PNMR is quite a useful technique for drug discovery when a paramagnetic center is present. The most relevant consequence of PNMR for drug discovery is paramagnetic relaxation enhancement (PRE), although there are a number of studies demonstrating the use of pseudocontact shift (PCS) effect in drug discovery research [341].

Paramagnetic relaxation enhancement (PRE) is proportional to the inverse sixth power of the distance between the paramagnetic center and the nucleus of interest (i.e., ^{1}H), although it does not reveal anything about relative orientation [341]. PRE can give quantitative information in the range of 10–25 Angstroms [346]. Several researchers have taken advantage of this outstanding property to study the structural and dynamic properties of complex biomolecular machineries in their native environment [347].

For example, Iwahara et al. (2003) demonstrated that a protein's binding polarity to DNA can be determined by PRE, using EDTA-derivatized deoxythymidine (dT-EDTA) with a chelated metal ion (such as Cu^{2+} or Mn^{2+}) as a probe. dT-EDTA with a chelated metal ion is a convenient choice, as it can be inserted into any position of a synthesized oligonucleotide. With data derived from the PRE effect, one can easily determine the polarity of the protein (or drug) binding to DNA [348]. Several researchers have investigated DNA as a drug target [349], and the study of Iwahara et al. clearly demonstrates, and even indicates, that PRE can potentially be used to study the interactions between a drug and DNA [348], provided that a paramagnetic center such as dT-EDTA or a metal ion is present.

Brasuń et al. [350] also used PRE derived distances between a paramagnetic center and a nucleus of interest. They replaced the Cys-S-S-Cys bridge found in oxytocin and vasopressin with the His-Cu^{2+}-His motif to investigate if doing so would alter the stability of oxytocin and vasopressin. They determined the distances between the Cu^{2+} ion and 1H nuclei (possible because of PRE), and used these values to generate three-dimensional models of the His-Cu^{2+}-His motifs in both oxytocin and vasopressin. In doing so, they indicated that such an approach using PRE can help in designing new biologically active compounds [350], and hence in drug discovery research, as many drug discovery studies require a reliable models for the successful generations of hit-lead molecules, especially in the case of in silico docking [351]. This study again proves the usefulness of PRE, and therefore, PNMR, in drug discovery research.

In two additional studies, Huang et al. [352,353] used PRE in their individual studies of protein binding and protein dynamics, respectively. In the Huang et al. case [352], these authors used PRE to establish a model of the binding between the G-actin protein, and thymosin β4, an actin-binding protein. Using PRE determined constraints (distances) and ^{1}H-^{15}N HSQC, they were able to establish a well-converging docking structure of the G-actin/thymonsin β4 complex [352]. On the other hand Huang et al. [353] did not measure protein binding, but studied the conformational changes and dynamics of select large membrane proteins utilizing ^{19}F-NMR spectroscopy, and Ni^{2+} as the paramagnetic center. Through a series of extensive experiments, they showed that conformational exchange rates of membrane proteins can be determined from measurements of the metal-enhanced longitudinal relaxation (i.e., PRE) of the ^{19}F nuclei [353], thus yielding additional information (i.e., protein conformation dynamics) that could be utilized in drug discovery projects targeting proteins (i.e., understanding how the protein changes shape based on its environment can be used to find potential binding sites for drug candidates).

All these examples prove that PNMR is powerful approach in drug discovery research, given that PRE can aid in generating trustworthy models of interacting molecules, and that it can help researchers understand better how the molecules interact in the first place.

3.4. Solid State NMR in Drug Discovery

Since the late 1970s solid state NMR (ssNMR) has demonstrated its usefulness in complex biomolecular systems such as collagen or lipid bilayers [354]. However, over the past years ssNMR has gained attention in the field of drug design and is slowly becoming a commonly used technique as its proving to be a powerful tool for structural analysis of membrane proteins and amyloid fibrils [354–356].

ssNMR is becoming a more attractive alternative for several different reasons. One of them is the fact that it enables the characterization of a chemical compound in a solid-state form such as in a tablet/pill [356–358]. Moreover, ssNMR is not only restricted to analyzing the chemical structure but it can also provide insight into the physical properties of a compound such as polymorphism (different crystalline structures of the same compound), disorder (crystal defects and amorphous solids in the compound) or the presence of cocrystals (multicomponent crystal made of a compound and one or more small organic molecules) [356,357]. ssNMR can also be used to quantify the amount of crystalline against the amount of amorphous material in the sample to establish phase purity (the amount of desired phase separated from other, undesirable phase) [356–358].

ssNMR differs from liquid state NMR by the presence of anisotropic interactions. In liquids NMR these effects are averaged to zero as a consequence of rapid molecular tumbling. In solid state however, the molecules are not tumbling rapidly and the residual effects of anisotropic (orientation depended) interactions such as anisotropic chemical shift, magnetic dipolar coupling, and quadrupolar coupling could be observed in the form of broad peaks, with could be much wider than the chemical shift range of the nucleus [355,358,359]. As a results, there has been a constant effort to improve the sensitivity and resolution of solid state NMR spectra, which increased the potential of ssNMR in future applications [360]. One of the methods that works for nuclei with spin value of I = 1/2 is called magic-angle spinning (MAS). It increases the resolution by rapidly rotating the sample around a fixed (or so-called magic) angle of 54.736° [360]. This method can be combined with decoupling, to remove the dipolar couplings between spins. This is done by applying radiofrequency pulses or cross-polarization (CP) transfer of magnetization from abundant and sensitive nuclei such as ^{1}H to less sensitive such as ^{13}C [328,333]. A broader comparison between ssNMR and liquid state NMR is provided in [361].

As mentioned before, ssNMR can provide information about membranes and membrane proteins. For this reason, ssNMR can be used to detect interactions of ligands with receptors embedded to the membrane which enables the mapping of binding site of a receptor by utilizing CP-MAS (cross-polarization magic-angle spinning) NMR and site specific mutagenesis [355]. ssNMR can provide the conformation of ligands bound to the receptor which can then be used to optimize future drug in terms of better affinity and efficiency [355]. Since ssNMR is also applicable to amyloid research, it can be used for probing polypeptide structures of amyloid and intermolecular contacts between fibrils. The potential is for the design a drug that will inhibit the process of aggregation of proteins and peptides [355]. Lastly, since ssNMR gains insight into physical properties of a chemical compound it can be used for control of the process of formulation and processing of a drug to help assess the purity of a compound [358].

An example of ssNMR application related to drug design is the work of Callari et al., who monitored the effect of drug loading on the properties of micelles [362]. Polymer micelles are widely used as nano-carries for drug delivery, but so far the effects of drug loading on the morphology of a drug carrier had not been thoroughly investigated [362]. They created a model consisting of a fructose hydrophilic block and a PMAA block (micelle), to which a different amount of platinum complex was anchored. The results from this experiment showed that micelles loaded with a higher amount of platinum complex had reduced cellular uptake, release, and cytotoxicity. The micelles with a lower load (LL) of platinum complex were more effective at targeting cancer cells (of cell lines MDA-MB-231 (breast cancer) and A549 (lung cancer) than the micelles with a higher load (HL) of the platinum complex. This is evidenced by the lower IC_{50} (half maximal inhibitory concentration) values of the LL micelles as compared to the HL micelles. Both of those results could be related to the micellar structure and their potential for interaction between the sugar moieties and the cell wall [362].

Another example of practical application of ssNMR is the work of Lee and colleagues [363] in which they investigated the structure of a designed zinc-binding amyloid fibril that catalyzed ester hydrolysis. Metals ions such as zinc where found to affect the process of protein aggregation which resulted in arise of amyloid like structures. Therefore, understanding the processes of aggregation and

the factors related to them is crucial for creation of new drugs for amyloid related diseases [364]. In the experiment Lee et al. used Ac-IHVHLQI-CONH$_2$ peptide (referred as HHQ) to form fibrils with varying Zn^{2+}:HHQ molar ratios. The results showed that Zn^{2+}-bound HHQ fibrils form parallel-in-register form of packing β-strand in each sheet and His residues are coordinated to Zn^{2+} via Nδ1, while half of the His residues are also coordinated to Zn^{2+} via Nε2. Additionally, Zn^{2+} binds in a 1:1 metal ion/peptide ratio. After further analysis using structural bioinformatics, it was concluded that each zinc ion was coordinated by three histidine nitrogens from two adjacent strands. Half of all histidines bridged to Zn^{2+} ions forming a metal–imidazolate chain [363].

3.5. NMR Validation in Drug Design

A "hit" is a molecule identified from a screening technique (HTS, FBDD, etc) as having a desirable effect (i.e., decreased cellular growth, high affinity score) on a target [365,366]. However, the question of whether the activity is related to actual binding to the target, or to interference with one of the components of the assay readout mechanism, is uncertain. Thus, a validation step is required. Hit-validation is therefore the process of confirming, or validating, that the molecule(s) identified previously have on target activity and selectivity [367,368]. One of the highest-impacts of NMR on drug discovery is the use as a hit-validation tool. Though the hit-validation or confirmation of drugs is mostly limited to the solution state [369], this aspect of NMR truly is a "gold standard" technique in drug discovery.

NMR by itself is a powerful tool for drug validation as in the case of Sharma et al. (2012) [370] who sought to identify potential drug-like inhibitors against L-Aspartate α-Decarboxylase (ADC) an enzyme responsible for the decarboxylation of L-aspartate in order to generate β-alanine and carbon dioxide [371], in *Mycobacterium tuberculosis*. They began with known inhibitors of ADC, and developed a protocol to measure the enzymatic activity of ADC. Upon addition of ADC to a solution of L-aspartate, L-aspartate gradually disappeared because ADC was converted to L-aspartate to β-alanine; therefore the peak intensity of L-aspartate decreased, and the peak intensity of β-alanine increased in the presence of ADC (no inhibitor drug present). Using this newly developed NMR-based protocol allowed direct measurement of ADC enzymatic activity, and Sharma et al. were able to confirm the enzymatic inhibiting activity of seven previously discovered inhibitors of ADC [370]. This study demonstrated that NMR can be an effective validation tool for known drugs and for new drugs generated by a screening approach.

NMR is also able to remove false positives that emerge from biochemical screens [372]. For example, an aptly named technique called A La Assay to detect Reactive Molecules by Nuclear Magnetic Resonance (ALARM NMR) is able to eliminate false positives from HTS methods [373], and in the presence of a test compound or mixture, measures dithiothreitol (DTT)-dependent ^{13}C chemical shift changes of the human La antigen [373]. Dahlin et al. provided an updated protocol of ALARM NMR to aid researchers in the production of the ^{13}C-labeled La antigen reporter protein, in testing compounds with the La protein, and in the analysis of obtained NMR spectra. Using ALARM NMR prioritized hits identified from HTS screening [374]. An example of ALARM NMR is found in the work of Dahlin et al., where they used this technique to test molecules that were assumed to be inhibitors of histone acetyltransferase (HAT) inhibitors, and from their studies, actually discovered that 65% (15 out of 23) of the most commonly reported HAT inhibitors were actually faulty. They were actually nonselective interference compounds, not necessarily specific to the inhibition of HAT [375]. Thus, ALARM NMR (and NMR in general) served as a useful validation method, especially for unvalidated hits identified from biochemical screens [372] or other screening techniques.

The last example highlights the need for cross validation, or the combination of two or more techniques to verify identified chemical hits. Of course, NMR is not the sole technique used for drug validation. Most often, NMR drug validation is coupled with additional methods [367] such as surface plasmon resonance (SPR) [376,377] X-ray crystallography [377–379], isothermal calorimetry (ITC) [379], UV-Vis and/or fluorescence spectroscopy [380].

The work of Goudreau et al. is an excellent example of combining NMR with another biophysical technique, in this case X-ray crystallography, for drug validation [378]. A series of benzodiazepine inhibitors of Human immunodeficiency virus 1 (HIV-1) was identified using an in vitro capsid assembly assay, and further characterized by ^{19}F-NMR. Analysis of the chemical shift perturbation and line broadening effect on the ^{19}F-NMR spectra of the benzodiazepine inhibitors revealed the specificity and reversibility of the binding inhibitors. The same set of ^{19}F-NMR spectra were used to identify the N-terminal domain of the capsid as the binding site of the benzodiazepine inhibitors. The specific amino acids involved in the binding of the benzodiazepine inhibitors were identified from the chemical shift perturbation of ^{1}H,^{15}N-TROSY NMR spectra. Later, use of X-ray co-crystallography confirmed binding locations of the benzodiazepine inhibitors and their binding modes, which was useful for further development and optimization of the benzodiazepine inhibitors [378]. The work of Goudreau et al. therefore showed how NMR could be used as a co-validation technique with another biophysical method [378].

NMR can be also coupled with multiple biophysical techniques to validate a molecule's ability to inhibit protein-protein interactions (PPIs) [367]. An example of the combination of NMR with SPR and X-ray crystallography can be found in the work of Fry et al., where the authors sought to understand how the nutlin molecule inhibits MDM2-p53, a protein-protein interaction that has been an important cancer therapy target for several years [381–383]. Fry et al. [377] gradually deconstructed RG7112, the first nutlin molecule to enter clinical trials [384], into 11 fragments so they could study the inhibitory effect of RG7112 on the MDM2-p53 interaction by SPR, NMR, and X-ray crystallography. SPR was used to determine the K_d values of the RG7112 fragments and confirmed that RG7112 and some of its fragments do bind to MDM2, inhibiting the MDM2-p53 interaction. ^{1}H,^{15}N-HSQC NMR chemical shift perturbation was also used to assess and verify binding identified by SPR. Of the six fragments of RG7112 confirmed by ^{1}H,^{15}N-HSQC NMR as binding to MDM2, SPR showed binding for five of them; thus, the two separate techniques were in good agreement with each other. The fragments of RG7112 that were confirmed to bind by both SPR and ^{1}H,^{15}N-HSQC NMR were further studied with X-ray crystallography, which can tell precisely where and how the molecules bind to the protein. Using co-crystallization, Fry et al. were able to obtain structures for several of the verified binding fragments in complex with MDM2 and were able to visualize the binding of the fragments to the MDM2 protein [377]. NMR is obviously a powerful drug binding validation tool, but it becomes much more powerful when coupled with additional biophysical techniques, as seen in the work of Fry et al. [377].

Dias et al. [379] took a similar approach as Fry et al. [377] in that they took known inhibitors of a protein-protein interaction, and dissected them into individual fragments to assess a protein's drug-ability. The interaction studied was that between the proteins von Hippel–Lindau (VHL), and the alpha subunit of hypoxia-inducible factor 1 (HIF-1α). Twelve compounds (known inhibitors and derived fragments) were developed using a crystal structure of HIF-1α peptide bound to the stable multiprotein complex pVHL-elongin C:elongin B (VCB). Each of these compounds was screened using three separate NMR techniques, Saturation Transfer Difference (STD), Carr–Purcell–Meiboom–Gill (CPMG) relaxation experiments, and WaterLOGSY (to assess drug binding and to predict drug binding mode. Each compound that was unambiguously detected (i.e., the molecule was identified as successfully binding by at least two of the three NMR methods of STD, CPMG, and WaterLOGSY) was subjected to further analysis by ITC and X-ray crystallography. ITC was used to determine the dissociation constants of binding molecules, and X-ray crystallography was used to confirm the binding mode predicted by the NMR studies. Generally speaking, the designed fragments had similar ligands efficacies compared to the parent molecules but had much higher dissociation constants (K_d values), meaning that the fragments bound less tightly than the original parent molecule [379]. With this example, it is possible to see the strength of using NMR as its own hit-validation tool (i.e., three different NMR techniques were used for screening compounds [379]), and yet, the follow-up of NMR studies with ITC and X-ray crystallography was useful in providing a basis for assessing the drug-ability of

a protein-protein interaction [385–388]. Thus, it is clear to see that NMR is a prominent method of hit-validation in drug discovery research, especially in combination with other biophysical techniques.

3.6. Other Methods Used to Determine the Drug-Target Complexes

Substantial progress has been made in the NMR field over the past 5–10 years, and various methods were established to determine the drug-target complexes. Most of them utilize either NOE or chemical shift perturbations (CSP) although in silico models/programs, using NMR-derivate data also exist.

3.6.1. DIRECTION

One of the methods called difference of inversion recovery rate with and without target irradiation (DIRECTION) is used to map pharmacophores and can be an alternative to STD experiments. This method uses the difference between longitudinal relaxation rates of ligand protons with- and with-out irradiation of the protons of the target protein. The DIRECTION approach, however cannot be used for slowly exchanging (strong binding) ligands. The practical approach of this method was demonstrated on the experiment when analyzed the interactions between p38 MAPK (p38 a mitogen-activated protein kinase) and its inhibitor-SB203580 [389,390]. The results from this experiment showed that protons H1, H4, H5, and H6 of SB203580, are in close neighborhood with the protons of p38 MAPK when compared with H2, H3, and methyl protons. It indicates that two aromatic rings (a pyridine ring and fluorophenyl ring) of SB203580 interact tightly with p38 MAPK. The results were later confirmed with proton density map of each ligand's proton, based on the crystal structure of SB203580–p38 MAPK complex [391]. Moreover, the same authors already created a new and improved protein–ligand docking method by combining the DIRECTION obtained NMR data with docking software. [392].

3.6.2. ILOE

A second method that can be used to map pharmacophores is called inter-ligand nuclear Overhauser effect (ILOE). This 2D NMR experiment detects when two ligands bind simultaneously to adjacent sites on a protein surface although both of the ligands do not have to bind to the same binding pocket (opposite to INPHARMA, see above) [5,393]. A negative ligand−ligand NOE signal will be created when ligands bind in close proximity to each other whereas ligands that do not bind will show no NOEs, or at most very weak positive ones [372,394]. ILOE also enables determination of the ligand orientations with respect to one another [393]. As in the case of INPHARMA, ILOE can be utilized even in the absence of a 3D protein structure and used with large proteins. Additionally, ILOE differs from INPHARMA in mixing times—for ILOE the mixing times are typically in the range of 600–800 ms [345]. Application of ILOE was first shown on glycolate+NAD$^+$ in the presence of porcine heart lactatedehydrogenase, and by glucose-6-phosphate+NADPH in the presence of *L. mesenteroides* glucose-6-phosphatedehydrogenase and from that time it has been widely used [393,395,396].

3.6.3. SOS-NMR

A third method called structural information using Overhauser effects and selective labeling (SOS-NMR), relies of STD experiments performed on ligand complexes with different protein samples that have been fully deuterated excluding a specific type of amino acid. In other words, the data obtained by SOS-NMR gives insight into the ligand-binding amino acid composition and when taken into consideration the 3D structure of targeted protein can be used to establish the structure of protein-ligand complex. This approach has been demonstrated using two complexes—FKBP complexed to 2-(3'-pyridyl)-benzimidazole and MurA complexed to uridine diphosphateN-acetylglucosamine (UDP-GlcNAc). The results showed that for FKBP and MurA, only four and three amino acids (FKBP: Ile, Val, Leu, Met; MurA: Trp, Phe, His) were needed to be selectively protonated in perdeuterated samples to establish the ligand-binding site. Additionally, on average only 6 amino acids were required

for accurate identification of ligand-binding surface. According to authors SOS-NMR can greatly improve the early stages of the drug discovery process [397]. Moreover, combining SOS-NMR with other methods can even further increase chances for a positive outcome of an experiment [398].

3.6.4. Tert-butyl Labelling

A completely different approach to this topic was taken by Chen et al. [399,400]. Instead of using isotope labeling, Chen's group decided to use a *tert*-butyl group contained within ligand-1 to obtain structural information about the protein-ligand complex [400]. The *tert*-butyl group formed an intense singlet in 1.0 to 1.5 ppm range thanks to rapid methyl rotation and methyl reorientation within that group. When compared with the protein's ^{1}H-NMR signal, the tert-butyl signal tended to be much narrower and resulted in easy detection without the need for isotopic enrichment even in protein complexes of high molecular mass such as *Bacillus stearothermophilus* DnaB hexamer (320 kDa) [399]. Additionally, the *tert*-butyl group produces intense NOESY cross peaks that can be observed even in the situations where normally cross-peaks of the proteins are barely detectable. This is partially because the signal corresponded to nine protons within *tert*-butyl group. Those aspects enable measurements of pseudo-contact shifts generated by paramagnetic tags attached to the protein. As a result, it allows positioning of the ligand on the protein. An example of this approach, is dengue virus NS2B-NS3 protease from serotype 2 (referred as DENpro) in complexed with ligand containing a *tert*-butyl group. The result of this experiment showed NOEs between the *tert*-butyl group of ligand-1 and residue Val155 from DENpro [400].

3.6.5. SALMON

Solvent accessibility, ligand binding, and mapping of ligand orientation by NMR spectroscopy (SALMON) is another method based on the data obtained via nuclear Overhauser effect. This method utilizes WaterLOGSY [401] to probe for solvent accessibility to the ligand and determine the orientation of the ligand by analyzing signal changes in WaterLOGSY spectra (positive signal from unbound ligand vs. negative for protein-bound ligands). This method was first used to determine the orientation of prodrug called tretazicar ((5-(aziridin-1-yl)-2,4-dinitrobenzamide) known as CB1954 in NQO2 (quinone oxidoreductase 2) binding site. Previous attempts had been made to obtain the orientation of tretazicar bounded to NQO2, however the results obtained from X-ray crystallography were inconclusive as two orientations of tretazicar could be possible. The information obtained via SALMON showed that the side chain of asparagine at position 161 formed a hydrogen bond with 2-nitrogroup of tretazicar, and that the aziridine moiety of tretazicar pointed toward the solvent [401].

3.6.6. LOGSY Titration

Another variant of WaterLOGSY method called LOGSY utilizes the titration slopes as a measure of solvent accessibility. The titration slopes are created by a constant increase of protein concentrations. This method also provides more insight into the process of ligand solvation by checking the influence of protein concentration onto the process. This approach was used on the bromodomain 1 of protein 4 (Brd4-BD1) by mapping epitopes of two ligands interacting with Brd4-BD1 and predicting ligands position. The results showed that the triazolopyridazine moiety of both ligands was implanted into the binding pocket of the Brd4. Additionally, the results from LOGSY titration showed that methyl-group 1 of ligand 1, aromatic proton 8 of ligand 2 and aromatic proton 8 of ligand 1 exhibit strong water NOE. This information enabled researchers to utilize a chemical replacement strategy (substitute bound water molecules by suitable functional groups) for aromatic proton 8 in a series of ligands containing the triazolopyridazine ring. Those protons were replaced with an amino or aminomethyl groups and as a result, the binding affinity of those ligands increased 100-fold. Finally, the results obtained from X-ray crystallography for ligands with such modifications allowed to find the binding mode of the triazolopyridazine ring of ligand 1 (with methyl group pointing internally) and the substituted amino group was found to create hydrogen bond to the side chain of Asn140 of Brd4-BD1 [402].

3.6.7. Nuclear Magnetic Resonance Molecular Replacement (NMR^2)

The most recent approach called Nuclear Magnetic Resonance Molecular Replacement (NMR^2) utilizes spatial data obtained through solution-state NMR in order to locate the binding pocket of a complex structure. For that, it uses a receptor model, e.g., a X-ray structure of a homolog, to conduct an analysis and at the same time excluding the need for protein resonance assignment. To conduct an experiment using such an approach requires a few steps. First, either the protein or ligand used in the complex must be uniformly ^{13}C and ^{15}N labeled. Then, an experiment to assign the ligand is needed such as 2D ^{13}C,^{1}H-HMQC or ^{13}C,^{1}H-HMBC. The next step is the evaluation of ligand intra- and ligand–protein intermolecular distances through NOE cross peaks obtained from F_1-^{15}N,^{13}C-filtered ^{1}H,^{1}H-NOESY. Lastly, choosing a proper input structure is required which can be either X-ray or NMR structures in apo form, with another bound ligand, or a homolog to the protein of interest. Then the NMR^2 program analyzes for all possible partial assignments (such as methyl groups of a protein) and calculates the complex structures for all options [403,404]. This method was already successfully used to resolve complex structures in case of slow and fast exchange ligands [403–406].

3.6.8. HECSP

In silico methods combined with NMR derived information can also be used to determine accurate drug-target complexes. ^{1}H empirical chemical shift perturbation (HECSP) is an empirical model that is based on chemical shift perturbation (CSP) of a protein. CSP represents the change in chemical shifts in a protein due to alteration of its chemical environment (which can happen upon ligand binding). The CSP of a target protein is obtained by a series of 2D HSQC experiments with a set of ligand titrations involving samples that contain ^{15}N-labelled protein. The calculation of ^{1}H-CSPs inside the protein are based on four contributors: 1) ring current, 2) electric field, 3) hydrogen bonding, and last 4) magnetic anisotropy. To show the value of the HECSP model two CSP examples were used: apo-neocarzinostatin (apoNCS)-naphthoate ester complex, and human intestinal fatty acid binding protein (hIFABP)-ketorolac-ANS complex. The results from the experiment showed that HECSP model can distinguish native ligand from decoys and more clearly define protein-ligand complex structures with NMR derived information [407].

3.6.9. SAMPLEX

Another program that can utilize CSP called Smoothed Automatic Mapping of Protein from Listed Extremes (SAMPLEX) can help to determine the interaction surface of proteins complexes. SAMPLEX takes the chemical shifts of the protein of interests in both the free and bound state and corresponding 3D structure of a protein in the free state. The programs returns a confidence value for each residue to be in a perturbed or unperturbed state (0.05 as being in a perturbed state, −0.05 as remaining in their unperturbed state). This approach was tested on five examples, one of which was Subtilisin BPN' (serine protease) complexed with its inhibitor–chymotrypsin inhibitor 2. The results showed that residue 2, and residues 56–62 of chymotrypsin inhibitor-2 were perturbed and residue 63 was in an ambiguous state. To compare, the X-ray crystallography data showed residues 50 and 54–61 to be involved in the interaction. For subtilisin BPN' the program predicted residues 33, 97, 99–109, 126-128, 141, 154–156, 167–171 and 218–219 to perturbed and residues 65, 98 and 220 to be in ambiguous state. That information was also confronted with the X-ray crystallography data which shown residues 99–104, 125–128, 154–157, 167, 218–221 to be perturbed [408].

4. In-Cell NMR Approaches

The interactions between targets (proteins) and ligands (small molecules) can be analyzed independently of the biological systems by using 'cell-based' NMR drug design approaches. Three basic approaches [409] are as follows: (1) Compound-detected *in-cell* NMR, (2) Target-detected *in-cell* NMR, and (3) Reporter-detected *in-cell* NMR.

These methods, with the exception of compound detected *in-cell* NMR, differ according to the isotopically labeled structure (protein, cell structure, etc.), which enables NMR detection. A cartoon representation of each of these methods is given in Figure 13.
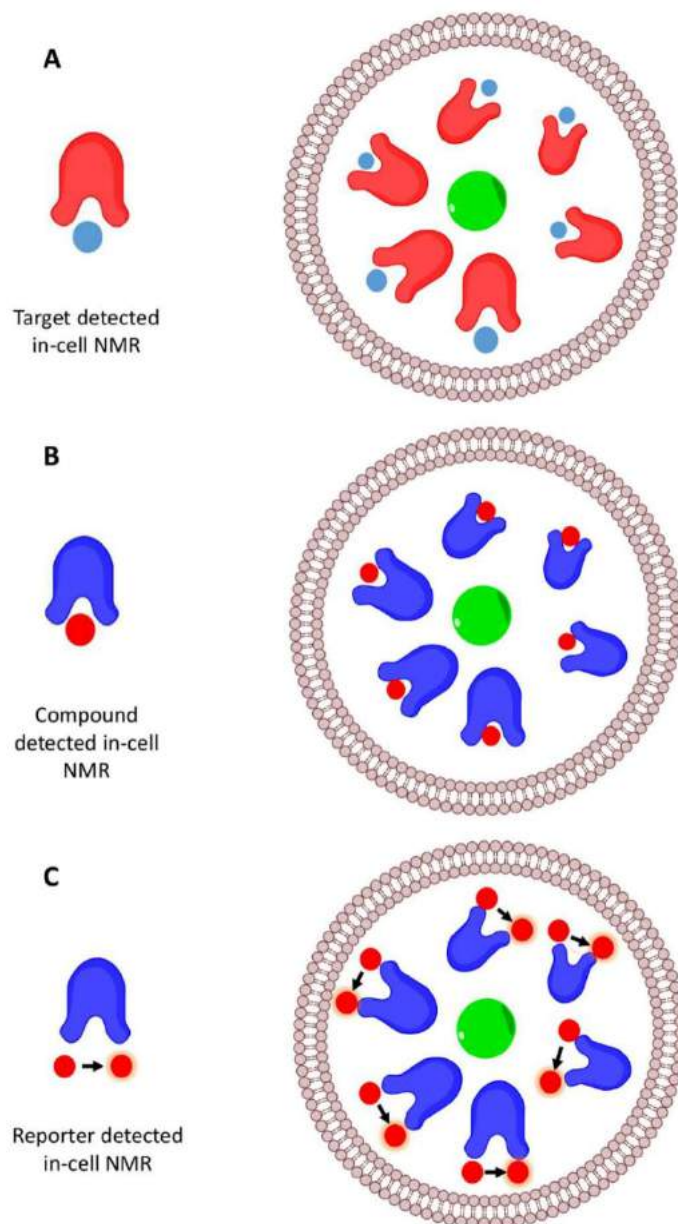
Figure 13. Representation of different in-cell NMR techniques. (**A**) Target-detected in-cell NMR, (**B**) compound-detected in-cell NMR, (**C**) Reporter-detected in-cell NMR. The red color is the isotopically labeled component of the system. Adapted with permission from [409].

4.1. Compound-Detected In-Cell NMR

STD NMR is a technique that lies within the compound-detected *in-cell* NMR method but does not require isotope-labelling of the studied compound. However isotopic labelling of the compound may be used to enhance the quality of the spectra.

4.2. Target-Detected In-Cell NMR

In the target-detected in-cell NMR only the target of interest is isotopically labeled (i.e., ^{15}N labeled protein). For instance, target proteins can be isotopically labeled during cell growth in isotopically

enriched (^{13}C, ^{15}N, or both ^{15}N/^{13}C) media [410]. The cell type and the labeling method may vary across experiments. Different cell types, including bacteria [411], oocytes [412], yeast cells [413], mammalian cells [414], HeLa cells [415] and even insect cells [416] have been reported in the literature. The fact that *in-cell* NMR applies to more than one cell type testifies of the versatility and potential application of this technique.

In terms of labeling, ^{15}N is one of the most commonly used approaches [417] when the targets of interest are proteins. Recently, ^{19}F labeling has been reported as a useful probe for protein-ligand interactions [418]. It was shown that ^{19}F can reveal information about the dynamics of protein-ligand interactions [419]. Methyl groups [420] have also been used as probes for proteins and complexes in vivo [420], proving that labeling specific chemical groups instead of the entire biomolecule (i.e., protein) is feasible.

4.3. Reporter-Detected In-Cell NMR

In-cell NMR extends beyond proteins, and has been applied successfully to DNA [93,421] and RNA molecules [422,423]. Telomeric repeats have also been studied using target detected *in-cell* NMR [424]. The reporter-detected *in-cell* NMR technique isotopically labels neither the ligand nor the target, but rather a receptor that indirectly measures the effects of ligand-target binding [409].

The "reporter" varies according to the experimental context. For instance, Dose et al. [425] used acetylation- and deacetylation-based assays to monitor the activity of histone deacetylase and acetyl-transferase. Thongwichian et al. [426] used peptide-based reporters to identify active kinases and phosphatases in cellular conditions. Lastly, Doura et al. [427] designed a ^{19}F probe that operates in biological conditions in order to study the adherence and dynamics of proteins found in human blood.

4.4. "In-Virus" NMR Strategy

In many viruses and phages, scaffolding proteins (SPs) are required to ensure the correct organization of coat proteins (CPs) and other minor capsid proteins into a precursor structure, called a procapsid [428,429]. Although SPs are critical for viral assembly and therefore potential therapeutic targets their structural properties (with only a few exceptions [430,431]) are poorly understood. The size limitation of NMR can be used advantageously as a filter to identify disordered segments even in very large supramolecular protein complexes. In this way, NMR can provide a unique perspective on the dynamic and disordered elements of macromolecules not accessible by other techniques. The procapsid encapsulation experiments described by Whitehead et al. [432] were conceptually analogous to *in-cell* NMR experiments [433–435] in which signals from small proteins, or flexible segments of proteins, can be observed when they are incorporated inside living cells, as long as the isotope-labeled proteins of interest do not interact strongly with other large cellular components [433–435]. The so called "in-virus" NMR strategy applied by Whitehead et al. [432] could be more generally used to study the dynamic properties of macromolecules encapsulated into virus particles, including cargo molecules encased in viral capsids for nanotechnology applications. Additionally, such studies could assess the level of interaction of cargo molecules with the virus and probe the release properties of cargo NMR [432].

5. Final Remarks

As we have attempted to emphasize and demonstrate, NMR has a powerful and unique role in drug design. NMR provides detailed structural information about a molecule along with kinetic information over extended time periods, i.e., not just a snapshot [24,25]. Moreover, NMR is quantitative and highly reproducible, allowing applications in diverse fields such as relaxometry, combinatorial chemistry, fluxomics, and targeted analysis [91]. NMR can be combined with other analytical techniques, such as mass spectrometry "in tandem" analysis of the molecules of interest [436–438]. ^{1}H 1D-NMR is used particularly in the analysis of metabolites, while the strength and intensity of the recorded signals is directly proportional to the concentration of the sample [44,439,440]. ^{1}H 1D-NMR can also be used to

follow "real-time" analysis of different molecules [441]. In the 1D ^{1}H-NMR experiment, there are no polarization transfer techniques required (the ^{1}H atom is already highly sensitive) and covers a spread of interesting nuclei in the molecule(s) being studied [91].

Assuming that the sample can be stored stably for extended periods of time, the non-destructive nature of NMR permits the re-use on the sample for different experiments [50,442]. Aiding in the reproducibility of NMR [91], sample-recycling offers a significant advantage of NMR [443,444].

While always important in drug design, sensitivity and resolution of NMR are two major factors that need special consideration. Since both factors improve with increasing magnetic field strength, we have seen a spike in the demand for ultra-high-field NMR spectrometers. Recently, 28.2 T (i.e., 1.2 GHz for ^{1}H) magnets have become commercially available, and with recent advances in magnet technology, such as liquid helium recycling and magnetic field shielding [91], NMR has begun to offer far better resolution and higher sensitivity while reducing the substantial costs of maintaining the instruments compared to past decades. Other steps have been taken to enhance the sensitivity of NMR including: the development of cryoprobes increasing the signal to noise ratio 3 to 4 times, and micro-coil probes that not only increased sensitivity but also reduced the amount of sample required for the measurements [445].

From another perspective, one can further optimize the process of obtaining spectra by using different methods of measurements. One of these, called SOFAST, helps to reduce the delay between scans resulting in lowering acquisition time for 2D experiments such as HMQC utilizing ^{1}H,^{15}N or ^{1}H,^{13}C [117,446,447]. The basic principle of this method is to use selective ^{1}H pulses that will excite only a small portion of the available nuclei pool, while the unperturbed spins provide a magnetization "heat sink" thus improving the spin-lattice relaxation (T_1) rate via dipolar interactions [446]. These methods can be highly efficient when studying drug binding and molecular interactions [117].

Another method, called ultrafast 2D NMR, enables obtaining a 2D spectra within a single scan but with the associated cost of reduced sensitivity [117,448]. The principle of this method is to divide the sample into *n* number of fractions, and apply the appropriate incremental aspect to each fraction, while recording them all simultaneously within the one scan [448]. This method has been applied to many metabolomic studies [177,447,449] as well as in the analysis of natural products [450]. The difficulty is that the effective concentration of the sample is lowered by the fractionation level. The more slices the sample is split into, the greater the reduction of combined signal that is obtained.

Lastly, a method termed non-uniform sampling (NUS) may provide an advantage by reducing the total time for measurement while maintaining the same resolution of spectra [117]. NUS effectively skips over parts of the total dataset, collecting only around 20 to 30% of the total. Usually sections containing higher concentrations of signal (over noise) are emphasized in the selection scheme, known as non-linear data acquisition. These methods reconstruct the complete data subset by applying various algorithms such as multidimensional decomposition (MDD), which essentially separates the sets of multidimensional data into one dimensional problems that are much easier to solve given the common process of signal overlapping in multidimensional NMR spectra [117]. Other algorithms such as compressed sensing (CS), Maximum entropy method (Max Ent) and Iterative soft threshold (IST) each have their own advantages but all focus on decreasing the time needed for collection of spectra [117,451]. The cost is in signal to noise, as no gain is ever absolutely free.

The inherent advantages of NMR do not eliminate the disadvantages (Table 3), which are namely being limited for some nuclei, and inherent insensitivity for many types of experiments. NMR can provide high quality resolution and sensitivity for some experiments [91,452] but the application can be challenging. When the experiments become multidimensional, there is often a tradeoff between the improved higher resolution and/or the resulting sensitivity and/or the amount of time an experiment takes, i.e., high-quality spectra for multidimensional experiments take much longer than their simple 1D counterparts [117] (Scheme 2). One must always choose between resolution, sensitivity, and the amount time; as you can only ever have two out of the three.

Table 3. Advantages and limitations of different NMR techniques developed in recent years.

NMR Technique	Advantages	Disadvantages
1D-NMR	Ability to identify simple chemical compounds. High quality resolution and sensitivity for many 1D experiments. Less time consuming compared to 2D NMR.	Compared to 2D NMR less details can be obtained for more complex molecules. For nuclei other than ^{1}H and ^{19}F, relative sensitivity is fairly low—requires extra labeling to obtain better spectra.
2D NMR	Ability to identify complex molecules and observe different interactions between the nuclei, e.g., correlations between all spins in one spin system using TOCSY experiment.	Requires long times to obtain a proper spectra (up to days).
Ultrafast 2D NMR	Greatly reduces time to obtain 2D spectra.	Reduced sensitivity.
SOFAST	Significantly reduces acquisition time of HMQC.	Relatively low resolution
NUS	Lowers the time of measurement while keeping the same level of resolution.	Requires use of reconstruction algorithms since missing data points can lead to artifacts in spectra.
MDD	Multidimensional data are "broken" to one dimensional, which are easier to analyze. Ability to resolve overlapping resonances.	Data must be (approximately) symmetrical (Lorentzian shape) to obtain good spectra.
CS	Good reconstruction of weaker peaks.	Large computational costs, low performance on noisy data.
MAX ENT	Significant reduction in acquisition time.	Nominally Lorentzian peak shapes may be distorted, and peak intensities may be altered.
IST	Greatly reduced time to obtain NMR spectra.	Requires a grid of uniformly sampled data points.
FBDD	Often makes stronger binding ligands from weakly binding fragments. Less time and resource intensive.	Can be used only for small fragments of compound of interest.
SAR	Direct observation of target binding to ligand. Several types of NMR experiments are possible.	Inability to distinguish binding modes, difficult to gage the "true" binding site of ligand to protein.
STD	Only requires a small amount of sample. Highly reproducible. Allows direct observations of ligand binding.	Only works for ligands with low binding affinity (fast chemical exchange). Inability to distinguish binding modes.
In cell **NMR**	In vivo studies are possible, can focus on specific cell parts.	Special labeling techniques may be required. Spectra may be more challenging to interpret.
In silico **+ NMR**	Can model protein drug interactions, helps speed up and reduce cost of drug delivery	Protein models need to be validated through experimental approach.
PNMR	Can observe proteins interacting with metal ions, long observation distance (10-25 angstroms) between paramagnetic left and nearby atoms.	Paramagnetic left required in the system.

Table 3. *Cont.*

NMR Technique	Advantages	Disadvantages
ALARM NMR	Elimination of false positives from HTS methods	It requires synthesis of human La antigen protein.
ssNMR	Enables the characterization of a chemical compound in a solid-state form such as a tablet/pill. Provides insight into the physical properties of a compound.	Significant broadening of the spectral lineshapes due to anisotropic spin interactions.
Relaxation editing	Noticeable difference in spectra of binding and non-binding ligands.	Sets the lower limit of time for which experiments can be performed.
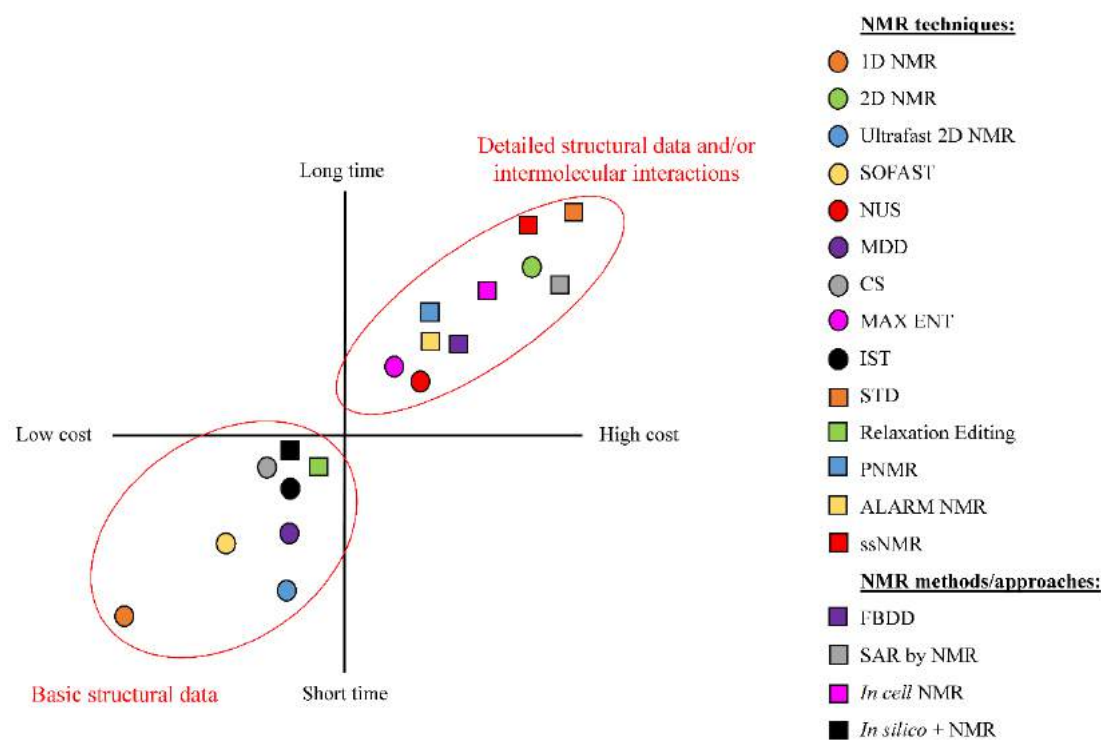
Scheme 2. Analysis of the cost and time between different NMR methods used in drug design. Meaning of some of the acronyms are listed below: SOFAST—Band-Selective Optimized Flip Angle Short Transient; NUS—Non-uniform sampling; MDD—Multidimensional Decomposition; CS—Compressed Signaling; MAX ENT—Maximum Entropy; IST—Iterative Soft Threshold; STD—Saturation Transfer Difference; PNMR—Paramagnetic NMR; ALARM—A La Assay to detect Reactive Molecules; ssNMR—Solid State NMR; FBDD—Fragment Based Drug Design; SAR—Structure Activity Relationship.

Unfortunately, in the real world, when working with NMR spectroscopy, we are mainly forced to choose between high or low precision data (Scheme 2) with fixed available instrument times. Scheme 2 can be useful, when choosing NMR technique and/or method/approaches in drug studies. It shows the general representation of different NMR techniques and method/approaches in cost-time matrix, bearing in mind that the exact position in the matrix can be influenced by the environmental conditions, pulse sequence and sample preparation (e.g., concentration). Regarding, NMR methods/approaches, the exact position depends on the choice of proper NMR technique. For the purposes of Scheme 2, the 2D techniques were chosen as described in the practical examples. Nevertheless, with relatively short times and at low cost, we can acquire numerous data sets and therefore the low precision can be partially compensated for by statistical analysis.

Fortunately, significant efforts have been undertaken to reduce the amount of time it takes to record multidimensional spectra, especially for 2D NMR, and still obtain high quality spectra (Table 3). Novel pulse sequences have been developed to decouple nuclei in Pure-shift NMR [117]. Dynamic Nuclear Polarization (DNP) can induce hyper-polarization in atoms (^{13}C, ^{15}N) with an inherently low sensitivity [453,454]. Parahydrogen-Induced Polarization (PHIP) and Signal Amplification by Reversible Exchange (SABRE) are other polarization techniques used to increase the sensitivity of inherently insensitive nuclei [455].

6. Conclusions

NMR has become a "gold standard" method in drug design due to its speed, simplicity, and reproducibility. The standardized ppm scale allows one to compare all NMR results and gather them in databases for the common use of researchers. Although sample labeling was limiting in the beginning, it has now become a strength of NMR that permits the observation of big molecules and/or biomolecular processes "through the door lock". NMR is the only analytical technique that permits qualitative and quantitative analysis without previous sample purification or separation. High precision NMR data still requires long experiment times and has elevated costs; however, these will no doubt be alleviated in the future.

References

1. Adams, C.P.; Brantner, V.V. Estimating the Cost Of New Drug Development: Is It Really \$802 Million? *Health Aff. (Millwood)* **2006**, *25*, 420–428. [CrossRef] [PubMed]

2. DiMasi, J.A.; Hansen, R.W.; Grabowski, H.G. The price of innovation: New estimates of drug development costs. *J. Health Econ.* **2003**, *22*, 151–185. [CrossRef]

3. Meigs, L.; Smirnova, L.; Rovida, C.; Leist, M.; Hartung, T. Animal testing and its alternatives—The most important omics is economics. *ALTEX Altern. Anim. Exp.* **2018**, *35*, 275–305. [CrossRef] [PubMed]

4. Friedman, L.M.; Furberg, C.D.; DeMets, D.L. What Is the Question? In *Fundamentals of Clinical Trials*; Friedman, L.M., Furberg, C.D., DeMets, D.L., Eds.; Springer: New York, NY, USA, 2010; pp. 37–53. ISBN 978-1-4419-1586-3.

5. Harner, M.J.; Mueller, L.; Robbins, K.J.; Reily, M.D. NMR in drug design. *Arch. Biochem. Biophys.* **2017**, *628*, 132–147. [CrossRef]

6. Chu, S.; Zhou, G.; Gochin, M. Evaluation of ligand-based NMR screening methods to characterize small molecule binding to HIV-1 glycoprotein-41. *Org. Biomol. Chem.* **2017**, *15*, 5210–5219. [CrossRef]

7. Zartler, E.R.; Hanson, J.; Jones, B.E.; Kline, A.D.; Martin, G.; Mo, H.; Shapiro, M.J.; Wang, R.; Wu, H.; Yan, J. RAMPED-UP NMR: Multiplexed NMR-Based Screening for Drug Discovery. *J. Am. Chem. Soc.* **2003**, *125*, 10941–10946. [CrossRef]

8. Dhahri, M.; Sioud, S.; Dridi, R.; Hassine, M.; Boughattas, N.A.; Almulhim, F.; Al Talla, Z.; Jaremko, M.; Emwas, A.-H.M. Extraction, Characterization, and Anticoagulant Activity of a Sulfated Polysaccharide from Bursatella leachii Viscera. *ACS Omega* **2020**, *5*, 14786–14795. [CrossRef]

9. Alahmari, F.; Dey, S.; Emwas, A.-H.; Davaasuren, B.; Rothenberger, A. Ultra-low thermal conductivity in Na/Sb chalcobismuthates: Synthesis, crystal structures, optical properties and 23Na NMR spectroscopy. *New J. Chem.* **2019**, *43*, 10814–10820. [CrossRef]

10. Alahmari, F.; Dey, S.; Emwas, A.-H.; Davaasuren, B.; Rothenberger, A. Layered copper thioaluminate K2Cu3AlS4: Synthesis, crystal structure, characterization and solid-state 27Al and 39K NMR studies. *J. Alloys Compd.* **2019**, *776*, 1041–1047. [CrossRef]

11. Manzoor, S.; Bilal, A.; Khan, S.; Ullah, R.; Iftikhar, S.; Emwas, A.-H.; Alazmi, M.; Gao, X.; Jawaid, A.; Saleem, R.S.Z.; et al. Identification and characterization of SSE15206, a microtubule depolymerizing agent that overcomes multidrug resistance. *Sci. Rep.* **2018**, *8*, 1–12. [CrossRef]

12. Qiu, X.; Redwine, D.; Beshah, K.; Livazovic, S.; Canlas, C.G.; Guinov, A.; Emwas, A.-H.M. Amide versus amine ratio in the discrimination layer of reverse osmosis membrane by solid state 15N NMR and DNP NMR. *J. Membr. Sci.* **2019**, *581*, 243–251. [CrossRef]

13. Dias, D.A.; Jones, O.A.H.; Beale, D.J.; Boughton, B.A.; Benheim, D.; Kouremenos, K.A.; Wolfender, J.-L.; Wishart, D.S. Current and Future Perspectives on the Structural Identification of Small Molecules in Biological Systems. *Metabolites* **2016**, *6*, 46. [CrossRef] [PubMed]

14. Duchardt-Ferner, E.; Wöhnert, J. NMR experiments for the rapid identification of P=O···H–X type hydrogen bonds in nucleic acids. *J. Biomol. NMR* **2017**, *69*, 101–110. [CrossRef]

15. Lee, H.-M.; Kim, C.S.; Jang, Y.M.; Kwon, S.W.; Lee, B.-J. Separation and structural elucidation of a novel analogue of vardenafil included as an adulterant in a dietary supplement by liquid chromatography–electrospray ionization mass spectrometry, infrared spectroscopy and nuclear magnetic resonance spectroscopy. *J. Pharm. Biomed. Anal.* **2011**, *54*, 491–496. [CrossRef] [PubMed]

16. Lu, X.; Skomski, D.; Thompson, K.C.; McNevin, M.J.; Xu, W.; Su, Y. Three-Dimensional NMR Spectroscopy of Fluorinated Pharmaceutical Solids under Ultrafast Magic Angle Spinning. *Anal. Chem.* **2019**, *91*, 6217–6224. [CrossRef]

17. Pauli, G.F.; Chen, S.-N.; Lankin, D.C.; Bisson, J.; Case, R.J.; Chadwick, L.R.; Gödecke, T.; Inui, T.; Krunic, A.; Jaki, B.U.; et al. Essential Parameters for Structural Analysis and Dereplication by 1H-NMR Spectroscopy. *J. Nat. Prod.* **2014**, *77*, 1473–1487. [CrossRef]

18. Silva, M.F.S.; Silva, L.M.A.; Quintela, A.L.; dos Santos, A.G.; Silva, F.A.N.; de Oliveira, F.d.C.E.; Alves Filho, E.G.; de Brito, E.S.; Canuto, K.M.; Pessoa, C.; et al. UPLC-HRMS and NMR applied in the evaluation of solid-phase extraction methods as a rational strategy of dereplication of Phyllanthus spp. aiming at the discovery of cytotoxic metabolites. *J. Chromatogr. B* **2019**, *1120*, 51–61. [CrossRef]

19. Samai, S.; Sapsanis, C.; Patil, S.P.; Ezzeddine, A.; Moosa, B.A.; Omran, H.; Emwas, A.-H.; Salama, K.N.; Khashab, N.M. A light responsive two-component supramolecular hydrogel: A sensitive platform for the fabrication of humidity sensors. *Soft Matter.* **2016**, *12*, 2842–2845. [CrossRef]

20. Oommen, J.M.; Hussain, M.M.; Emwas, A.-H.M.; Agarwal, P.; Archer, L.A. Nuclear Magnetic Resonance Study of Nanoscale Ionic Materials. *Electrochem. Solid State Lett.* **2010**, *13*, K87. [CrossRef]

21. Santos, S.C.; Carvalho, A.G.; Fortes, G.A.C.; Ferri, P.H.; De Oliveira, A. Variable-temperature NMR and conformational analysis of Oenothein, B. *J. Braz. Chem. Soc.* **2014**, *25*, 282–289. [CrossRef]

22. Tycko, R. NMR at Low and Ultralow Temperatures. *Acc. Chem. Res.* **2013**, *46*, 1923–1932. [CrossRef]

23. Xia, Z.; Nguyen, B.D.; Brunori, M.; Cutruzzolà, F.; La Mar, G.N. 1H-NMR Study of the Effect of Temperature through Reversible Unfolding on the Heme Pocket Molecular Structure and Magnetic Properties of Aplysia limacina Cyano-Metmyoglobin. *Biophys. J.* **2005**, *89*, 4149–4158. [CrossRef] [PubMed]

24. Mattar, S.M.; Emwas, A.H.; Calhoun, L.A. Spectroscopic Studies of the Intermediates in the Conversion of 1,4,11,12-Tetrahydro-9,10-anthraquinone to 9,10-Anthraquinone by Reaction with Oxygen under Basic Conditions. *J. Phys. Chem. A* **2004**, *108*, 11545–11553. [CrossRef]

25. Davaasuren, B.; Emwas, A.-H.; Rothenberger, A. MAu2GeS4-Chalcogel (M = Co, Ni): Heterogeneous Intra- and Intermolecular Hydroamination Catalysts. *Inorg. Chem.* **2017**, *56*, 9609–9616. [CrossRef] [PubMed]

26. Blindauer, C.A.; Emwas, A.H.; Holý, A.; Dvořáková, H.; Sletten, E.; Sigel, H. Complex Formation of the Antiviral 9-[2-(Phosphonomethoxy)Ethyl]Adenine (PMEA) and of Its N 1, N 3, and N 7 Deaza Derivatives with Copper(II) in Aqueous Solution. *Chem. Eur. J.* **1997**, *3*, 1526–1536. [CrossRef]

27. Jacquemmoz, C.; Giraud, F.; Dumez, J.-N. Online reaction monitoring by single-scan 2D NMR under flow conditions. *Analyst* **2020**, *145*, 478–485. [CrossRef] [PubMed]

28. Leverick, G.; Tatara, R.; Feng, S.; Crabb, E.; France-Lanord, A.; Tułodziecki, M.; Lopez, J.; Stephens, R.M.; Grossman, J.C.; Shao-Horn, Y. Solvent- and Anion-Dependent Li+–O2– Coupling Strength and Implications on the Thermodynamics and Kinetics of Li–O2 Batteries. *J. Phys. Chem. C* **2020**, *124*, 4953–4967. [CrossRef]

29. Dias, D.M.; Ciulli, A. NMR approaches in structure-based lead discovery: Recent developments and new frontiers for targeting multi-protein complexes. *Prog. Biophys. Mol. Biol.* **2014**, *116*, 101–112. [CrossRef]

30. Foot, J.N.; Feracci, M.; Dominguez, C. Screening protein–Single stranded RNA complexes by NMR spectroscopy for structure determination. *Methods* **2014**, *65*, 288–301. [CrossRef]

31. Kijewska, M.; Czerwińska, A.; Al-Harthi, S.; Wołczański, G.; Waliczek, M.; Emwas, A.-H.; Jaremko, M.; Jaremko, Ł.; Stefanowicz, P.; Szewczuk, Z. Intramolecularly stapled amphipathic peptides via a boron–sugar interaction. *Chem. Commun.* **2020**, *56*, 8814–8817. [CrossRef]

32. Takeuchi, K.; Baskaran, K.; Arthanari, H. Structure determination using solution NMR: Is it worth the effort? *J. Magn. Reson.* **2019**, *306*, 195–201. [CrossRef] [PubMed]

33. Baldwin, A.J.; Kay, L.E. NMR spectroscopy brings invisible protein states into focus. *Nat. Chem. Biol.* **2009**, *5*, 808–814. [CrossRef] [PubMed]

34. Jhoti, H.; Cleasby, A.; Verdonk, M.; Williams, G. Fragment-based screening using X-ray crystallography and NMR spectroscopy. *Curr. Opin. Chem. Biol.* **2007**, *11*, 485–493. [CrossRef] [PubMed]

35. Emwas, A.-H.M.; Al-Talla, Z.A.; Guo, X.; Al-Ghamdi, S.; Al-Masri, H.T. Utilizing NMR and EPR spectroscopy to probe the role of copper in prion diseases. *Magn. Reson. Chem.* **2013**, *51*, 255–268. [CrossRef]

36. Wyss, D.F.; Wang, Y.-S.; Eaton, H.L.; Strickland, C.; Voigt, J.H.; Zhu, Z.; Stamford, A.W. Combining NMR and X-ray Crystallography in Fragment-Based Drug Discovery: Discovery of Highly Potent and Selective BACE-1 Inhibitors. In *Fragment-Based Drug Discovery and X-Ray Crystallography*; Topics in Current Chemistry; Davies, T.G., Hyvönen, M., Eds.; Springer: Berlin, Germany, 2012; pp. 83–114. ISBN 978-3-642-27540-1.

37. Jack, R.; Sem, D.; Yu, L. Real-time structure-based drug development—Tutorial: Triad's NMR-based structural determinations are smart chemistry. *Genet. Eng. News* **2001**, *21*, 34.

38. Jadeja, Y.; Chomal, B.; Patel, M.; Jebaliya, H.; Khunt, R.; Shah, A. Method development and validation: Quantitation of telmisartan bulk drug and its tablet formulation by 1H-NMR spectroscopy. *Magn. Reson. Chem.* **2017**, *55*, 634–638. [CrossRef]

39. Kozlova, A.S.; Cross, T.A.; Brey, W.W.; Gor'kov, P.L. 31P and 15N Solid-State NMR Study for the Development of a Novel Membrane Protein Drug-Screening Methodology. *Biophys. J.* **2012**, *102*, 390a. [CrossRef]

40. Shimada, I. Functional analyses of target proteins for drug development by NMR. *Proc. J. Pharmacol. Sci.* **2015**, *128*, 54.

41. Soulsby, D. Band-selective excitation NMR spectroscopy and quantitative time-domain analysis using Complete Reduction to Amplitude-Frequency Table (CRAFT) to determine distribution coefficients during drug development. *Magn. Reson. Chem.* **2019**, *57*, 953–960. [CrossRef]

42. Ali, M.; Shaw, D.R.; Zhang, L.; Haroon, M.F.; Narita, Y.; Emwas, A.-H.; Saikaly, P.E.; Okabe, S. Aggregation ability of three phylogenetically distant anammox bacterial species. *Water Res.* **2018**, *143*, 10–18. [CrossRef]

43. Cui, G.; Liew, Y.J.; Li, Y.; Kharbatia, N.; Zahran, N.I.; Emwas, A.-H.; Eguiluz, V.M.; Aranda, M. Host-dependent nitrogen recycling as a mechanism of symbiont control in Aiptasia. *PLoS Genet.* **2019**, *15*, e1008189. [CrossRef] [PubMed]

44. Emwas, A.-H.; Saccenti, E.; Gao, X.; McKay, R.T.; dos Santos, V.A.P.M.; Roy, R.; Wishart, D.S. Recommended strategies for spectral processing and post-processing of 1D 1H-NMR data of biofluids with a particular focus on urine. *Metabolomics* **2018**, *14*, 31. [CrossRef] [PubMed]

45. Hajjar, D.; Kremb, S.; Sioud, S.; Emwas, A.-H.; Voolstra, C.R.; Ravasi, T. Anti-cancer agents in Saudi Arabian herbals revealed by automated high-content imaging. *PLoS ONE* **2017**, *12*. [CrossRef] [PubMed]

46. Iftikhar, S.; Khan, S.; Bilal, A.; Manzoor, S.; Abdullah, M.; Emwas, A.-H.; Sioud, S.; Gao, X.; Chotana, G.A.; Faisal, A.; et al. Synthesis and evaluation of modified chalcone based p53 stabilizing agents. *Bioorg. Med. Chem. Lett.* **2017**, *27*, 4101–4106. [CrossRef] [PubMed]

47. Alqahtani, F.Y.; Aleanizy, F.S.; El Tahir, E.; Alkahtani, H.M.; AlQuadeib, B.T. Chapter Three-Paclitaxel. In *Profiles of Drug Substances, Excipients and Related Methodology*; Brittain, H.G., Ed.; Academic Press: Cambridge, MA, USA, 2019; Volume 44, pp. 205–238. ISBN 978-0-12-817165-3.

48. Dey, R.; Samantaray, M.K.; Poater, A.; Hamieh, A.; Kavitake, S.; Abou-Hamad, E.; Callens, E.; Emwas, A.-H.; Cavallo, L.; Basset, J.-M. Synthesis and characterization of a homogeneous and silica supported homoleptic cationic tungsten(VI) methyl complex: Application in olefin metathesis. *Chem. Commun.* **2016**, *52*, 11270–11273. [CrossRef]

49. Elbaz, A.M.; Gani, A.; Hourani, N.; Emwas, A.-H.; Sarathy, S.M.; Roberts, W.L. TG/DTG, FT-ICR Mass Spectrometry, and NMR Spectroscopy Study of Heavy Fuel Oil. *Energy Fuels* **2015**, *29*, 7825–7835. [CrossRef]

50. Emwas, A.-H.; Roy, R.; McKay, R.T.; Ryan, D.; Brennan, L.; Tenori, L.; Luchinat, C.; Gao, X.; Zeri, A.C.; Gowda, G.A.N.; et al. Recommendations and Standardization of Biomarker Quantification Using NMR-Based Metabolomics with Particular Focus on Urinary Analysis. *J. Proteome Res.* **2016**, *15*, 360–373. [CrossRef]

51. Li, S.; Winters, H.; Jeong, S.; Emwas, A.-H.; Vigneswaran, S.; Amy, G.L. Marine bacterial transparent exopolymer particles (TEP) and TEP precursors: Characterization and RO fouling potential. *Desalination* **2016**, *379*, 68–74. [CrossRef]

52. Fordwour, O.B.; Wolthers, K.R. Active site arginine controls the stereochemistry of hydride transfer in cyclohexanone monooxygenase. *Arch. Biochem. Biophys.* **2018**, *659*, 47–56. [CrossRef]

53. Hamzi, I.; Fray, M.; Abidi, R.; Barhoumi-Slimi, T. Synthesis, characterization and conformational study of new α,β-unsaturated acylhydrazones based on calix [4] arene backbone. *J. Mol. Struct.* **2019**, *1185*, 78–84. [CrossRef]

54. Jeziorowski, S.; Thiele, C.M. Poly-γ-p-Biphenylmethyl-Glutamate as Enantiodifferentiating Alignment Medium for NMR Spectroscopy with Temperature-Tunable Properties. *Chem. Eur. J.* **2018**, *24*, 15631–15637. [CrossRef] [PubMed]

55. Mazzola, E.P.; Deeds, J.R.; Stutts, W.L.; Ridge, C.D.; Dickey, R.W.; White, K.D.; Williamson, R.T.; Martin, G.E. Elucidation and partial NMR assignment of monosulfated maitotoxins from the Caribbean. *Toxicon* **2019**, *164*, 44–50. [CrossRef] [PubMed]

56. Mphahlele, M.J.; Maluleka, M.M.; Mampa, R.M. Elucidation of the Structure of the 2-amino-3,5-Dibromochalcone Epoxides in Solution and Solid State. *Crystals* **2019**, *9*, 277. [CrossRef]

57. Kobyłka, K.; Żuchowski, G.; Tejchman, W.; Zborowski, K.K. Synthesis, spectroscopy, and theoretical calculations of some 2-thiohydantoin derivatives as possible new fungicides. *J. Mol. Model.* **2019**, *25*, 268. [CrossRef]

58. Li, P.; Deng, J.; Xiao, N.; Cai, X.; Wu, Q.; Lu, Z.; Yang, Y.; Du, B. Identification of polyunsaturated triacylglycerols and CC location isomers in sacha inchi oil by photochemical reaction mass spectrometry combined with nuclear magnetic resonance spectroscopy. *Food Chem.* **2020**, *307*, 125568. [CrossRef]

59. Ólafsson, S.N.; Bjornsson, R.; Helgason, Ö.; Jonsdottir, S.; Suman, S.G. Coordination geometry determination of stannane compounds with phosphinoyldithioformate ligands using multinuclear NMR, Sn Mössbauer and DFT methods. *J. Organomet. Chem.* **2016**, *825–826*, 125–138. [CrossRef]

60. Selent, M.; Nyman, J.; Roukala, J.; Ilczyszyn, M.; Oilunkaniemi, R.; Bygrave, P.J.; Laitinen, R.; Jokisaari, J.; Day, G.M.; Lantto, P. Clathrate Structure Determination by Combining Crystal Structure Prediction with Computational and Experimental 129Xe NMR Spectroscopy. *Chem. Eur. J.* **2017**, *23*, 5258–5269. [CrossRef]

61. Şenkardeş, S.; Tatar, E.; Nepravishta, R.; Cela, D.; Paci, M.; Özakpınar, Ö.B.; Şekerler, T.; De Clercq, E.; Pannecouque, C.; Küçükgüzel, Ş.G.; et al. Synthesis and Biological Activity of N-(arylsulfonyl) Valine Hydrazones and Assistance of NMR Spectroscopy for Definitive 3D Structure. *Lett. Drug Des. Discov.* **2019**, *16*, 974–983. [CrossRef]

62. Sousa, F.F.O.; Luzardo-Álvarez, A.; Blanco-Méndez, J.; Otero-Espinar, F.J.; Martín-Pastor, M.; Sández Macho, I. Use of 1H-NMR STD, WaterLOGSY, and Langmuir monolayer techniques for characterization of drug–zein protein complexes. *Eur. J. Pharm. Biopharm.* **2013**, *85*, 790–798. [CrossRef]

63. Meyer, B.; Peters, T. NMR Spectroscopy Techniques for Screening and Identifying Ligand Binding to Protein Receptors. *Angew. Chem. Int. Ed.* **2003**, *42*, 864–890. [CrossRef]

64. Mohanty, S.; Sieker, L.C.; Drobny, G.P. Sequential 1H-NMR Assignment of the Complex of Aponeocarzinostatin with Ethidium Bromide and Investigation of Protein-Drug Interactions in the Chromophore Binding Site. *Biochemistry* **1994**, *33*, 10579–10590. [CrossRef] [PubMed]

65. Chen, C.; Gao, J.; Wang, T.-S.; Guo, C.; Yan, Y.-J.; Mao, C.-Y.; Gu, L.-W.; Yang, Y.; Li, Z.-F.; Liu, A. NMR-based Metabolomic Techniques Identify the Toxicity of Emodin in HepG2 Cells. *Sci. Rep.* **2018**, *8*, 1–10. [CrossRef] [PubMed]

66. Xu, C.; Rezeng, C.; Li, J.; Zhang, L.; Yan, Y.; Gao, J.; Wang, Y.; Li, Z.; Chen, J. 1H-NMR-Based Metabolomics Study of the Toxicological Effects in Rats Induced by "Renqing Mangjue" Pill, a Traditional Tibetan Medicine. *Front. Pharmacol.* **2017**, *8*. [CrossRef] [PubMed]

67. Dallons, M.; Schepkens, C.; Dupuis, A.; Tagliatti, V.; Colet, J.-M. New Insights About Doxorubicin-Induced Toxicity to Cardiomyoblast-Derived H9C2 Cells and Dexrazoxane Cytoprotective Effect: Contribution of In Vitro 1H-NMR Metabonomics. *Front. Pharmacol.* **2020**, *11*. [CrossRef]

68. Zhang, X.; Wu, H.; Liao, P.; Li, X.; Ni, J.; Pei, F. NMR-based metabonomic study on the subacute toxicity of aristolochic acid in rats. *Food Chem. Toxicol.* **2006**, *44*, 1006–1014. [CrossRef]

69. Al-Talla, Z.A.; Akrawi, S.H.; Emwas, A.-H.M. Solid state NMR and bioequivalence comparison of the pharmacokinetic parameters of two formulations of clindamycin. *Int. J. Clin. Pharmacol. Ther.* **2011**, *49*, 469–476. [CrossRef]

70. Cai, H.; Wang, Y.; McCarthy, D.; Wen, H.; Borchelt, D.R.; Price, D.L.; Wong, P.C. BACE1 is the major β-secretase for generation of Aβ peptides by neurons. *Nat. Neurosci.* **2001**, *4*, 233–234. [CrossRef]

71. Huang, C.; Rossi, P.; Saio, T.; Kalodimos, C.G. Structural basis for the antifolding activity of a molecular chaperone. *Nature* **2016**, *537*, 202–206. [CrossRef]

72. Ziarek, J.J.; Peterson, F.C.; Lytle, B.L.; Volkman, B.F. Chapter ten—Binding Site Identification and Structure Determination of Protein–Ligand Complexes by NMR: A Semiautomated Approach. In *Methods in Enzymology*; Fragment-Based Drug Design; Kuo, L.C., Ed.; Academic Press: San Diego, CA, USA, 2011; Volume 493, pp. 241–275. ISBN 978-0-12-381274-2.

73. Keiffer, S.; Carneiro, M.G.; Hollander, J.; Kobayashi, M.; Pogoryelev, D.; AB, E.; Theisgen, S.; Müller, G.; Siegal, G. NMR in target driven drug discovery: Why not? *J. Biomol. NMR* **2020**. [CrossRef]

74. Marshall, C.B.; KleinJan, F.; Gebregiworgis, T.; Lee, K.-Y.; Fang, Z.; Eves, B.J.; Liu, N.F.; Gasmi-Seabrook, G.M.C.; Enomoto, M.; Ikura, M. NMR in integrated biophysical drug discovery for RAS: Past, present, and future. *J. Biomol. NMR* **2020**. [CrossRef]

75. Norton, R.S.; Jahnke, W. NMR in pharmaceutical discovery and development. *J. Biomol. NMR* **2020**. [CrossRef] [PubMed]

76. Cady, E.B. *Clinical Magnetic Resonance Spectroscopy*; Springer: New York, NY, USA, 1990; ISBN 978-0-306-43449-5.

77. Farrar, T.C. Principles of Pulse NMR Spectroscopy. In *NMR: Principles and Applications to Biomedical Research*; Pettegrew, J.W., Ed.; Springer: New York, NY, USA, 1990; pp. 1–36. ISBN 978-1-4612-3300-8.

78. Levitt, M.H. *Spin Dynamics: Basics of Nuclear Magnetic Resonance*; John Wiley & Sons: Hoboken, NJ, USA, 2013; ISBN 978-1-118-68184-8.

79. Jacobsen, N.E. *NMR Spectroscopy Explained: Simplified Theory, Applications and Examples for Organic Chemistry and Structural Biology*; John Wiley & Sons: Hoboken, NJ, USA, 2007; ISBN 0-470-17334-3.

80. Chu, S.; Maltsev, S.; Emwas, A.-H.; Lorigan, G.A. Solid-state NMR paramagnetic relaxation enhancement immersion depth studies in phospholipid bilayers. *J. Magn. Reson.* **2010**, *207*, 89–94. [CrossRef] [PubMed]

81. Ishima, R.; Torchia, D.A. Protein dynamics from NMR. *Nat. Struct. Biol.* **2000**, *7*, 740–743. [CrossRef] [PubMed]

82. Kleckner, I.R.; Foster, M.P. An introduction to NMR-based approaches for measuring protein dynamics. *Biochim. Biophys. Acta* **2011**, *1814*, 942–968. [CrossRef] [PubMed]

83. Alsiary, R.A.; Alghrably, M.; Saoudi, A.; Al-Ghamdi, S.; Jaremko, L.; Jaremko, M.; Emwas, A.-H. Using NMR spectroscopy to investigate the role played by copper in prion diseases. *Neurol. Sci. Off. J. Ital. Neurol. Soc. Ital. Soc. Clin. Neurophysiol.* **2020**, *41*, 2389–2406. [CrossRef]

84. Taraban, M.B.; Deredge, D.J.; Smith, M.E.; Briggs, K.T.; Li, Y.; Jiang, Z.-X.; Wintrode, P.L.; Yu, Y.B. Monitoring dendrimer conformational transition using 19F and 1H2O NMR. *Magn. Reson. Chem.* **2019**, *57*, 861–872. [CrossRef]

85. Kumar Patel, A.; Kumar Mishra, S.; Krishnamurthy, K.; Suryaprakash, N. Retention of strong intramolecular hydrogen bonds in high polarity solvents in binaphthalene–benzamide derivatives: Extensive NMR studies. *RSC Adv.* **2019**, *9*, 32759–32770. [CrossRef]

86. Feng, X.; Xu, H.; Chen, J.-F.; Ruan, L.-Y.; Zhao, W.-L.; Meng, H.-H.; Liu, W.-Y.; Zhao, W.-L.; Zheng, Q.; Liu, Z.-C.; et al. Potential hepatoxicity risk of the shell of Herpetospermum caudigerum Wall in rats based on 1H-NMR metabonomics. *J. Pharm. Biomed. Anal.* **2019**, *176*, 112800. [CrossRef]

87. Liu, X.; Zhu, W.; Guan, S.; Feng, R.; Zhang, H.; Liu, Q.; Sun, P.; Lin, D.; Zhang, N.; Shen, J. Metabolomic Analysis of Anti-Hypoxia and Anti-anxiety Effects of Fu Fang Jin Jing Oral Liquid. *PLoS ONE* **2013**, *8*. [CrossRef]

88. Zhang, Z.-Z.; Fan, M.-L.; Hao, X.; Qin, X.-M.; Li, Z.-Y. Integrative drug efficacy assessment of Danggui and European Danggui using NMR-based metabolomics. *J. Pharm. Biomed. Anal.* **2016**, *120*, 1–9. [CrossRef]

89. Gimeno, A.; Reichardt, N.-C.; Cañada, F.J.; Perkams, L.; Unverzagt, C.; Jiménez-Barbero, J.; Ardá, A. NMR and Molecular Recognition of N-Glycans: Remote Modifications of the Saccharide Chain Modulate Binding Features. *ACS Chem. Biol.* **2017**, *12*, 1104–1112. [CrossRef] [PubMed]

90. Palivec, V.; Bour, P.; Jungwirth, P.; Kaminsky, J.; Martinez-Seara, H. Obtaining 3D Atomistic Structure of Saccharides from Raman/ROA/NMR Spectroscopic Techniques. *Biophys. J.* **2020**, *118*, 298a. [CrossRef]

91. Emwas, A.-H.; Roy, R.; McKay, R.T.; Tenori, L.; Saccenti, E.; Gowda, G.A.N.; Raftery, D.; Alahmari, F.; Jaremko, L.; Jaremko, M.; et al. NMR Spectroscopy for Metabolomics Research. *Metabolites* **2019**, *9*, 123. [CrossRef] [PubMed]

92. Emwas, A.-H.M. The Strengths and Weaknesses of NMR Spectroscopy and Mass Spectrometry with Particular Focus on Metabolomics Research. In *Metabonomics: Methods and Protocols*; Methods in Molecular Biology; Bjerrum, J.T., Ed.; Humana Press: New York, NY, USA, 2015; Volume 1277, pp. 161–193. ISBN 978-1-4939-2377-9.

93. Krafcikova, M.; Dzatko, S.; Caron, C.; Granzhan, A.; Fiala, R.; Loja, T.; Teulade-Fichou, M.-P.; Fessl, T.; Hänsel-Hertsch, R.; Mergny, J.-L.; et al. Monitoring DNA–Ligand Interactions in Living Human Cells Using NMR Spectroscopy. *J. Am. Chem. Soc.* **2019**, *141*, 13281–13285. [CrossRef]

94. Overall, S.A.; Zhu, S.; Hanssen, E.; Separovic, F.; Sani, M.-A. In Situ Monitoring of Bacteria under Antimicrobial Stress Using 31P Solid-State NMR. *Int. J. Mol. Sci.* **2019**, *20*, 181. [CrossRef]

95. Kay, L.E. NMR studies of protein structure and dynamics. *J. Magn. Reson.* **2011**, *213*, 477–491. [CrossRef]

96. Shockcor, J.P.; Unger, S.E.; Wilson, I.D.; Foxall, P.J.D.; Nicholson, J.K.; Lindon, J.C. Combined HPLC, NMR Spectroscopy, and Ion-Trap Mass Spectrometry with Application to the Detection and Characterization of Xenobiotic and Endogenous Metabolites in Human Urine. *Anal. Chem.* **1996**, *68*, 4431–4435. [CrossRef]

97. Al-Talla, Z.A.; Akrawi, S.H.; Tolley, L.T.; Sioud, S.H.; Zaater, M.F.; Emwas, A.-H.M. Bioequivalence assessment of two formulations of ibuprofen. *Drug Des. Devel. Ther.* **2011**, *5*, 427–433. [CrossRef]

98. Corcoran, O.; Spraul, M. LC–NMR–MS in drug discovery. *Drug Discov. Today* **2003**, *8*, 624–631. [CrossRef]

99. Tardivel, P.J.C.; Canlet, C.; Lefort, G.; Tremblay-Franco, M.; Debrauwer, L.; Concordet, D.; Servien, R. ASICS: An automatic method for identification and quantification of metabolites in complex 1D 1H-NMR spectra. *Metabolomics* **2017**, *13*, 109. [CrossRef]

100. Cui, Q.; Lewis, I.A.; Hegeman, A.D.; Anderson, M.E.; Li, J.; Schulte, C.F.; Westler, W.M.; Eghbalnia, H.R.; Sussman, M.R.; Markley, J.L. Metabolite identification via the Madison Metabolomics Consortium Database. *Nat. Biotechnol.* **2008**, *26*, 162–164. [CrossRef] [PubMed]

101. Cañueto, D.; Gómez, J.; Salek, R.M.; Correig, X.; Cañellas, N. rDolphin: A GUI R package for proficient automatic profiling of 1D 1H-NMR spectra of study datasets. *Metabolomics* **2018**, *14*, 24. [CrossRef] [PubMed]

102. Lewis, I.A.; Schommer, S.C.; Markley, J.L. rNMR: Open source software for identifying and quantifying metabolites in NMR spectra. *Magn. Reson. Chem.* **2009**, *47*, S123–S126. [CrossRef] [PubMed]

103. Cavanagh, J.; Fairbrother, W.J.; Palmer, A.G.; Rance, M.; Skelton, N.J. Chapter 3—experimental aspects of NMR spectroscopy. In *Protein NMR Spectroscopy. Principles and Practice*, 2nd ed.; Cavanagh, J., Fairbrother, W.J., Palmer, A.G., Rance, M., Skelton, N.J., Eds.; Academic Press: Burlington, MA, USA, 2007; pp. 114–270. ISBN 978-0-12-164491-8.

104. Rule, G.S.; Hitchens, T.K. (Eds.) Practical Aspects of N-Dimensional Data Acquisition and Processing. In *Fundamentals of Protein NMR Spectroscopy*; Focus on Structural Biology; Springer: Dordrecht, The Netherlands, 2006; pp. 313–351. ISBN 978-1-4020-3500-5.

105. Tsang-Lin, H.; Shaka, A.J. Water suppression that works. Excitation sculpting using arbitrary waveforms and pulsed field gradients. *Water Suppr. Works Excit. Sculpt. Using Arbitr. Waveforms Pulsed Field Gradients* **1995**, *112*, 275–279.

106. Callihan, D.; West, J.; Kumar, S.; Schweitzer, B.I.; Logan, T.M. Simple, Distortion-Free Homonuclear Spectra of Peptides and Nucleic Acids in Water Using Excitation Sculpting. *J. Magn. Reson. B* **1996**, *1*, 82–85. [CrossRef] [PubMed]

107. Hwang, T.L.; Shaka, A.J. Water Suppression That Works. Excitation Sculpting Using Arbitrary Wave-Forms and Pulsed-Field Gradients. *J. Magn. Reson. A* **1995**, *112*, 275–279. [CrossRef]

108. Piotto, M.; Saudek, V.; Sklenár, V. Gradient-tailored excitation for single-quantum NMR spectroscopy of aqueous solutions. *J. Biomol. NMR* **1992**, *2*, 661–665. [CrossRef] [PubMed]

109. Zheng, G.; Price, W.S. Solvent signal suppression in NMR. *Prog. Nucl. Magn. Reson. Spectrosc.* **2010**, 267–288. [CrossRef]

110. Levitt, M.H. Experiments on AX systems. In *Spin Dynamics: Basics of Nuclear Magnetic Resonance*; John Wiley & Son: Hoboken, NJ, USA, 2008; pp. 409–452. ISBN 978-0-470-51117-6.

111. Doddrell, D.M.; Pegg, D.T.; Bendall, M.R. Distortionless enhancement of NMR signals by polarization transfer. *J. Magn. Reson. 1969* **1982**, *48*, 323–327. [CrossRef]

112. Tsujimoto, T.; Yoshitomi, T.; Maruyama, T.; Yamamoto, Y.; Hakamatsuka, T.; Uchiyama, N. 13C-NMR-based metabolic fingerprinting of Citrus-type crude drugs. *J. Pharm. Biomed. Anal.* **2018**, *161*, 305–312. [CrossRef]

113. Ye, T.; Mo, H.; Shanaiah, N.; Gowda, G.A.N.; Zhang, S.; Raftery, D. Chemoselective 15N Tag for Sensitive and High-Resolution Nuclear Magnetic Resonance Profiling of the Carboxyl-Containing Metabolome. *Anal. Chem.* **2009**, *81*, 4882–4888. [CrossRef] [PubMed]

114. Tayyari, F.; Gowda, G.A.N.; Gu, H.; Raftery, D. 15N-Cholamine—A Smart Isotope Tag for Combining NMR- and MS-Based Metabolite Profiling. *Anal. Chem.* **2013**, *85*, 8715–8721. [CrossRef] [PubMed]

115. Luo, J.; Zeng, Q.; Wu, K.; Lin, Y. Fast reconstruction of non-uniform sampling multidimensional NMR spectroscopy via a deep neural network. *J. Magn. Reson.* **2020**, *317*, 106772. [CrossRef]

116. Rossi, P.; Xia, Y.; Khanra, N.; Veglia, G.; Kalodimos, C.G. 15N and 13C-SOFAST-HMQC editing enhances 3D-NOESY sensitivity in highly deuterated, selectively [1H,13C]-labeled proteins. *J. Biomol. NMR* **2016**, *66*, 259–271. [CrossRef]

117. Emwas, A.-H.; Alghrably, M.; Al-Harthi, S.; Poulson, B.; Szczepski, K.; Chandra, K.; Jaremko, M. Chapter 5—New Advances in Fast Methods of 2D NMR Experiments. In *Nuclear Magnetic Resonance*; Khaneja, N., Ed.; IntechOpen: London, UK, 2019; pp. 83–106. ISBN 978-1-83880-420-6.

118. Kovtunov, K.V.; Kovtunova, L.M.; Gemeinhardt, M.E.; Bukhtiyarov, A.V.; Gesiorski, J.; Bukhtiyarov, V.I.; Chekmenev, E.Y.; Koptyug, I.V.; Goodson, B.M. Heterogeneous Microtesla SABRE Enhancement of 15N NMR Signals. *Angew. Chem. Int. Ed.* **2017**, *56*, 10433–10437. [CrossRef]

119. Kaplan, O.; van Zijl, P.C.M.; Cohen, J.S. Information from combined 1H and 31P NMR studies of cell extracts: Differences in metabolism between drug-sensitive and drug-resistant MCF-7 human breast cancer cells. *Biochem. Biophys. Res. Commun.* **1990**, *169*, 383–390. [CrossRef]

120. Nunnally, R.L.; Bottomley, P.A. Assessment of pharmacological treatment of myocardial infarction by phosphorus-31 NMR with surface coils. *Science* **1981**, *211*, 177–180. [CrossRef] [PubMed]

121. DeSilva, M.A.; Shanaiah, N.; Gowda, G.A.N.; Rosa-Pérez, K.; Hanson, B.A.; Raftery, D. Application of 31P NMR spectroscopy and chemical derivatization for metabolite profiling of lipophilic compounds in human serum. *Magn. Reson. Chem.* **2009**, *47*, S74–S80. [CrossRef] [PubMed]

122. Carvalho, J.; Alves, S.; Castro, M.M.C.A.; Geraldes, C.F.G.C.; Queiroz, J.A.; Fonseca, C.P.; Cruz, C. Development of a bioreactor system for cytotoxic evaluation of pharmacological compounds in living cells using NMR spectroscopy. *J. Pharmacol. Toxicol. Methods* **2019**, *95*, 70–78. [CrossRef] [PubMed]

123. Findeisen, M.; Berger, S. The organic set of NMR spectra. In *50 and More Essential NMR Experiments: A Detailed Guide*; Wiley-VCH: Weinheim, Germany, 2013; pp. 11–16. ISBN 978-3-527-33694-4.

124. Jeener, J.; Alewaeters, G. Pulse pair technique in high resolution NMR a reprint of the historical 1971 lecture notes on two-dimensional spectroscopy. *Prog. Nucl. Magn. Reson. Spectrosc.* **2016**, *94–95*, 75–80. [CrossRef]

125. Reynolds, W.F.; Enríquez, R.G. Choosing the Best Pulse Sequences, Acquisition Parameters, Postacquisition Processing Strategies, and Probes for Natural Product Structure Elucidation by NMR Spectroscopy. *J. Nat. Prod.* **2002**, *65*, 221–244. [CrossRef] [PubMed]

126. Lewis, P.; Kaltia, S.; Wähälä, K. The phase transfer catalysed synthesis of isoflavone-O-glucosides. *J. Chem. Soc. Perkin 1* **1998**, 2481–2484. [CrossRef]

127. Fontaine, X.L.R.; Kennedy, J.D.; Shaw, B.L.; Vila, J.M. Determination of the relative signs of 2J(31P–31P) in complexes of tungsten(0) and molybdenum(0) using two-dimensional [31P–31P]-COSY-45 nuclear magnetic resonance chemical shift correlation. *J. Chem. Soc. Dalton Trans.* **1987**, 2401–2405. [CrossRef]

128. Keeler, J. Two dimentional NMR. In *Understanding NMR Spectroscopy*; John Wiley & Sons: Hoboken, NJ, USA, 2011; pp. 139–162. ISBN 978-1-119-96493-3.

129. Bingol, K.; Brüschweiler, R. Knowns and unknowns in metabolomics identified by multidimensional NMR and hybrid MS/NMR methods. *Curr. Opin. Biotechnol.* **2017**, *43*, 17–24. [CrossRef] [PubMed]

130. Kingsley, P.B. Product operators, coherence pathways, and phase cycling. Part III: Phase cycling. *Concepts Magn. Reson.* **1995**, *7*, 167–192. [CrossRef]

131. Bain, A.D.; Burton, I.W.; Reynolds, W.F. Artifacts in two-dimensional NMR. *Prog. Nucl. Magn. Reson. Spectrosc.* **1994**, *26*, 59–89. [CrossRef]

132. Claridge, T.D.W. Chapter 6-Correlations through the Chemical Bond I: Homonuclear Shift Correlation. In *High-Resolution NMR Techniques in Organic Chemistry*, 3rd ed.; Claridge, T.D.W., Ed.; Elsevier: Amsterdam, The Netherlands, 2016; pp. 203–241. ISBN 978-0-08-099986-9.

133. Coote, P.; Bermel, W.; Wagner, G.; Arthanari, H. Analytical optimization of active bandwidth and quality factor for TOCSY experiments in NMR spectroscopy. *J. Biomol. NMR* **2016**, *66*, 9–20. [CrossRef] [PubMed]

134. MacKinnon, N.; While, P.T.; Korvink, J.G. Novel selective TOCSY method enables NMR spectral elucidation of metabolomic mixtures. *J. Magn. Reson.* **2016**, *272*, 147–157. [CrossRef]

135. Thrippleton, M.J.; Keeler, J. Elimination of Zero-Quantum Interference in Two-Dimensional NMR Spectra. *Angew. Chem. Int. Ed.* **2003**, *42*, 3938–3941. [CrossRef]

136. Li, Z.-Y.; Ding, L.-L.; Li, J.-M.; Xu, B.-L.; Yang, L.; Bi, K.-S.; Wang, Z.-T. 1H-NMR and MS Based Metabolomics Study of the Intervention Effect of Curcumin on Hyperlipidemia Mice Induced by High-Fat Diet. *PLoS ONE* **2015**, *10*. [CrossRef]

137. Jiang, L.; Lee, S.C.; Ng, T.C. Pharmacometabonomics Analysis Reveals Serum Formate and Acetate Potentially Associated with Varying Response to Gemcitabine-Carboplatin Chemotherapy in Metastatic Breast Cancer Patients. *J. Proteome Res.* **2018**, *17*, 1248–1257. [CrossRef] [PubMed]

138. Vermathen, M.; Paul, L.E.H.; Diserens, G.; Vermathen, P.; Furrer, J. 1H HR-MAS NMR Based Metabolic Profiling of Cells in Response to Treatment with a Hexacationic Ruthenium Metallaprism as Potential Anticancer Drug. *PLoS ONE* **2015**, *10*. [CrossRef] [PubMed]

139. Powder-George, Y.; Frank, J.; Ramsewak, R.S.; Reynolds, W.F. The Use of Coupled HSQC Spectra to Aid in Stereochemical Assignments of Molecules with Severe Proton Spectral Overlap. *Phytochem. Anal.* **2012**, *23*, 274–277. [CrossRef] [PubMed]

140. Parkinson, J.A. Chapter 2—NMR Spectroscopy Methods in Metabolic Phenotyping. In *The Handbook of Metabolic Phenotyping*; Lindon, J.C., Nicholson, J.K., Holmes, E., Eds.; Elsevier: Amsterdam, The Netherlands, 2019; pp. 53–96. ISBN 978-0-12-812293-8.

141. Claridge, T.D.W. *High-Resolution NMR Techniques in Organic Chemistry*; Elsevier: Cambridge, MA, USA, 2016; ISBN 978-0-08-099993-7.

142. Hu, H.; Krishnamurthy, K. Doubly compensated multiplicity-edited HSQC experiments utilizing broadband inversion pulses. *Magn. Reson. Chem.* **2008**, *46*, 683–689. [CrossRef]

143. Szakács, Z.; Sánta, Z. Chapter 7-NMR Methodological Overview. In *Anthropic Awareness*; Szántay, C., Ed.; Elsevier: Amsterdam, The Netherlands, 2015; pp. 257–289. ISBN 978-0-12-419963-7.

144. Norwood, T.J. Product Operator Formalism in NMR. In *Encyclopedia of Spectroscopy and Spectrometry*; Lindon, J.C., Ed.; Academic Press: Oxford, UK, 1999; pp. 1875–1884. ISBN 978-0-12-226680-5.

145. De Castro, F.; Benedetti, M.; Antonaci, G.; Del Coco, L.; De Pascali, S.A.; Muscella, A.; Marsigliante, S.; Fanizzi, F.P. Response of Cisplatin Resistant Skov-3 Cells to [Pt(O,O′-Acac)(γ-Acac)(DMS)] Treatment Revealed by a Metabolomic 1H-NMR Study. *Molecules* **2018**, *23*, 2301. [CrossRef]

146. Mandal, P.K.; Majumdar, A. A comprehensive discussion of HSQC and HMQC pulse sequences. *Concepts Magn. Reson. Part A* **2004**, *20A*, 1–23. [CrossRef]

147. Caytan, E.; Ligny, R.; Carpentier, J.-F.; Guillaume, S.M. Evaluation of Band-Selective HSQC and HMBC: Methodological Validation on the Cyclosporin Cyclic Peptide and Application for Poly(3-hydroxyalkanoate)s Stereoregularity Determination. *Polymers* **2018**, *10*, 533. [CrossRef]

148. Airoldi, C.; Merlo, S.; Sironi, E. Chapter 4—NMR Molecular Recognition Studies for the Elucidation of Protein and Nucleic Acid Structure and Function. In *Applications of NMR Spectroscopy*; ur-Rahman, A., Choudhary, M.I., Eds.; Elsevier: Amsterdam, The Netherlands, 2015; pp. 147–219. ISBN 978-1-60805-999-7.

149. Xia, J.; Bjorndahl, T.C.; Tang, P.; Wishart, D.S. MetaboMiner–semi-automated identification of metabolites from 2D NMR spectra of complex biofluids. *BMC Bioinform.* **2008**, *9*, 507. [CrossRef]

150. Hansen, D.F.; Vallurupalli, P.; Kay, L.E. An Improved 15N Relaxation Dispersion Experiment for the Measurement of Millisecond Time-Scale Dynamics in Proteins. *J. Phys. Chem. B* **2008**, *112*, 5898–5904. [CrossRef]

151. Mulder, F.A.A.; Spronk, C.A.E.M.; Slijper, M.; Kaptein, R.; Boelens, R. Improved HSQC experiments for the observation of exchange broadened signals. *J. Biomol. NMR* **1996**, *8*, 223–228. [CrossRef]

152. Wallmeier, J.; Samol, C.; Ellmann, L.; Zacharias, H.U.; Vogl, F.C.; Garcia, M.; Dettmer, K.; Oefner, P.J.; Gronwald, W. Quantification of Metabolites by NMR Spectroscopy in the Presence of Protein. *J. Proteome Res.* **2017**, *16*, 1784–1796. [CrossRef] [PubMed]

153. Cavanagh, J.; Fairbrother, W.J.; Palmer, A.G.; Rance, M.; Skelton, N.J. Chapter 5—relaxation and dynamic processes. In *Protein NMR Spectroscopy. Principles and Practice*, 2nd ed.; Cavanagh, J., Fairbrother, W.J., Palmer, A.G., Rance, M., Skelton, N.J., Eds.; Academic Press: Burlington, MA, USA, 2007; pp. 333–404. ISBN 978-0-12-164491-8.

154. Teng, Q. Basic Principles of NMR. In *Structural Biology: Practical NMR Applications*; Springer: New York, NY, USA, 2013; pp. 1–65. ISBN 978-1-4614-3963-9.

155. Macomber, R.S. *A Complete Introduction to Modern Nmr Spectroscopy*; John Wiley & Sons: New York, NY, USA, 1998; ISBN 0-471-15736-8.

156. Pellecchia, M.; Sem, D.S.; Wüthrich, K. NMR in drug discovery. *Nat. Rev. Drug Discov.* **2002**, *1*, 211–219. [CrossRef] [PubMed]

157. Liu, M.; Nicholson, J.K.; Lindon, J.C. High-Resolution Diffusion and Relaxation Edited One- and Two-Dimensional 1H-NMR Spectroscopy of Biological Fluids. *Anal. Chem.* **1996**, *68*, 3370–3376. [CrossRef] [PubMed]

158. Vold, R.L.; Waugh, J.S.; Klein, M.P.; Phelps, D.E. Measurement of Spin Relaxation in Complex Systems. *J. Chem. Phys.* **1968**, *48*, 3831–3832. [CrossRef]

159. Balci, M. 15—Multiple-Pulse NMR Experiments. In *Basic 1H- and 13C-NMR Spectroscopy*; Balci, M., Ed.; Elsevier Science: Amsterdam, The Netherlands, 2005; pp. 339–375. ISBN 978-0-444-51811-8.

160. Smith, P.E.S.; Donovan, K.J.; Szekely, O.; Baias, M.; Frydman, L. Ultrafast NMR T1 Relaxation Measurements: Probing Molecular Properties in Real Time. *Chem. Phys. Chem.* **2013**, *14*, 3138–3145. [CrossRef] [PubMed]

161. Wang, H.; Zhao, M.; Ackerman, J.L.; Song, Y. Saturation-inversion-recovery: A method for T1 measurement. *J. Magn. Reson.* **2017**, *274*, 137–143. [CrossRef]

162. Günther, H. Chapter 8—The Physical Basis of the Nuclear Magnetic Resonance Experiment. Part II: Pulse and Fourier-Transform NMR. In *NMR Spectroscopy: Basic Principles, Concepts and Applications in Chemistry*; Wiley-VCH: Weinheim, Germany, 2013; pp. 233–280. ISBN 978-3-527-67477-0.

163. Figueroa-Villar, J.D.; Tinoco, L.W. Spin-Lattice Relaxation Time in Drug Discovery and Design. *Curr. Top. Med. Chem.* **2009**, *9*, 811–823. [CrossRef]

164. Maity, S.; Gundampati, R.K.; Suresh Kumar, T.K. NMR Methods to Characterize Protein-Ligand Interactions. *Nat. Prod. Commun.* **2019**, *14*. [CrossRef]

165. Casu, M.; Puligheddu, S.; Saba, G.; Marincola, F.C.; Orellana, G.; Lai, A. The Interaction of DNA with Intercalating Agents Probed by Sodium-23 NMR Relaxation Rates. *J. Biomol. Struct. Dyn.* **1997**, *15*, 37–43. [CrossRef]

166. Stockman, B.J.; Dalvit, C. NMR screening techniques in drug discovery and drug design. *Prog. Nucl. Magn. Reson. Spectrosc.* **2002**, *41*, 187–231. [CrossRef]

167. Hajduk, P.J.; Olejniczak, E.T.; Fesik, S.W. One-Dimensional Relaxation- and Diffusion-Edited NMR Methods for Screening Compounds That Bind to Macromolecules. *J. Am. Chem. Soc.* **1997**, *119*, 12257–12261. [CrossRef]

168. Tang, H.; Wang, Y.; Nicholson, J.K.; Lindon, J.C. Use of relaxation-edited one-dimensional and two dimensional nuclear magnetic resonance spectroscopy to improve detection of small metabolites in blood plasma. *Anal. Biochem.* **2004**, *325*, 260–272. [CrossRef]

169. Jaremko, Ł.; Jaremko, M.; Nowakowski, M.; Ejchart, A. The Quest for Simplicity: Remarks on the Free-Approach Models. *J. Phys. Chem. B* **2015**, *119*, 11978–11987. [CrossRef] [PubMed]

170. Jaremko, Ł.; Jaremko, M.; Ejchart, A.; Nowakowski, M. Fast evaluation of protein dynamics from deficient 15N relaxation data. *J. Biomol. NMR* **2018**, *70*, 219–228. [CrossRef] [PubMed]

171. Carr, H.Y.; Purcell, E.M. Effects of Diffusion on Free Precession in Nuclear Magnetic Resonance Experiments. *Phys. Rev.* **1954**, *94*, 630–638. [CrossRef]

172. Meiboom, S.; Gill, D. Modified Spin-Echo Method for Measuring Nuclear Relaxation Times. *Rev. Sci. Instrum.* **1958**, *29*, 688–691. [CrossRef]

173. Kowalewski, J.; Maler, L. Measuring T1 and T2 Relaxation Rates. In *Nuclear Spin Relaxation in Liquids: Theory, Experiments, and Applications*, 2nd ed.; CRC Press: Boca Raton, FL, USA, 2017; pp. 139–152. ISBN 978-1-351-26459-4.

174. Baldwin, A.J. An exact solution for R2, eff in CPMG experiments in the case of two site chemical exchange. *J. Magn. Reson.* **2014**, *244*, 114–124. [CrossRef]

175. Hajduk, P.J.; Meadows, R.P.; Fesik, S.W. NMR-based screening in drug discovery. *Q. Rev. Biophys.* **1999**, *32*, 211–240. [CrossRef]

176. Mladenov, G.; Dimitrov, V.S. Extraction of T2 from NMR linewidths in simple spin systems by use of reference deconvolution. *Magn. Reson. Chem.* **2001**, *39*, 672–680. [CrossRef]

177. Ghosh, S.; Sengupta, A.; Chandra, K. Quantitative metabolic profiling of NMR spectral signatures of branched chain amino acids in blood serum. *Amino Acids* **2015**, *47*, 2229–2236. [CrossRef]

178. Ruan, L.-Y.; Fan, J.-T.; Hong, W.; Zhao, H.; Li, M.-H.; Jiang, L.; Fu, Y.-H.; Xing, Y.-X.; Chen, C.; Wang, J.-S. Isoniazid-induced hepatotoxicity and neurotoxicity in rats investigated by 1H-NMR based metabolomics approach. *Toxicol. Lett.* **2018**, *295*, 256–269. [CrossRef] [PubMed]

179. Jung, J.; Park, M.; Park, H.J.; Shim, S.B.; Cho, Y.H.; Kim, J.; Lee, H.-S.; Ryu, D.H.; Choi, D.; Hwang, G.-S. 1H-NMR-based metabolic profiling of naproxen-induced toxicity in rats. *Toxicol. Lett.* **2011**, *200*, 1–7. [CrossRef] [PubMed]

180. Ryu, S.H.; Lee, J.D.; Kim, J.W.; Kim, S.; Kim, S.; Kim, K.-B. 1H-NMR toxicometabolomics following cisplatin-induced nephrotoxicity in male rats. *J. Toxicol. Sci.* **2019**, *44*, 57–71. [CrossRef] [PubMed]

181. Li, Y.; Man, S.; Li, J.; Chai, H.; Fan, W.; Liu, Z.; Gao, W. The antitumor effect of formosanin C on HepG2 cell as revealed by 1H-NMR based metabolic profiling. *Chem. Biol. Interact.* **2014**, *220*, 193–199. [CrossRef]

182. Sun, Y.-J.; Wang, H.-P.; Liang, Y.-J.; Yang, L.; Li, W.; Wu, Y.-J. An NMR-based metabonomic investigation of the subacute effects of melamine in rats. *J. Proteome Res.* **2012**, *11*, 2544–2550. [CrossRef]

183. Sweeney, S.R.; Kavanaugh, A.; Lodi, A.; Wang, B.; Boyle, D.; Tiziani, S.; Guma, M. Metabolomic profiling predicts outcome of rituximab therapy in rheumatoid arthritis. *RMD Open* **2016**, *2*, e000289. [CrossRef]

184. Al Zweiri, M.; Sills, G.J.; Leach, J.P.; Brodie, M.J.; Robertson, C.; Watson, D.G.; Parkinson, J.A. Response to drug treatment in newly diagnosed epilepsy: A pilot study of 1H-NMR- and MS-based metabonomic analysis. *Epilepsy Res.* **2010**, *88*, 189–195. [CrossRef]

185. Maulidiani; Abas, F.; Khatib, A.; Perumal, V.; Suppaiah, V.; Ismail, A.; Hamid, M.; Shaari, K.; Lajis, N.H. Metabolic alteration in obese diabetes rats upon treatment with Centella asiatica extract. *J. Ethnopharmacol.* **2016**, *180*, 60–69. [CrossRef]

186. Raj, V.; Bhadauria, A.S.; Singh, A.K.; Kumar, U.; Rai, A.; Keshari, A.K.; Kumar, P.; Kumar, D.; Maity, B.; Nath, S.; et al. Novel 1,3,4-thiadiazoles inhibit colorectal cancer via blockade of IL-6/COX-2 mediated JAK2/STAT3 signals as evidenced through data-based mathematical modeling. *Cytokine* **2019**, *118*, 144–159. [CrossRef]

187. Liu, C.-C.; Wu, Y.-F.; Feng, G.-M.; Gao, X.-X.; Zhou, Y.-Z.; Hou, W.-J.; Qin, X.-M.; Du, G.-H.; Tian, J.-S. Plasma-metabolite-biomarkers for the therapeutic response in depressed patients by the traditional Chinese medicine formula Xiaoyaosan: A 1H-NMR-based metabolomics approach. *J. Affect. Disord.* **2015**, *185*, 156–163. [CrossRef]

188. Tan, G.; Liao, W.; Dong, X.; Yang, G.; Zhu, Z.; Li, W.; Chai, Y.; Lou, Z. Metabonomic Profiles Delineate the Effect of Traditional Chinese Medicine Sini Decoction on Myocardial Infarction in Rats. *PLoS ONE* **2012**, *7*. [CrossRef] [PubMed]

189. Mason, S.; Reinecke, C.J.; Solomons, R.; Wevers, R.A.; Engelke, U.F.H. 1H-NMR spectral identification of medication in cerebrospinal fluid of pediatric meningitis. *J. Pharm. Biomed. Anal.* **2017**, *143*, 56–61. [CrossRef] [PubMed]

190. Tian, J.-S.; Zhao, L.; Shen, X.-L.; Liu, H.; Qin, X.-M. 1H-NMR-based metabolomics approach to investigating the renal protective effects of Genipin in diabetic rats. *Chin. J. Nat. Med.* **2018**, *16*, 261–270. [CrossRef]

191. Kim, K.-B.; Yang, J.-Y.; Kwack, S.J.; Kim, H.S.; Ryu, D.H.; Kim, Y.-J.; Bae, J.Y.; Lim, D.S.; Choi, S.M.; Kwon, M.J.; et al. Potential metabolomic biomarkers for evaluation of adriamycin efficacy using a urinary 1H-NMR spectroscopy. *J. Appl. Toxicol.* **2013**, *33*, 1251–1259. [CrossRef] [PubMed]

192. Rawat, A.; Dubey, D.; Guleria, A.; Kumar, U.; Keshari, A.K.; Chaturvedi, S.; Prakash, A.; Saha, S.; Kumar, D. 1H-NMR-based serum metabolomics reveals erythromycin-induced liver toxicity in albino Wistar rats. *J. Pharm. Bioallied Sci.* **2016**, *8*, 327–334. [CrossRef]

193. Sun, B.; Wang, X.; Cao, R.; Zhang, Q.; Liu, Q.; Xu, M.; Zhang, M.; Du, X.; Dong, F.; Yan, X. NMR-based metabonomics study on the effect of Gancao in the attenuation of toxicity in rats induced by Fuzi. *J. Ethnopharmacol.* **2016**, *193*, 617–626. [CrossRef] [PubMed]

194. Singh, M.; Tam, B.; Akabayov, B. NMR-Fragment Based Virtual Screening: A Brief Overview. *Molecules* **2018**, *23*, 233. [CrossRef]

195. Shuker, S.B.; Hajduk, P.J.; Meadows, R.P.; Fesik, S.W. Discovering High-Affinity Ligands for Proteins: SAR by NMR. *Science* **1996**, *274*, 1531–1534. [CrossRef]

196. Romasanta, A.K.S.; van der Sijde, P.; Hellsten, I.; Hubbard, R.E.; Keseru, G.M.; van Muijlwijk-Koezen, J.; de Esch, I.J.P. When fragments link: A bibliometric perspective on the development of fragment-based drug discovery. *Drug Discov. Today* **2018**, *23*, 1596–1609. [CrossRef]

197. van Montfort, R.L.M.; Workman, P.; Lamoree, B.; Hubbard, R.E. Current perspectives in fragment-based lead discovery (FBLD). *Essays Biochem.* **2017**, *61*, 453–464. [CrossRef]

198. Szymański, P.; Markowicz, M.; Mikiciuk-Olasik, E. Adaptation of High-Throughput Screening in Drug Discovery—Toxicological Screening Tests. *Int. J. Mol. Sci.* **2012**, *13*, 427–452. [CrossRef] [PubMed]

199. Martis, E.A.; Radhakrishnan, R.; Badve, R.R. High-throughput screening: The hits and leads of drug discovery-An overview. *J. Appl. Pharm. Sci.* **2011**, *1*, 2–10.

200. Lightbody, G.; Haberland, V.; Browne, F.; Taggart, L.; Zheng, H.; Parkes, E.; Blayney, J.K. Review of applications of high-throughput sequencing in personalized medicine: Barriers and facilitators of future progress in research and clinical application. *Brief. Bioinform.* **2019**, *20*, 1795–1811. [CrossRef] [PubMed]

201. Zhu, Z.; Cuozzo, J. Review Article: High-Throughput Affinity-Based Technologies for Small-Molecule Drug Discovery. *J. Biomol. Screen.* **2009**, *14*, 1157–1164. [CrossRef]

202. Keserű, G.M.; Erlanson, D.A.; Ferenczy, G.G.; Hann, M.M.; Murray, C.W.; Pickett, S.D. Design Principles for Fragment Libraries: Maximizing the Value of Learnings from Pharma Fragment-Based Drug Discovery (FBDD) Programs for Use in Academia. *J. Med. Chem.* **2016**, *59*, 8189–8206. [CrossRef]

203. Shi, Y.; von Itzstein, M. How Size Matters: Diversity for Fragment Library Design. *Molecules* **2019**, *24*, 2838. [CrossRef]

204. Fox, S.; Farr-Jones, S.; Sopchak, L.; Boggs, A.; Nicely, H.W.; Khoury, R.; Biros, M. High-Throughput Screening: Update on Practices and Success. *J. Biomol. Screen.* **2006**, *11*, 864–869. [CrossRef]

205. Clare, R.H.; Bardelle, C.; Harper, P.; Hong, W.D.; Börjesson, U.; Johnston, K.L.; Collier, M.; Myhill, L.; Cassidy, A.; Plant, D.; et al. Industrial scale high-throughput screening delivers multiple fast acting macrofilaricides. *Nat. Commun.* **2019**, *10*, 1–8. [CrossRef]

206. Mballo, C.; Makarenkov, V. Virtual High Throughput Screening Using Machine Learning Methods. In Proceedings of the Classification as a Tool for Research, Dresden, Germany, 13–18 March 2009; Locarek-Junge, H., Weihs, C., Eds.; Springer: Berlin, Germany, 2010; pp. 517–524.

207. Erlanson, D.A. Introduction to Fragment-Based Drug Discovery. In *Fragment-Based Drug Discovery and X-Ray Crystallography*; Topics in Current Chemistry; Davies, T.G., Hyvönen, M., Eds.; Springer: Berlin, Germany, 2012; Volume 317, pp. 1–32. ISBN 978-3-642-27540-1.

208. Keserü, G.M.; Makara, G.M. The influence of lead discovery strategies on the properties of drug candidates. *Nat. Rev. Drug Discov.* **2009**, *8*, 203–212. [CrossRef]

209. Robson-Tull, J. Biophysical screening in fragment-based drug design: A brief overview. *Biosci. Horiz. Int. J. Stud. Res.* **2018**, *11*. [CrossRef]

210. Pellecchia, M. High-Throughput Screening and Fragment-Based Design: General Considerations for Lead Discovery and Optimization. In *NMR of Biomolecules: Towards Mechanistic Systems Biology*; Bertini, I., McGreevy, K.S., Parigi, G., Eds.; Wiley-VCH: Weinheim, Germany, 2012; pp. 253–263. ISBN 978-3-527-64450-6.

211. Campos-Olivas, R. NMR Screening and Hit Validation in Fragment Based Drug Discovery. *Curr. Top. Med. Chem.* **2011**, *11*, 43–67. [CrossRef] [PubMed]

212. Murray, C.W.; Blundell, T.L. Structural biology in fragment-based drug design. *Curr. Opin. Struct. Biol.* **2010**, *20*, 497–507. [CrossRef] [PubMed]

213. Harner, M.J.; Frank, A.O.; Fesik, S.W. Fragment-Based Drug Discovery Using NMR Spectroscopy. *J. Biomol. NMR* **2013**, *56*, 65–75. [CrossRef] [PubMed]

214. Lepre, C.A. Chapter Nine—Practical Aspects of NMR-Based Fragment Screening. In *Methods in Enzymology*; Fragment-Based Drug Design; Kuo, L.C., Ed.; Academic Press: San Diego, CA, USA, 2011; Volume 493, pp. 219–239.

215. Klages, J.; Coles, M.; Kessler, H. NMR-based screening: A powerful tool in fragment-based drug discovery. *Analyst* **2007**, *132*, 692–705. [CrossRef] [PubMed]

216. Gossert, A.D.; Jahnke, W. NMR in drug discovery: A practical guide to identification and validation of ligands interacting with biological macromolecules. *Prog. Nucl. Magn. Reson. Spectrosc.* **2016**, *97*, 82–125. [CrossRef] [PubMed]

217. Coyle, J.; Walser, R. Applied Biophysical Methods in Fragment-Based Drug Discovery. *SLAS Discov. Adv. Sci. Drug Discov.* **2020**, *25*, 471–490. [CrossRef] [PubMed]

218. Kirsch, P.; Hartman, A.M.; Hirsch, A.K.H.; Empting, M. Concepts and Core Principles of Fragment-Based Drug Design. *Molecules* **2019**, *24*, 4309. [CrossRef]

219. Li, Q. Application of Fragment-Based Drug Discovery to Versatile Targets. *Front. Mol. Biosci.* **2020**, *7*. [CrossRef]

220. Mashalidis, E.H.; Śledź, P.; Lang, S.; Abell, C. A three-stage biophysical screening cascade for fragment-based drug discovery. *Nat. Protoc.* **2013**, *8*, 2309–2324. [CrossRef]

221. Blundell, T.L. Protein crystallography and drug discovery: Recollections of knowledge exchange between academia and industry. *IUCrJ* **2017**, *4*, 308–321. [CrossRef]

222. Erlanson, D.A.; Fesik, S.W.; Hubbard, R.E.; Jahnke, W.; Jhoti, H. Twenty years on: The impact of fragments on drug discovery. *Nat. Rev. Drug Discov.* **2016**, *15*, 605–619. [CrossRef] [PubMed]

223. Hughes, T.; Baldwin, I.; Churcher, I. Fragment-based drug discovery—From hit discovery to FDA approval: Lessons learned and future challenge. *Int. Drug Discov.* **2011**, *6*, 34.

224. Bollag, G.; Tsai, J.; Zhang, J.; Zhang, C.; Ibrahim, P.; Nolop, K.; Hirth, P. Vemurafenib: The first drug approved for BRAF -mutant cancer. *Nat. Rev. Drug Discov.* **2012**, *11*, 873–886. [CrossRef] [PubMed]

225. Juárez-Salcedo, L.M.; Desai, V.; Dalia, S. Venetoclax: Evidence to date and clinical potential. *Drugs Context* **2019**, *8*. [CrossRef] [PubMed]

226. Chen, H.; Zhou, X.; Gao, Y.; Chen, H.; Zhou, J. Fragment-based drug design: Strategic advances and lessons learned. *Drug Discov. Technol.* **2017**, 212–232. [CrossRef]

227. Bancet, A.; Raingeval, C.; Lomberget, T.; Le Borgne, M.; Guichou, J.-F.; Krimm, I. Fragment Linking Strategies for Structure-Based Drug Design. *J. Med. Chem.* **2020**. [CrossRef]

228. Fairbrother, W.J.; Leverson, J.D.; Sampath, D.; Souers, A.J. Discovery and Development of Venetoclax, a Selective Antagonist of BCL-2. In *Successful Drug Discovery*; John Wiley & Sons: Hoboken, NJ, USA, 2019; pp. 225–245. ISBN 978-3-527-81469-5.

229. Oltersdorf, T.; Elmore, S.W.; Shoemaker, A.R.; Armstrong, R.C.; Augeri, D.J.; Belli, B.A.; Bruncko, M.; Deckwerth, T.L.; Dinges, J.; Hajduk, P.J.; et al. An inhibitor of Bcl-2 family proteins induces regression of solid tumours. *Nature* **2005**, *435*, 677–681. [CrossRef]

230. Muchmore, S.W.; Sattler, M.; Liang, H.; Meadows, R.P.; Harlan, J.E.; Yoon, H.S.; Nettesheim, D.; Chang, B.S.; Thompson, C.B.; Wong, S.-L.; et al. X-ray and NMR structure of human Bcl-x L, an inhibitor of programmed cell death. *Nature* **1996**, *381*, 335–341. [CrossRef]

231. Hortobagyi, G.N. Ribociclib for the first-line treatment of advanced hormone receptor-positive breast cancer: A review of subgroup analyses from the MONALEESA-2 trial. *Breast Cancer Res.* **2018**, *20*, 123. [CrossRef]

232. Merry, T.L.; Brooks, A.E.S.; Masson, S.W.; Adams, S.E.; Jaiswal, J.K.; Jamieson, S.M.F.; Shepherd, P.R. The CSF1 receptor inhibitor pexidartinib (PLX3397) reduces tissue macrophage levels without affecting glucose homeostasis in mice. *Int. J. Obes.* **2020**, *44*, 245–253. [CrossRef]

233. Tap, W.D.; Wainberg, Z.A.; Anthony, S.P.; Ibrahim, P.N.; Zhang, C.; Healey, J.H.; Chmielowski, B.; Staddon, A.P.; Cohn, A.L.; Shapiro, G.I.; et al. Structure-Guided Blockade of CSF1R Kinase in Tenosynovial Giant-Cell Tumor. *N. Engl. J. Med.* **2015**, *373*, 428–437. [CrossRef] [PubMed]

234. Smith, C.C.; Zhang, C.; Lin, K.C.; Lasater, E.A.; Zhang, Y.; Massi, E.; Damon, L.E.; Pendleton, M.; Bashir, A.; Sebra, R.; et al. Characterizing and Overriding the Structural Mechanism of the Quizartinib-Resistant FLT3 "Gatekeeper" F691L Mutation with PLX3397. *Cancer Discov.* **2015**, *5*, 668–679. [CrossRef] [PubMed]

235. Thaisrivongs, D.A.; Morris, W.J.; Scott, J.D. Discovery and Chemical Development of Verubecestat, a BACE1 Inhibitor for the Treatment of Alzheimer's Disease. In *Complete Accounts of Integrated Drug Discovery and Development: Recent Examples from the Pharmaceutical Industry Volume 1*; ACS Symposium Series; American Chemical Society: Washington, DC, USA, 2018; Volume 1307, pp. 53–89. ISBN 978-0-8412-3398-0.

236. Scott, J.D.; Li, S.W.; Brunskill, A.P.J.; Chen, X.; Cox, K.; Cumming, J.N.; Forman, M.; Gilbert, E.J.; Hodgson, R.A.; Hyde, L.A.; et al. Discovery of the 3-Imino-1,2,4-thiadiazinane 1,1-Dioxide Derivative Verubecestat (MK-8931)–A β-Site Amyloid Precursor Protein Cleaving Enzyme 1 Inhibitor for the Treatment of Alzheimer's Disease. *J. Med. Chem.* **2016**, *59*, 10435–10450. [CrossRef] [PubMed]

237. Murray, C.W.; Carr, M.G.; Callaghan, O.; Chessari, G.; Congreve, M.; Cowan, S.; Coyle, J.E.; Downham, R.; Figueroa, E.; Frederickson, M.; et al. Fragment-Based Drug Discovery Applied to Hsp90. Discovery of Two Lead Series with High Ligand Efficiency. *J. Med. Chem.* **2010**, *53*, 5942–5955. [CrossRef] [PubMed]

238. Woodhead, A.J.; Angove, H.; Carr, M.G.; Chessari, G.; Congreve, M.; Coyle, J.E.; Cosme, J.; Graham, B.; Day, P.J.; Downham, R.; et al. Discovery of (2,4-Dihydroxy-5-isopropylphenyl)-[5-(4-methylpiperazin -1-ylmethyl)-1,3-dihydroisoindol-2-yl]methanone (AT13387), a Novel Inhibitor of the Molecular Chaperone Hsp90 by Fragment Based Drug Design. *J. Med. Chem.* **2010**, *53*, 5956–5969. [CrossRef]

239. Basarab, G.S.; Hill, P.J.; Garner, C.E.; Hull, K.; Green, O.; Sherer, B.A.; Dangel, P.B.; Manchester, J.I.; Bist, S.; Hauck, S.; et al. Optimization of Pyrrolamide Topoisomerase II Inhibitors Toward Identification of an Antibacterial Clinical Candidate (AZD5099). *J. Med. Chem.* **2014**, *57*, 6060–6082. [CrossRef]

240. Lamoree, B.; Hubbard, R.E. Using Fragment-Based Approaches to Discover New Antibiotics. *SLAS Discov. Adv. Sci. Drug Discov.* **2018**, *23*, 495–510. [CrossRef]

241. Wyatt, P.G.; Woodhead, A.J.; Berdini, V.; Boulstridge, J.A.; Carr, M.G.; Cross, D.M.; Davis, D.J.; Devine, L.A.; Early, T.R.; Feltell, R.E.; et al. Identification of N-(4-Piperidinyl)-4-(2,6-dichlorobenzoylamino)- 1H-pyrazole-3-carboxamide (AT7519), a Novel Cyclin Dependent Kinase Inhibitor Using Fragment-Based X-Ray Crystallography and Structure Based Drug Design. *J. Med. Chem.* **2008**, *51*, 4986–4999. [CrossRef]

242. Dolman, M.E.M.; Poon, E.; Ebus, M.E.; den Hartog, I.J.M.; van Noesel, C.J.M.; Jamin, Y.; Hallsworth, A.; Robinson, S.P.; Petrie, K.; Sparidans, R.W.; et al. Cyclin-Dependent Kinase Inhibitor AT7519 as a Potential Drug for MYCN-Dependent Neuroblastoma. *Clin. Cancer Res.* **2015**, *21*, 5100–5109. [CrossRef]

243. Squires, M.S.; Feltell, R.E.; Wallis, N.G.; Lewis, E.J.; Smith, D.-M.; Cross, D.M.; Lyons, J.F.; Thompson, N.T. Biological characterization of AT7519, a small-molecule inhibitor of cyclin-dependent kinases, in human tumor cell lines. *Mol. Cancer Ther.* **2009**, *8*, 324–332. [CrossRef]

244. Hazlitt, R.A.; Teitz, T.; Bonga, J.D.; Fang, J.; Diao, S.; Iconaru, L.; Yang, L.; Goktug, A.N.; Currier, D.G.; Chen, T.; et al. Development of Second-Generation CDK2 Inhibitors for the Prevention of Cisplatin-Induced Hearing Loss. *J. Med. Chem.* **2018**, *61*, 7700–7709. [CrossRef] [PubMed]

245. Erlanson, D. Practical Fragments: Fragments in the clinic: 2016 edition. *Pract. Fragm.* **2016**, 489–499.

246. Hajduk, P.J. SAR by NMR: Putting the Pieces Together. *Mol. Interv.* **2006**, *6*, 266. [CrossRef] [PubMed]

247. Oschkinat, H. SAR-by-NMR. In *Encyclopedia of Molecular Pharmacology*; Offermanns, S., Rosenthal, W., Eds.; Springer: Berlin, Germany, 2008; pp. 1107–1109. ISBN 978-3-540-38918-7.

248. Barile, E.; Pellecchia, M. NMR-Based Approaches for the Identification and Optimization of Inhibitors of Protein–Protein Interactions. *Chem. Rev.* **2014**, *114*, 4749–4763. [CrossRef]

249. Hajduk, P.J.; Augeri, D.J.; Mack, J.; Mendoza, R.; Yang, J.; Betz, S.F.; Fesik, S.W. NMR-Based Screening of Proteins Containing 13C-Labeled Methyl Groups. *J. Am. Chem. Soc.* **2000**, *122*, 7898–7904. [CrossRef]

250. Shortridge, M.D.; Hage, D.S.; Harbison, G.S.; Powers, R. Estimating Protein−Ligand Binding Affinity Using High-Throughput Screening by NMR. *J. Comb. Chem.* **2008**, *10*, 948–958. [CrossRef]

251. Kang, C.; Gayen, S.; Wang, W.; Severin, R.; Chen, A.S.; Lim, H.A.; Chia, C.S.B.; Schüller, A.; Doan, D.N.P.; Poulsen, A.; et al. Exploring the binding of peptidic West Nile virus NS2B–NS3 protease inhibitors by NMR. *Antiviral Res.* **2013**, *97*, 137–144. [CrossRef]

252. Chiou, J.W.; Fu, B.; Chou, R.-H.; Yu, C. Blocking the Interactions between Calcium-Bound S100A12 Protein and the V Domain of RAGE Using Tranilast. *PLoS ONE* **2016**, *11*. [CrossRef]

253. Zech, S.G.; Olejniczak, E.; Hajduk, P.; Mack, J.; McDermott, A.E. Characterization of Protein−Ligand Interactions by High-Resolution Solid-State NMR Spectroscopy. *J. Am. Chem. Soc.* **2004**, *126*, 13948–13953. [CrossRef]

254. Williamson, M.P. Using chemical shift perturbation to characterise ligand binding. *Prog. Nucl. Magn. Reson. Spectrosc.* **2013**, *73*, 1–16. [CrossRef]

255. Jang, R.; Gao, X.; Li, M. Combining automated peak tracking in SAR by NMR with structure-based backbone assignment from 15N-NOESY. *BMC Bioinform.* **2012**, *13*, S4. [CrossRef] [PubMed]

256. Rahman, A.U.; Choudhary, M.I. Atia-tul-Wahab Chapter 6—Nuclear Overhauser Effect. In *Solving Problems with NMR Spectroscopy*; Rahman, A., Choudhary, M.I., Wahab, A., Eds.; Academic Press: London, UK, 2016; pp. 227–264. ISBN 978-0-12-411589-7.

257. Kumar, A.; Christy Rani Grace, R. Nuclear Overhauser Effect. In *Encyclopedia of Spectroscopy and Spectrometry*; Lindon, J.C., Ed.; Academic Press: Oxford, UK, 1999; pp. 1643–1653. ISBN 978-0-12-226680-5.

258. Jones, C.R.; Butts, C.P.; Harvey, J.N. Accuracy in determining interproton distances using Nuclear Overhauser Effect data from a flexible molecule. *Beilstein, J. Org. Chem.* **2011**, *7*, 145–150. [CrossRef] [PubMed]

259. Günther, H. Chapter 10—More 1D and 2D NMR Experiments: The Nuclear Overhauser Effect—Polarization Transfer–Spin Lock Experiments–3D NMR. In *NMR Spectroscopy: Basic Principles, Concepts and Applications in Chemistry*; Wiley-VCH: Weinheim, Germany, 2013; pp. 341–376. ISBN 978-3-527-67477-0.

260. Venkitakrishnan, R.P.; Benard, O.; Max, M.; Markley, J.L.; Assadi-Porter, F.M. Use of NMR Saturation Transfer Difference Spectroscopy to Study Ligand Binding to Membrane Proteins. In *Membrane Protein Structure and Dynamics: Methods and Protocols*; Methods in Molecular Biology; Vaidehi, N., Klein-Seetharaman, J., Eds.; Humana Press: New York, NY, USA, 2012; pp. 47–63. ISBN 978-1-62703-023-6.

261. Dalvit, C.; Fogliatto, G.; Stewart, A.; Veronesi, M.; Stockman, B. WaterLOGSY as a method for primary NMR screening: Practical aspects and range of applicability. *J. Biomol. NMR* **2001**, *21*, 349–359. [CrossRef] [PubMed]

262. Mayer, M.; Meyer, B. Characterization of Ligand Binding by Saturation Transfer Difference NMR Spectroscopy. *Angew. Chem. Int. Ed.* **1999**, *38*, 1784–1788. [CrossRef]

263. Klein, J.; Meinecke, R.; Mayer, M.; Meyer, B. Detecting Binding Affinity to Immobilized Receptor Proteins in Compound Libraries by HR-MAS STD NMR. *J. Am. Chem. Soc.* **1999**, *121*, 5336–5337. [CrossRef]

264. Ludwig, C.; Guenther, U.L. Ligand based NMR methods for drug discovery. *Front. Biosci. Landmark Ed.* **2009**, *14*, 4565–4574. [CrossRef]

265. Benie, A.J.; Moser, R.; Bäuml, E.; Blaas, D.; Peters, T. Virus-Ligand Interactions: Identification and Characterization of Ligand Binding by NMR Spectroscopy. *J. Am. Chem. Soc.* **2003**, *125*, 14–15. [CrossRef]

266. Peters, T.; Meyer, B. *Method for Detecting Biologically Active Compounds from Compound Libraries*; APExBIO: Houston, TX, USA, 2001.

267. Keller, R.M.; Wüthrich, K. Evolutionary change of the heme C electronic structure: Ferricytochrome c-551 from Pseudomonas aeruginosa and horse heart ferricytochrome c. *Biochem. Biophys. Res. Commun.* **1978**, *83*, 1132–1139. [CrossRef]

268. Cayley, P.J.; Albrand, J.P.; Feeney, J.; Roberts, G.C.K.; Piper, E.A.; Burgen, A.S.V. Nuclear magnetic resonance studies of the binding of trimethoprim to dihydrofolate reductase. *Biochemistry* **1979**, *18*, 3886–3895. [CrossRef]

269. Vogtherr, M.; Peters, T. Application of NMR Based Binding Assays to Identify Key Hydroxy Groups for Intermolecular Recognition. *J. Am. Chem. Soc.* **2000**, *122*, 6093–6099. [CrossRef]

270. Lane, A.N.; Kelly, G.; Ramos, A.; Frenkiel, T.A. Determining binding sites in protein–nucleic acid complexes by cross-saturation. *J. Biomol. NMR* **2001**, *21*, 127–139. [CrossRef] [PubMed]

271. Mayer, M.; Meyer, B. Group Epitope Mapping by Saturation Transfer Difference NMR To Identify Segments of a Ligand in Direct Contact with a Protein Receptor. *J. Am. Chem. Soc.* **2001**, *123*, 6108–6117. [CrossRef] [PubMed]

272. Artico, M.; Corelli, F.; Massa, S.; Mai, A.; Tramontano, E. *Synthetic Derivatives of Pyrrole and Pyrrolidine Suitable for the Therapy of Infections Caused by Rhinoviruses*; ACS Publications: Washington, DC, USA, 1994.

273. Ahmed, S.M.; Hall, A.J.; Robinson, A.E.; Verhoef, L.; Premkumar, P.; Parashar, U.D.; Koopmans, M.; Lopman, B.A. Global prevalence of norovirus in cases of gastroenteritis: A systematic review and meta-analysis. *Lancet Infect. Dis.* **2014**, *14*, 725–730. [CrossRef]

274. Lee, B.Y.; McGlone, S.M.; Bailey, R.R.; Wettstein, Z.S.; Umscheid, C.A.; Muder, R.R. Economic Impact of Outbreaks of Norovirus Infection in Hospitals. *Infect. Control Hosp. Epidemiol.* **2011**, *32*, 191–193. [CrossRef]

275. Tan, M.; Jiang, X. Norovirus–host interaction: Implications for disease control and prevention. *Expert Rev. Mol. Med.* **2007**, *9*, 1–22. [CrossRef]

276. Prasad, B.V.V.; Hardy, M.E.; Dokland, T.; Bella, J.; Rossmann, M.G.; Estes, M.K. X-ray Crystallographic Structure of the Norwalk Virus Capsid. *Science* **1999**, *286*, 287–290. [CrossRef]

277. Chen, R.; Neill, J.D.; Estes, M.K.; Prasad, B.V.V. X-ray structure of a native calicivirus: Structural insights into antigenic diversity and host specificity. *Proc. Natl. Acad. Sci. USA* **2006**, *103*, 8048–8053. [CrossRef]

278. Cao, S.; Lou, Z.; Tan, M.; Chen, Y.; Liu, Y.; Zhang, Z.; Zhang, X.C.; Jiang, X.; Li, X.; Rao, Z. Structural Basis for the Recognition of Blood Group Trisaccharides by Norovirus. *J. Virol.* **2007**, *81*, 5949–5957. [CrossRef]

279. Fiege, B.; Leuthold, M.; Parra, F.; Dalton, K.P.; Meloncelli, P.J.; Lowary, T.L.; Peters, T. Epitope mapping of histo blood group antigens bound to norovirus VLPs using STD NMR experiments reveals fine details of molecular recognition. *Glycoconj. J.* **2017**, *34*, 679–689. [CrossRef]

280. Meloncelli, P.J.; West, L.J.; Lowary, T.L. Synthesis and NMR studies on the ABO histo-blood group antigens: Synthesis of type III and IV structures and NMR characterization of type I–VI antigens. *Carbohydr. Res.* **2011**, *346*, 1406–1426. [CrossRef]

281. Rademacher, C.; Krishna, N.R.; Palcic, M.; Parra, F.; Peters, T. NMR Experiments Reveal the Molecular Basis of Receptor Recognition by a Calicivirus. *J. Am. Chem. Soc.* **2008**, *130*, 3669–3675. [CrossRef] [PubMed]

282. Balaram, P.; Bothner-By, A.A.; Dadok, J. Negative nuclear Overhuaser effects as probes of macromolecular structure. *J. Am. Chem. Soc.* **1972**, *94*, 4015–4017. [CrossRef] [PubMed]

283. Henrichsen, D.; Ernst, B.; Magnani, J.L.; Wang, W.-T.; Meyer, B.; Peters, T. Bioaffinity NMR Spectroscopy: Identification of an E-Selectin Antagonist in a Substance Mixture by Transfer NOE. *Angew. Chem. Int. Ed.* **1999**, *38*, 98–102. [CrossRef]

284. Sánchez-Pedregal, V.M.; Reese, M.; Meiler, J.; Blommers, M.J.J.; Griesinger, C.; Carlomagno, T. The Inpharma Method: Protein-Mediated Interligand NOEs for Pharmacophore Mapping. *Angew. Chem. Int. Ed.* **2005**, *44*, 4172–4175. [CrossRef] [PubMed]

285. Cohen, Y.; Avram, L.; Frish, L. Diffusion NMR Spectroscopy in Supramolecular and Combinatorial Chemistry: An Old Parameter—New Insights. *Angew. Chem. Int. Ed.* **2005**, *44*, 520–554. [CrossRef] [PubMed]

286. Metcalfe, G.; Speetjens, M.F.M.; Lester, D.R.; Clercx, H.J.H. Beyond Passive: Chaotic Transport in Stirred Fluids. In *Advances in Applied Mechanics*; van der Giessen, E., Aref, H., Eds.; Academic Press: San Diego, CA, USA, 2012; Volume 45, pp. 109–188. ISBN 978-0-12-380876-9.

287. Molnar, C.; Gair, J. 3.5 Passive Transport. In *Concepts of Biology-1st Canadian ed.*; BCcampus: Houston, TE, USA, 2019; pp. 92–98. ISBN 978-1-989623-99-2.

288. Chhabra, R.P.; Richardson, J.F. Chapter 7—Momentum, heat and mass transfer in boundary layers. In *Non-Newtonian Flow and Applied Rheology*, 2nd ed.; Chhabra, R.P., Richardson, J.F., Eds.; Butterworth-Heinemann: Oxford, UK, 2008; pp. 343–375. ISBN 978-0-7506-8532-0.

289. Nicolay, K.; Braun, K.P.J.; De Graaf, R.A.; Dijkhuizen, R.M.; Kruiskamp, M.J. Diffusion NMR spectroscopy. *NMR Biomed.* **2001**, *14*, 94–111. [CrossRef] [PubMed]

290. Claridge, T.D.W. Chapter 10-Diffusion NMR Spectroscopy. In *High-Resolution NMR Techniques in Organic Chemistry*, 3rd ed.; Claridge, T.D.W., Ed.; Elsevier: Amsterdam, The Netherlands, 2016; pp. 381–419. ISBN 978-0-08-099986-9.

291. Crank, J. The diffusion equation. In *The Mathematics of Diffusion*; Oxford University Press: Oxford, UK, 1975; pp. 1–10. ISBN 0-19-853411-6.

292. Cussler, E.L. Models for Diffusion. In *Diffusion: Mass Transfer in Fluid Systems*, 3rd ed.; Cambridge University Press: Cambridge, UK, 2009; pp. 1–10. ISBN 978-0-521-87121-1.

293. Stejskal, E.O.; Tanner, J.E. Spin Diffusion Measurements: Spin Echoes in the Presence of a Time-Dependent Field Gradient. *J. Chem. Phys.* **1965**, *42*, 288–292. [CrossRef]

294. Kerssebaum, R.; Salnikov, G. *DOSY and Diffusion by NMR*; Bruker BioSpin GmbH: Rheinstetten, Germany, 2006; Volume 1.

295. Sinnaeve, D. The Stejskal–Tanner equation generalized for any gradient shape—An overview of most pulse sequences measuring free diffusion. *Concepts Magn. Reson. Part A* **2012**, *40A*, 39–65. [CrossRef]

296. Johnson, C.S. Diffusion ordered nuclear magnetic resonance spectroscopy: Principles and applications. *Prog. Nucl. Magn. Reson. Spectrosc.* **1999**, *34*, 203–256. [CrossRef]

297. Lucas, L.H.; Larive, C.K. Measuring ligand-protein binding using NMR diffusion experiments. *Concepts Magn. Reson. Part A* **2004**, *20A*, 24–41. [CrossRef]

298. Gilard, V.; Trefi, S.; Balayssac, S.; Delsuc, M.-A.; Gostan, T.; Malet-Martino, M.; Martino, R.; Prigent, Y.; Taulelle, F. Chapter 6—DOSY NMR for Drug Analysis. In *NMR Spectroscopy in Pharmaceutical Analysis*; Holzgrabe, U., Wawer, I., Diehl, B., Eds.; Elsevier: Amsterdam, The Netherlands, 2008; pp. 269–289. ISBN 978-0-444-53173-5.

299. Valette, J.; Chaumeil, M.; Guillermier, M.; Bloch, G.; Hantraye, P.; Lebon, V. Diffusion-weighted NMR spectroscopy allows probing of 13C labeling of glutamate inside distinct metabolic compartments in the brain. *Magn. Reson. Med.* **2008**, *60*, 306–311. [CrossRef] [PubMed]

300. Dumez, J.-N. Spatial encoding and spatial selection methods in high-resolution NMR spectroscopy. *Prog. Nucl. Magn. Reson. Spectrosc.* **2018**, *109*, 101–134. [CrossRef] [PubMed]

301. Guduff, L.; Kuprov, I.; van Heijenoort, C.; Dumez, J.-N. Spatially encoded 2D and 3D diffusion-ordered NMR spectroscopy. *Chem. Commun.* **2017**, *53*, 701–704. [CrossRef]

302. Ruddigkeit, L.; van Deursen, R.; Blum, L.C.; Reymond, J.-L. Enumeration of 166 Billion Organic Small Molecules in the Chemical Universe Database GDB-17. *J. Chem. Inf. Model.* **2012**, *52*, 2864–2875. [CrossRef] [PubMed]

303. Reymond, J.-L.; Awale, M. Exploring Chemical Space for Drug Discovery Using the Chemical Universe Database. *ACS Chem. Neurosci.* **2012**, *3*, 649–657. [CrossRef] [PubMed]

304. Xu, C.; Wan, Y.; Chen, D.; Gao, C.; Yin, H.; Fetherston, D.; Kupce, E.; Lopez, G.; Ameduri, B.; Twum, E.B.; et al. 19F DOSY diffusion-NMR spectroscopy of fluoropolymers. *Magn. Reson. Chem.* **2017**, *55*, 472–484. [CrossRef]

305. Pagès, G.; Gilard, V.; Martino, R.; Malet-Martino, M. Pulsed-field gradient nuclear magnetic resonance measurements (PFG NMR) for diffusion ordered spectroscopy (DOSY) mapping. *Analyst* **2017**, *142*, 3771–3796. [CrossRef]

306. Nishimura, N.; Yoza, K.; Kobayashi, K. Guest-Encapsulation Properties of a Self-Assembled Capsule by Dynamic Boronic Ester Bonds. *J. Am. Chem. Soc.* **2010**, *132*, 777–790. [CrossRef]

307. Mathias, E.V.; Aponte, J.; Kornfield, J.A.; Ba, Y. Properties of small molecular drug loading and diffusion in a fluorinated PEG hydrogel studied by 1H molecular diffusion NMR and 19F spin diffusion NMR. *Colloid Polym. Sci.* **2010**, *288*, 1655–1663. [CrossRef]

308. Kramer, M.; Kleinpeter, E. STD-DOSY: A new NMR method to analyze multi-component enzyme/substrate systems. *J. Magn. Reson.* **2010**, *202*, 245–249. [CrossRef]

309. Tanoli, S.; Tanoli, N.; Usmani, S.; Zaheer-Ul-Haq; Ferreira, A. The exploration of interaction studies of smaller size, mostly ignored yet intrinsically inestimable molecules towards BSA; An example of STD and DOSY NMR. *Open Chem.* **2014**, *12*, 332–340. [CrossRef]

310. Lionta, E.; Spyrou, G.; Vassilatis, D.K.; Cournia, Z. Structure-Based Virtual Screening for Drug Discovery: Principles, Applications and Recent Advances. *Curr. Top. Med. Chem.* **2014**, *14*, 1923–1938. [CrossRef] [PubMed]

311. Danchin, A.; Médigue, C.; Gascuel, O.; Soldano, H.; Hénaut, A. From data banks to data bases. *Res. Microbiol.* **1991**, *142*, 913–916. [CrossRef]

312. Ekins, S.; Mestres, J.; Testa, B. In silico pharmacology for drug discovery: Methods for virtual ligand screening and profiling. *Br. J. Pharmacol.* **2007**, *152*, 9–20. [CrossRef]

313. Lin, X.; Li, X.; Lin, X. A Review on Applications of Computational Methods in Drug Screening and Design. *Molecules* **2020**, *25*, 1375. [CrossRef] [PubMed]

314. Johnson, D.K.; Karanicolas, J. Ultra-High-Throughput Structure-Based Virtual Screening for Small-Molecule Inhibitors of Protein–Protein Interactions. *J. Chem. Inf. Model.* **2016**, *56*, 399–411. [CrossRef] [PubMed]

315. Plouffe, D.; Brinker, A.; McNamara, C.; Henson, K.; Kato, N.; Kuhen, K.; Nagle, A.; Andreson, P.; Zhou, Y.; Gray, N.S.; et al. In silico activity profiling reveals the mechanism of action of antimalarials discovered in a high-throughput screen. *Proc. Natl. Acad. Sci. USA* **2008**, *105*, 9059–9064. [CrossRef]

316. Chiddarwar, R.K.; Rohrer, S.G.; Wolf, A.; Tresch, S.; Wollenhaupt, S.; Bender, A. In silico target prediction for elucidating the mode of action of herbicides including prospective validation. *J. Mol. Graph. Model.* **2017**, *71*, 70–79. [CrossRef]

317. Zoete, V.; Grosdidier, A.; Michielin, O. Docking, virtual high throughput screening and in silico fragment-based drug design. *J. Cell. Mol. Med.* **2009**, *13*, 238–248. [CrossRef]

318. Murgueitio, M.S.; Bermudez, M.; Mortier, J.; Wolber, G. In silico virtual screening approaches for anti-viral drug discovery. *Drug Discov. Today Technol.* **2012**, *9*, e219–e225. [CrossRef]

319. Kumar, V.; Krishna, S.; Siddiqi, M.I. Virtual screening strategies: Recent advances in the identification and design of anti-cancer agents. *Methods* **2015**, *71*, 64–70. [CrossRef]

320. Banegas-Luna, A.-J.; Cerón-Carrasco, J.P.; Pérez-Sánchez, H. A review of ligand-based virtual screening web tools and screening algorithms in large molecular databases in the age of big data. *Future Med. Chem.* **2018**, *10*, 2641–2658. [CrossRef] [PubMed]

321. Subramaniam, S.; Mehrotra, M.; Gupta, D. Virtual high throughput screening (vHTS)—A perspective. *Bioinformation* **2008**, *3*, 14–17. [CrossRef] [PubMed]

322. Stark, J.L.; Powers, R. Application of NMR and Molecular Docking in Structure-Based Drug Discovery. In *NMR of Proteins and Small Biomolecules*; Topics in Current Chemistry; Zhu, G., Ed.; Springer: Berlin, Germany, 2012; pp. 1–34. ISBN 978-3-642-28917-0.

323. Fan, H.; Irwin, J.J.; Sali, A. Virtual Ligand Screening Against Comparative Protein Structure Models. *Methods Mol. Biol. Clifton NJ* **2012**, *819*, 105–126. [CrossRef]

324. Ciulli, A. Biophysical Screening for the Discovery of Small-Molecule Ligands. *Methods Mol. Biol. Clifton NJ* **2013**, *1008*, 357–388. [CrossRef]

325. Amaning, K.; Lowinski, M.; Vallee, F.; Steier, V.; Marcireau, C.; Ugolini, A.; Delorme, C.; Foucalt, F.; McCort, G.; Derimay, N.; et al. The use of virtual screening and differential scanning fluorimetry for the rapid identification of fragments active against MEK1. *Bioorg. Med. Chem. Lett.* **2013**, *23*, 3620–3626. [CrossRef]

326. Tanrikulu, Y.; Krüger, B.; Proschak, E. The holistic integration of virtual screening in drug discovery. *Drug Discov. Today* **2013**, *18*, 358–364. [CrossRef] [PubMed]

327. Xu, H. Retrospect and prospect of virtual screening in drug discovery. *Curr. Top. Med. Chem.* **2002**, *2*, 1305–1320. [CrossRef]

328. Kitchen, D.B.; Decornez, H.; Furr, J.R.; Bajorath, J. Docking and scoring in virtual screening for drug discovery: Methods and applications. *Nat. Rev. Drug Discov.* **2004**, *3*, 935–949. [CrossRef]

329. Rudisser, S.; Jahnke, W. NMR and in silico Screening. *Comb. Chem. High Throughput Screen.* **2002**, *5*, 591–603. [CrossRef]

330. Morelli, X.; Rigby, A.C. Acceleration of the Drug Discovery Process: A Combinatorial Approach Using NMR Spectroscopy and Virtual Screening. *Curr. Comput. Aided Drug Des.* **2007**, *3*, 33–49. [CrossRef]

331. Chen, D.; Ranganathan, A.; IJzerman, A.P.; Siegal, G.; Carlsson, J. Complementarity between in Silico and Biophysical Screening Approaches in Fragment-Based Lead Discovery against the A2A Adenosine Receptor. *J. Chem. Inf. Model.* **2013**, *53*, 2701–2714. [CrossRef] [PubMed]

332. Cieślak, M.; Komoszyński, M.; Wojtczak, A. Adenosine A2A receptors in Parkinson's disease treatment. *Purinergic Signal.* **2008**, *4*, 305–312. [CrossRef] [PubMed]

333. Di Lello, P.; Pastor, R.; Murray, J.M.; Blake, R.A.; Cohen, F.; Crawford, T.D.; Drobnick, J.; Drummond, J.; Kategaya, L.; Kleinheinz, T.; et al. Discovery of Small-Molecule Inhibitors of Ubiquitin Specific Protease 7 (USP7) Using Integrated NMR and in Silico Techniques. *J. Med. Chem.* **2017**, *60*, 10056–10070. [CrossRef] [PubMed]

334. Sheng, Y.; Saridakis, V.; Sarkari, F.; Duan, S.; Wu, T.; Arrowsmith, C.H.; Frappier, L. Molecular recognition of p53 and MDM2 by USP7/HAUSP. *Nat. Struct. Mol. Biol.* **2006**, *13*, 285–291. [CrossRef] [PubMed]

335. Baurin, N.; Aboul-Ela, F.; Barril, X.; Davis, B.; Drysdale, M.; Dymock, B.; Finch, H.; Fromont, C.; Richardson, C.; Simmonite, H.; et al. Design and Characterization of Libraries of Molecular Fragments for Use in NMR Screening against Protein Targets. *J. Chem. Inf. Comput. Sci.* **2004**, *44*, 2157–2166. [CrossRef]

336. Potamitis, C.; Zervou, M.; Katsiaras, V.; Zoumpoulakis, P.; Durdagi, S.; Papadopoulos, M.G.; Hayes, J.M.; Grdadolnik, S.G.; Kyrikou, I.; Argyropoulos, D.; et al. Antihypertensive Drug Valsartan in Solution and at the AT1 Receptor: Conformational Analysis, Dynamic NMR Spectroscopy, in Silico Docking, and Molecular Dynamics Simulations. *J. Chem. Inf. Model.* **2009**, *49*, 726–739. [CrossRef]

337. Bertini, I.; Fragai, M.; Giachetti, A.; Luchinat, C.; Maletta, M.; Parigi, G.; Yeo, K.J. Combining in Silico Tools and NMR Data to Validate Protein–Ligand Structural Models: Application to Matrix Metalloproteinases. *J. Med. Chem.* **2005**, *48*, 7544–7559. [CrossRef]

338. Li, G.-B.; Abboud, M.I.; Brem, J.; Someya, H.; Lohans, C.T.; Yang, S.-Y.; Spencer, J.; Wareham, D.W.; McDonough, M.A.; Schofield, C.J. NMR-filtered virtual screening leads to non-metal chelating metallo-β-lactamase inhibitors. *Chem. Sci.* **2017**, *8*, 928–937. [CrossRef]

339. Palacios, A.R.; Rossi, M.-A.; Mahler, G.S.; Vila, A.J. Metallo-β-Lactamase Inhibitors Inspired on Snapshots from the Catalytic Mechanism. *Biomolecules* **2020**, *10*, 854. [CrossRef]

340. Shan, J.; Zhang, X.; Bao, J.; Cassell, R.; Zheng, J.J. Synthesis of Potent Dishevelled PDZ Domain Inhibitors Guided by Virtual Screening and NMR Studies. *Chem. Biol. Drug Des.* **2012**, *79*, 376–383. [CrossRef] [PubMed]

341. Softley, C.A.; Bostock, M.J.; Popowicz, G.M.; Sattler, M. Paramagnetic NMR in drug discovery. *J. Biomol. NMR* **2020**, *74*, 287–309. [CrossRef] [PubMed]

342. Cetiner, E.C.; Schwalbe, H. Chapter 9: Paramagnetic NMR in Drug Discovery. In *Paramagnetism in Experimental Biomolecular NMR.*; The Royal Society of Chemistry: London, UK, 2018; pp. 258–282.

343. Pell, A.J.; Pintacuda, G.; Grey, C.P. Paramagnetic NMR in solution and the solid state. *Prog. Nucl. Magn. Reson. Spectrosc.* **2019**, *111*, 1–271. [CrossRef] [PubMed]

344. Prudencio, M.; Impagliazzo, A.; Ubbink, M.; Rohovec, J.; Peters, J. CLaNP-An artificial paramagnetic centre to study proteins by NMR. *J. Inorg. Biochem.* **2003**, *1*, 213. [CrossRef]

345. Sugiki, T.; Furuita, K.; Fujiwara, T.; Kojima, C. Current NMR Techniques for Structure-Based Drug Discovery. *Molecules* **2018**, *23*, 148. [CrossRef]

346. Gottstein, D.; Reckel, S.; Dötsch, V.; Güntert, P. Requirements on Paramagnetic Relaxation Enhancement Data for Membrane Protein Structure Determination by NMR. *Structure* **2012**, *20*, 1019–1027. [CrossRef]

347. Ubbink, M.; Perrakis, A.; Ravera, E.; Carlon, A.; Fragai, M.; Parigi, G.; Luchinat, C. Paramagnetic NMR as a new tool in structural biology. *Emerg. Top. Life Sci.* **2018**, *2*, 19–28. [CrossRef]

348. Iwahara, J.; Anderson, D.E.; Murphy, E.C.; Clore, G.M. EDTA-Derivatized Deoxythymidine as a Tool for Rapid Determination of Protein Binding Polarity to DNA by Intermolecular Paramagnetic Relaxation Enhancement. *J. Am. Chem. Soc.* **2003**, *125*, 6634–6635. [CrossRef]

349. Hurley, L.H.; Boyd, F.L. DNA as a target for drug action. *Trends Pharmacol. Sci.* **1988**, *9*, 402–407. [CrossRef]

350. Brasuń, J.; Cebrat, M.; Jaremko, Ł.; Jaremko, M.; Ilc, G.; Gładysz, O.; Zhukov, I. The structural effects of the Cys-S-S-Cys bridge exchange by the His-Cu(II)-His motif studied on natural peptides—A promising tool for natural compounds-based design. *Dalton Trans.* **2009**, 4853–4857. [CrossRef]

351. Schaduangrat, N.; Lampa, S.; Simeon, S.; Gleeson, M.P.; Spjuth, O.; Nantasenamat, C. Towards reproducible computational drug discovery. *J. Cheminformatics* **2020**, *12*, 9. [CrossRef]

352. Huang, S.; Umemoto, R.; Tamura, Y.; Kofuku, Y.; Uyeda, T.Q.P.; Nishida, N.; Shimada, I. Utilization of paramagnetic relaxation enhancements for structural analysis of actin-binding proteins in complex with actin. *Sci. Rep.* **2016**, *6*, 33690. [CrossRef] [PubMed]

353. Huang, Y.; Wang, X.; Lv, G.; Razavi, A.M.; Huysmans, G.H.M.; Weinstein, H.; Bracken, C.; Eliezer, D.; Boudker, O. Monitoring Dynamics of Large Membrane Proteins by 19F Paramagnetic Longitudinal Relaxation: Domain Movement in a Glutamate Transporter Homolog. *bioRxiv* **2019**, 832121. [CrossRef]

354. Renault, M.; Cukkemane, A.; Baldus, M. Solid-State NMR Spectroscopy on Complex Biomolecules. *Angew. Chem. Int. Ed.* **2010**, *49*, 8346–8357. [CrossRef] [PubMed]

355. Middleton, D.A. Solid-state NMR spectroscopy as a tool for drug design: From membrane-embedded targets to amyloid fibrils. *Biochem. Soc. Trans.* **2007**, *35*, 985–990. [CrossRef] [PubMed]

356. Vogt, F.G.; Clawson, J.S.; Strohmeier, M.; Pham, T.N.; Watson, S.A.; Edwards, A.J. New Approaches to the Characterization of Drug Candidates by Solid-State NMR. In *Pharmaceutical Sciences Encyclopedia*; American Cancer Society: Atlanta, GA, USA, 2011; pp. 1–77. ISBN 978-0-470-57122-4.

357. Pranitha, D.; Parthiban, N.; Dinakaran, S.; Ghosh, S.; Banji, D. Saikiran Solid state nuclear magnetic resonance spectroscopy-A review. *Asian J. Pharm. Clin. Res.* **2011**, *4*, 9–14.

358. Berendt, R.T.; Sperger, D.M.; Munson, E.J.; Isbester, P.K. Solid-state NMR spectroscopy in pharmaceutical research and analysis. *TrAC Trends Anal. Chem.* **2006**, *25*, 977–984. [CrossRef]

359. Bugay, D.E. Solid-State Nuclear Magnetic Resonance Spectroscopy: Theory and Pharmaceutical Applications. *Pharm. Res.* **1993**, *10*, 317–327. [CrossRef]

360. Ashbrook, S.E.; Griffin, J.M.; Johnston, K.E. Recent Advances in Solid-State Nuclear Magnetic Resonance Spectroscopy. *Annu. Rev. Anal. Chem.* **2018**, *11*, 485–508. [CrossRef]

361. Watts, A. Solid-state NMR in drug design and discovery for membrane-embedded targets. *Nat. Rev. Drug Discov.* **2005**, *4*, 555–568. [CrossRef]

362. Callari, M.; De Souza, P.L.; Rawal, A.; Stenzel, M.H. The Effect of Drug Loading on Micelle Properties: Solid-State NMR as a Tool to Gain Structural Insight. *Angew. Chem. Int. Ed.* **2017**, *56*, 8441–8445. [CrossRef] [PubMed]

363. Lee, M.; Wang, T.; Makhlynets, O.V.; Wu, Y.; Polizzi, N.F.; Wu, H.; Gosavi, P.M.; Stöhr, J.; Korendovych, I.V.; DeGrado, W.F.; et al. Zinc-binding structure of a catalytic amyloid from solid-state NMR. *Proc. Natl. Acad. Sci. USA* **2017**, *114*, 6191–6196. [CrossRef] [PubMed]

364. Poulson, B.G.; Szczepski, K.; Izabela Lachowicz, J.; Jaremko, L.; Emwas, A.-H.; Jaremko, M. Aggregation of biologically important peptides and proteins: Inhibition or acceleration depending on protein and metal ion concentrations. *RSC Adv.* **2020**, *10*, 215–227. [CrossRef]

365. Hughes, J.P.; Rees, S.; Kalindjian, S.B.; Philpott, K.L. Principles of early drug discovery. *Br. J. Pharmacol.* **2011**, *162*, 1239–1249. [CrossRef]

366. Keserű, G.M.; Makara, G.M. Hit discovery and hit-to-lead approaches. *Drug Discov. Today* **2006**, *11*, 741–748. [CrossRef]

367. Hevener, K.E.; Pesavento, R.; Ren, J.; Lee, H.; Ratia, K.; Johnson, M.E. Chapter Twelve—Hit-to-Lead: Hit Validation and Assessment. In *Methods in Enzymology*; Modern Approaches in Drug Discovery; Lesburg, C.A., Ed.; Academic Press: Cambridge, MA, USA, 2018; Volume 610, pp. 265–309.

368. Genick, C.C.; Wright, S.K. Biophysics: For HTS hit validation, chemical lead optimization, and beyond. *Expert Opin. Drug Discov.* **2017**, *12*, 897–907. [CrossRef]

369. Sillerud, L.O.; Larson, R.S. Advances in Nuclear Magnetic Resonance for Drug Discovery. In *Bioinformatics and Drug Discovery*; Methods in Molecular Biology; Larson, R.S., Ed.; Humana Press: New York, NY, USA, 2012; pp. 195–266. ISBN 978-1-61779-965-5.

370. Sharma, R.; Florea, M.; Nau, W.M.; Swaminathan, K. Validation of Drug-Like Inhibitors against Mycobacterium Tuberculosis L-Aspartate α-Decarboxylase Using Nuclear Magnetic Resonance (1H-NMR). *PLoS ONE* **2012**, *7*, e45947. [CrossRef]

371. Fouad, W.M.; Rathinasabapathi, B. Expression of bacterial L-aspartate-alpha-decarboxylase in tobacco increases beta-alanine and pantothenate levels and improves thermotolerance. *Plant Mol. Biol.* **2006**, *60*, 495–505. [CrossRef]

372. Zega, A. NMR Methods for Identification of False Positives in Biochemical Screens. *J. Med. Chem.* **2017**, *60*, 9437–9447. [CrossRef]

373. Huth, J.R.; Mendoza, R.; Olejniczak, E.T.; Johnson, R.W.; Cothron, D.A.; Liu, Y.; Lerner, C.G.; Chen, J.; Hajduk, P.J. ALARM NMR: A Rapid and Robust Experimental Method to Detect Reactive False Positives in Biochemical Screens. *J. Am. Chem. Soc.* **2005**, *127*, 217–224. [CrossRef]

374. Dahlin, J.L.; Cuellar, M.; Singh, G.; Nelson, K.M.; Strasser, J.M.; Rappe, T.; Xia, Y.; Veglia, G.; Walters, M.A. ALARM NMR for HTS Triage and Chemical Probe Validation. *Curr. Protoc. Chem. Biol.* **2018**, *10*, 91–117. [CrossRef] [PubMed]

375. Dahlin, J.L.; Nelson, K.M.; Strasser, J.M.; Barsyte-Lovejoy, D.; Szewczyk, M.M.; Organ, S.; Cuellar, M.; Singh, G.; Shrimp, J.H.; Nguyen, N.; et al. Assay interference and off-target liabilities of reported histone acetyltransferase inhibitors. *Nat. Commun.* **2017**, *8*, 1527. [CrossRef] [PubMed]

376. Nagatoishi, S.; Yamaguchi, S.; Katoh, E.; Kajita, K.; Yokotagawa, T.; Kanai, S.; Furuya, T.; Tsumoto, K. A combination of 19F NMR and surface plasmon resonance for site-specific hit selection and validation of fragment molecules that bind to the ATP-binding site of a kinase. *Bioorg. Med. Chem.* **2018**, *26*, 1929–1938. [CrossRef] [PubMed]

377. Fry, D.C.; Wartchow, C.; Graves, B.; Janson, C.; Lukacs, C.; Kammlott, U.; Belunis, C.; Palme, S.; Klein, C.; Vu, B. Deconstruction of a Nutlin: Dissecting the Binding Determinants of a Potent Protein–Protein Interaction Inhibitor. *ACS Med. Chem. Lett.* **2013**, *4*, 660–665. [CrossRef]

378. Goudreau, N.; Coulombe, R.; Faucher, A.-M.; Grand-Maître, C.; Lacoste, J.-E.; Lemke, C.T.; Malenfant, E.; Bousquet, Y.; Fader, L.; Simoneau, B.; et al. Monitoring Binding of HIV-1 Capsid Assembly Inhibitors Using 19F Ligand-and 15N Protein-Based NMR and X-ray Crystallography: Early Hit Validation of a Benzodiazepine Series. *Chem. Med. Chem.* **2013**, *8*, 405–414. [CrossRef]

379. Dias, D.M.; Van Molle, I.; Baud, M.G.J.; Galdeano, C.; Geraldes, C.F.G.C.; Ciulli, A. Is NMR Fragment Screening Fine-Tuned to Assess Druggability of Protein–Protein Interactions? *ACS Med. Chem. Lett.* **2014**, *5*, 23–28. [CrossRef]

380. Arjmand, F.; Sharma, G.C.; Sayeed, F.; Muddassir, M.; Tabassum, S. De novo design of chiral organotin cancer drug candidates: Validation of enantiopreferential binding to molecular target DNA and 5′-GMP by UV–visible, fluorescence, 1H and 31P NMR. *J. Photochem. Photobiol. B* **2011**, *105*, 167–174. [CrossRef]

381. Chène, P. Inhibiting the p53–MDM2 interaction: An important target for cancer therapy. *Nat. Rev. Cancer* **2003**, *3*, 102–109. [CrossRef]

382. Hai, J.; Sakashita, S.; Allo, G.; Ludkovski, O.; Ng, C.; Shepherd, F.A.; Tsao, M.-S. Inhibiting MDM2-p53 Interaction Suppresses Tumor Growth in Patient-Derived Non–Small Cell Lung Cancer Xenograft Models. *J. Thorac. Oncol.* **2015**, *10*, 1172–1180. [CrossRef]

383. Zhang, Q.; Zeng, S.X.; Lu, H. Targeting p53-MDM2-MDMX Loop for Cancer Therapy. In *Mutant p53 and MDM2 in Cancer*; Subcellular Biochemistry; Deb, S.P., Deb, S., Eds.; Springer: Dordrecht, The Netherlands, 2014; pp. 281–319. ISBN 978-94-017-9211-0.

384. Tovar, C.; Graves, B.; Packman, K.; Filipovic, Z.; Xia, B.H.M.; Tardell, C.; Garrido, R.; Lee, E.; Kolinsky, K.; To, K.-H.; et al. MDM2 Small-Molecule Antagonist RG7112 Activates p53 Signaling and Regresses Human Tumors in Preclinical Cancer Models. *Cancer Res.* **2013**, *73*, 2587–2597. [CrossRef]

385. Scott, D.E.; Bayly, A.R.; Abell, C.; Skidmore, J. Small molecules, big targets: Drug discovery faces the protein–protein interaction challenge. *Nat. Rev. Drug Discov.* **2016**, *15*, 533–550. [CrossRef] [PubMed]

386. Goncearenco, A.; Li, M.; Simonetti, F.L.; Shoemaker, B.A.; Panchenko, A.R. Exploring Protein-Protein Interactions as Drug Targets for Anti-cancer Therapy with in Silico Workflows. In *Proteomics for Drug Discovery: Methods and Protocols*; Methods in Molecular Biology; Lazar, I.M., Kontoyianni, M., Lazar, A.C., Eds.; Humana Press: New York, NY, USA, 2017; pp. 221–236. ISBN 978-1-4939-7201-2.

387. Fry, D.C. Targeting Protein-Protein Interactions for Drug Discovery. In *Protein-Protein Interactions: Methods and Applications*; Methods in Molecular Biology; Meyerkord, C.L., Fu, H., Eds.; Humana Press: New York, NY, USA, 2015; pp. 93–106. ISBN 978-1-4939-2425-7.

388. Mabonga, L.; Kappo, A.P. Protein-protein interaction modulators: Advances, successes and remaining challenges. *Biophys. Rev.* **2019**, *11*, 559–581. [CrossRef] [PubMed]

389. Cuenda, A.; Rouse, J.; Doza, Y.N.; Meier, R.; Cohen, P.; Gallagher, T.F.; Young, P.R.; Lee, J.C. SB 203580 is a specific inhibitor of a MAP kinase homologue which is stimulated by cellular stresses and interleukin-1. *FEBS Lett.* **1995**, *364*, 229–233. [CrossRef] [PubMed]

390. Kumar, S.; McDonnell, P.C.; Gum, R.J.; Hand, A.T.; Lee, J.C.; Young, P.R. Novel Homologues of CSBP/p38 MAP Kinase: Activation, Substrate Specificity and Sensitivity to Inhibition by Pyridinyl Imidazoles. *Biochem. Biophys. Res. Commun.* **1997**, *235*, 533–538. [CrossRef]

391. Mizukoshi, Y.; Abe, A.; Takizawa, T.; Hanzawa, H.; Fukunishi, Y.; Shimada, I.; Takahashi, H. An Accurate Pharmacophore Mapping Method by NMR Spectroscopy. *Angew. Chem. Int. Ed.* **2012**, *51*, 1362–1365. [CrossRef]

392. Fukunishi, Y.; Mizukoshi, Y.; Takeuchi, K.; Shimada, I.; Takahashi, H.; Nakamura, H. Protein–ligand docking guided by ligand pharmacophore-mapping experiment by NMR. *J. Mol. Graph. Model.* **2011**, *31*, 20–27. [CrossRef]

393. Li, D.; DeRose, E.F.; London, R.E. The inter-ligand Overhauser effect: A powerful new NMR approach for mapping structural relationships of macromolecular ligands. *J. Biomol. NMR* **1999**, *15*, 71–76. [CrossRef]

394. Becattini, B.; Pellecchia, M. SAR by ILOEs: An NMR-Based Approach to Reverse Chemical Genetics. *Chem. Eur. J.* **2006**, *12*, 2658–2662. [CrossRef]

395. Becattini, B.; Sareth, S.; Zhai, D.; Crowell, K.J.; Leone, M.; Reed, J.C.; Pellecchia, M. Targeting Apoptosis via Chemical Design: Inhibition of Bid-Induced Cell Death by Small Organic Molecules. *Chem. Biol.* **2004**, *11*, 1107–1117. [CrossRef]

396. Lucas, L.H.; Price, K.E.; Larive, C.K. Epitope Mapping and Competitive Binding of HSA Drug Site II Ligands by NMR Diffusion Measurements. *J. Am. Chem. Soc.* **2004**, *126*, 14258–14266. [CrossRef]

397. Hajduk, P.J.; Mack, J.C.; Olejniczak, E.T.; Park, C.; Dandliker, P.J.; Beutel, B.A. SOS-NMR: A Saturation Transfer NMR-Based Method for Determining the Structures of Protein−Ligand Complexes. *J. Am. Chem. Soc.* **2004**, *126*, 2390–2398. [CrossRef]

398. Schieborr, U.; Vogtherr, M.; Elshorst, B.; Betz, M.; Grimme, S.; Pescatore, B.; Langer, T.; Saxena, K.; Schwalbe, H. How Much NMR Data Is Required to Determine a Protein–Ligand Complex Structure? *Chem. Bio. Chem.* **2005**, *6*, 1891–1898. [CrossRef] [PubMed]

399. Chen, W.-N.; Kuppan, K.V.; Lee, M.D.; Jaudzems, K.; Huber, T.; Otting, G. O-tert-Butyltyrosine, an NMR Tag for High-Molecular-Weight Systems and Measurements of Submicromolar Ligand Binding Affinities. *J. Am. Chem. Soc.* **2015**, *137*, 4581–4586. [CrossRef]

400. Chen, W.-N.; Nitsche, C.; Pilla, K.B.; Graham, B.; Huber, T.; Klein, C.D.; Otting, G. Sensitive NMR Approach for Determining the Binding Mode of Tightly Binding Ligand Molecules to Protein Targets. *J. Am. Chem. Soc.* **2016**, *138*, 4539–4546. [CrossRef] [PubMed]

401. Ludwig, C.; Michiels, P.J.A.; Wu, X.; Kavanagh, K.L.; Pilka, E.; Jansson, A.; Oppermann, U.; Günther, U.L. SALMON: Solvent Accessibility, Ligand binding, and Mapping of ligand Orientation by NMR Spectroscopy. *J. Med. Chem.* **2008**, *51*, 1–3. [CrossRef] [PubMed]

402. Geist, L.; Mayer, M.; Cockcroft, X.-L.; Wolkerstorfer, B.; Kessler, D.; Engelhardt, H.; McConnell, D.B.; Konrat, R. Direct NMR Probing of Hydration Shells of Protein Ligand Interfaces and Its Application to Drug Design. *J. Med. Chem.* **2017**, *60*, 8708–8715. [CrossRef] [PubMed]

403. Orts, J.; Riek, R. Protein—Ligand structure determination with the NMR molecular replacement tool, NMR2. *J. Biomol. NMR* **2020**. [CrossRef] [PubMed]

404. Orts, J.; Wälti, M.A.; Marsh, M.; Vera, L.; Gossert, A.D.; Güntert, P.; Riek, R. NMR-Based Determination of the 3D Structure of the Ligand–Protein Interaction Site without Protein Resonance Assignment. *J. Am. Chem. Soc.* **2016**, *138*, 4393–4400. [CrossRef]

405. Wälti, M.A.; Orts, J. The NMR2 Method to Determine Rapidly the Structure of the Binding Pocket of a Protein–Ligand Complex with High Accuracy. *Magnetochemistry* **2018**, *4*, 12. [CrossRef]

406. Torres, F.; Ghosh, D.; Strotz, D.; Chi, C.N.; Davis, B.; Orts, J. Protein–fragment complex structures derived by NMR molecular replacement. *RSC Med. Chem.* **2020**, *11*, 591–596. [CrossRef]

407. Yu, Z.; Li, P.; Merz, K.M. Using Ligand-Induced Protein Chemical Shift Perturbations To Determine Protein–Ligand Structures. *Biochemistry* **2017**, *56*, 2349–2362. [CrossRef] [PubMed]

408. Krzeminski, M.; Loth, K.; Boelens, R.; Bonvin, A.M. SAMPLEX: Automatic mapping of perturbed and unperturbed regions of proteins and complexes. *BMC Bioinform.* **2010**, *11*, 51. [CrossRef] [PubMed]

409. Siegal, G.; Selenko, P. Cells, drugs and NMR. *J. Magn. Reson.* **2019**, *306*, 202–212. [CrossRef] [PubMed]

410. Kang, C. Applications of In-Cell NMR in Structural Biology and Drug Discovery. *Int. J. Mol. Sci.* **2019**, *20*, 139. [CrossRef]

411. Li, C.; Wang, G.-F.; Wang, Y.; Creager-Allen, R.; Lutz, E.A.; Scronce, H.; Slade, K.M.; Ruf, R.A.S.; Mehl, R.A.; Pielak, G.J. Protein 19F NMR in Escherichia coli. *J. Am. Chem. Soc.* **2010**, *132*, 321–327. [CrossRef]

412. Pan, B.-B.; Yang, F.; Ye, Y.; Wu, Q.; Li, C.; Huber, T.; Su, X.-C. 3D structure determination of a protein in living cells using paramagnetic NMR spectroscopy. *Chem. Commun.* **2016**, *52*, 10237–10240. [CrossRef]

413. Bertrand, K.; Reverdatto, S.; Burz, D.S.; Zitomer, R.; Shekhtman, A. Structure of Proteins in Eukaryotic Compartments. *J. Am. Chem. Soc.* **2012**, *134*, 12798–12806. [CrossRef]

414. Mercatelli, E.; Barbieri, L.; Luchinat, E.; Banci, L. Direct structural evidence of protein redox regulation obtained by in-cell NMR. *Biochim. Biophys. Acta BBA Mol. Cell Res.* **2016**, *1863*, 198–204. [CrossRef]

415. Ohno, A.; Inomata, K.; Tochio, H.; Shirakawa, M. In-Cell NMR Spectroscopy in Protein Chemistry and Drug Discovery. *Curr. Top. Med. Chem.* **2011**, *11*, 68–73. [CrossRef]

416. Hamatsu, J.; O'Donovan, D.; Tanaka, T.; Shirai, T.; Hourai, Y.; Mikawa, T.; Ikeya, T.; Mishima, M.; Boucher, W.; Smith, B.O.; et al. High-Resolution Heteronuclear Multidimensional NMR of Proteins in Living Insect Cells Using a Baculovirus Protein Expression System. *J. Am. Chem. Soc.* **2013**, *135*, 1688–1691. [CrossRef]

417. Verardi, R.; Traaseth, N.J.; Masterson, L.R.; Vostrikov, V.V.; Veglia, G. Isotope Labeling for Solution and Solid-State NMR Spectroscopy of Membrane Proteins. In *Isotope Labeling in Biomolecular NMR*; Advances in Experimental Medicine and Biology; Atreya, H.S., Ed.; Springer: Dordrecht, The Netherlands, 2012; pp. 35–62. ISBN 978-94-007-4954-2.

418. Kang, C. 19F-NMR in Target-based Drug Discovery. *Curr. Med. Chem.* **2019**, *26*, 4964–4983. [CrossRef] [PubMed]

419. Norton, R.S.; Leung, E.W.W.; Chandrashekaran, I.R.; MacRaild, C.A. Applications of 19F-NMR in Fragment-Based Drug Discovery. *Molecules* **2016**, *21*, 860. [CrossRef] [PubMed]

420. Serber, Z.; Straub, W.; Corsini, L.; Nomura, A.M.; Shimba, N.; Craik, C.S.; Ortiz de Montellano, P.; Dötsch, V. Methyl Groups as Probes for Proteins and Complexes in In-Cell NMR Experiments. *J. Am. Chem. Soc.* **2004**, *126*, 7119–7125. [CrossRef] [PubMed]

421. Iwahara, J.; Zandarashvili, L.; Kemme, C.A.; Esadze, A. NMR-based investigations into target DNA search processes of proteins. *Methods* **2018**, *148*, 57–66. [CrossRef]

422. Lu, K.; Miyazaki, Y.; Summers, M.F. Isotope labeling strategies for NMR studies of RNA. *J. Biomol. NMR* **2009**, *46*, 113. [CrossRef]

423. Yamaoki, Y.; Kiyoishi, A.; Miyake, M.; Kano, F.; Murata, M.; Nagata, T.; Katahira, M. The first successful observation of in-cell NMR signals of DNA and RNA in living human cells. *Phys. Chem. Chem. Phys.* **2018**, *20*, 2982–2985. [CrossRef]

424. Salgado, G.; Cazenave, C.; Kerkour, A.; Mergny, J.-L. G-quadruplex DNA and ligand interaction in living cells using NMR spectroscopy. *Chem. Sci.* **2015**, *6*, 3314–3320. [CrossRef]

425. Dose, A.; Liokatis, S.; Theillet, F.-X.; Selenko, P.; Schwarzer, D. NMR Profiling of Histone Deacetylase and Acetyl-transferase Activities in Real Time. *ACS Chem. Biol.* **2011**, *6*, 419–424. [CrossRef]

426. Thongwichian, R.; Kosten, J.; Benary, U.; Rose, H.M.; Stuiver, M.; Theillet, F.-X.; Dose, A.; Koch, B.; Yokoyama, H.; Schwarzer, D.; et al. A Multiplexed NMR-Reporter Approach to Measure Cellular Kinase and Phosphatase Activities in Real-Time. *J. Am. Chem. Soc.* **2015**, *137*, 6468–6471. [CrossRef]

427. Doura, T.; Hata, R.; Nonaka, H.; Sugihara, F.; Yoshioka, Y.; Sando, S. An adhesive 19F MRI chemical probe allows signal off-to-on-type molecular sensing in a biological environment. *Chem. Commun.* **2013**, *49*, 11421–11423. [CrossRef]

428. Dokland, T. Scaffolding proteins and their role in viral assembly. *Cell. Mol. Life Sci. CMLS* **1999**, *56*, 580–603. [CrossRef] [PubMed]

429. Fane, B.A.; Prevelige, P.E. Mechanism of Scaffolding-Assisted Viral Assembly. In *Advances in Protein Chemistry*; Virus Structure; Academic Press: San Diego, CA, USA, 2003; Volume 64, pp. 259–299.

430. Sun, Y.; Parker, M.H.; Weigele, P.; Casjens, S.; Prevelige Jr, P.E.; Krishna, N.R. Structure of the coat protein-binding domain of the scaffolding protein from a double-stranded DNA virus11Edited by M. Summers. *J. Mol. Biol.* **2000**, *297*, 1195–1202. [CrossRef] [PubMed]

431. Xu, J.; Wang, D.; Gui, M.; Xiang, Y. Structural assembly of the tailed bacteriophage φ29. *Nat. Commun.* **2019**, *10*, 1–16. [CrossRef]

432. Whitehead, R.D.; Teschke, C.M.; Alexandrescu, A.T. NMR Mapping of Disordered Segments from a Viral Scaffolding Protein Enclosed in a 23 MDa Procapsid. *Biophys. J.* **2019**, *117*, 1387–1392. [CrossRef]

433. Croke, R.L.; Sallum, C.O.; Watson, E.; Watt, E.D.; Alexandrescu, A.T. Hydrogen exchange of monomeric α-synuclein shows unfolded structure persists at physiological temperature and is independent of molecular crowding in Escherichia coli. *Protein Sci.* **2008**, *17*, 1434–1445. [CrossRef] [PubMed]

434. Serber, Z.; Selenko, P.; Hänsel, R.; Reckel, S.; Löhr, F.; Ferrell, J.E.; Wagner, G.; Dötsch, V. Investigating macromolecules inside cultured and injected cells by in-cell NMR spectroscopy. *Nat. Protoc.* **2006**, *1*, 2701–2709. [CrossRef]

435. Theillet, F.-X.; Binolfi, A.; Frembgen-Kesner, T.; Hingorani, K.; Sarkar, M.; Kyne, C.; Li, C.; Crowley, P.B.; Gierasch, L.; Pielak, G.J.; et al. Physicochemical Properties of Cells and Their Effects on Intrinsically Disordered Proteins (IDPs). *Chem. Rev.* **2014**, *114*, 6661–6714. [CrossRef] [PubMed]

436. Marshall, D.D.; Powers, R. Beyond the paradigm: Combining mass spectrometry and nuclear magnetic resonance for metabolomics. *Prog. Nucl. Magn. Reson. Spectrosc.* **2017**, *100*, 1–16. [CrossRef]

437. Emwas, A.-H.M.; Al-Talla, Z.A.; Kharbatia, N.M. Sample Collection and Preparation of Biofluids and Extracts for Gas Chromatography–Mass Spectrometry. In *Metabonomics: Methods and Protocols*; Methods in Molecular Biology; Bjerrum, J.T., Ed.; Humana Press: New York, NY, USA, 2015; Volume 1277, pp. 75–90. ISBN 978-1-4939-2377-9.

438. Emwas, A.-H.M.; Al-Talla, Z.A.; Yang, Y.; Kharbatia, N.M. Gas Chromatography–Mass Spectrometry of Biofluids and Extracts. In *Metabonomics: Methods and Protocols*; Methods in Molecular Biology; Bjerrum, J.T., Ed.; Humana Press: New York, NY, USA, 2015; Volume 1277, pp. 91–112. ISBN 978-1-4939-2377-9.

439. Gebregiworgis, T.; Powers, R. Application of NMR Metabolomics to Search for Human Disease Biomarkers. *Comb. Chem. High Throughput Screen.* **2012**, *15*, 595–610. [CrossRef]

440. Tiziani, S.; Emwas, A.-H.; Lodi, A.; Ludwig, C.; Bunce, C.M.; Viant, M.R.; Günther, U.L. Optimized metabolite extraction from blood serum for 1H nuclear magnetic resonance spectroscopy. *Anal. Biochem.* **2008**, *377*, 16–23. [CrossRef]

441. Krishnan, V.V. Molecular Thermodynamics Using Nuclear Magnetic Resonance (NMR) Spectroscopy. *Inventions* **2019**, *4*, 13. [CrossRef] [PubMed]

442. Matzkanin, G.A. A Review of Nondestructive Characterization of Composites Using NMR. In Proceedings of the Nondestructive Characterization of Materials, Berlin, Germany, 24–28 July 2002; Höller, P., Hauk, V., Dobmann, G., Ruud, C.O., Green, R.E., Eds.; Springer: Berlin, Germany, 1989; pp. 655–669.

443. Rockwood, A.L.; Kushnir, M.M.; Clarke, N.J. Chapter 2-Mass Spectrometry. In *Principles and Applications of Clinical Mass Spectrometry*; Rifai, N., Horvath, A.R., Wittwer, C.T., Eds.; Elsevier: Amsterdam, The Netherlands, 2018; pp. 33–65. ISBN 978-0-12-816063-3.

444. Raji, M.; Amad, M.; Emwas, A.-H. Dehydrodimerization of pterostilbene during electrospray ionization mass spectrometry. *Rapid Commun. Mass Spectrom. RCM* **2013**, *27*, 1260–1266. [CrossRef] [PubMed]

445. Keun, H.C.; Beckonert, O.; Griffin, J.L.; Richter, C.; Moskau, D.; Lindon, J.C.; Nicholson, J.K. Cryogenic Probe 13C NMR Spectroscopy of Urine for Metabonomic Studies. *Anal. Chem.* **2002**, *74*, 4588–4593. [CrossRef] [PubMed]

446. Schanda, P.; Kupče, Ē.; Brutscher, B. SOFAST-HMQC Experiments for Recording Two-dimensional Deteronuclear Correlation Spectra of Proteins within a Few Seconds. *J. Biomol. NMR* **2005**, *33*, 199–211. [CrossRef]

447. Ghosh, S.; Sengupta, A.; Chandra, K. SOFAST-HMQC—An efficient tool for metabolomics. *Anal. Bioanal. Chem.* **2017**, *409*, 6731–6738. [CrossRef]

448. Giraudeau, P.; Frydman, L. Ultrafast 2D NMR: An Emerging Tool in Analytical Spectroscopy. *Annu. Rev. Anal. Chem.* **2014**, *7*, 129–161. [CrossRef]

449. Guennec, A.L.; Giraudeau, P.; Caldarelli, S. Evaluation of Fast 2D NMR for Metabolomics. *Anal. Chem.* **2014**, *86*, 5946–5954. [CrossRef]

450. Júnior, L.H.K.Q.; Queiroz, D.P.K.; Dhooghe, L.; Ferreira, A.G.; Giraudeau, P. Real-time separation of natural products by ultrafast 2D NMR coupled to on-line HPLC. *Analyst* **2012**, *137*, 2357–2361. [CrossRef]

451. Shrot, Y.; Frydman, L. Compressed sensing and the reconstruction of ultrafast 2D NMR data: Principles and biomolecular applications. *J. Magn. Reson.* **2011**, *209*, 352–358. [CrossRef]

452. Ludwig, C.; Marin-Montesinos, I.; Saunders, M.G.; Emwas, A.-H.; Pikramenou, Z.; Hammond, S.P.; Günther, U.L. Application of ex situ dynamic nuclear polarization in studying small molecules. *Phys. Chem. Chem. Phys.* **2010**, *12*, 5868–5871. [CrossRef]

453. Lilly Thankamony, A.S.; Wittmann, J.J.; Kaushik, M.; Corzilius, B. Dynamic nuclear polarization for sensitivity enhancement in modern solid-state NMR. *Prog. Nucl. Magn. Reson. Spectrosc.* **2017**, *102–103*, 120–195. [CrossRef] [PubMed]

454. Emwas, A.-H.; Saunders, M.; Ludwig, C.; Günther, U.L. Determinants for Optimal Enhancement in Ex Situ DNP Experiments. *Appl. Magn. Reson.* **2008**, *3–4*, 483–494. [CrossRef]

455. Kovtunov, K.V.; Pokochueva, E.V.; Salnikov, O.G.; Cousin, S.F.; Kurzbach, D.; Vuichoud, B.; Jannin, S.; Chekmenev, E.Y.; Goodson, B.M.; Barskiy, D.A.; et al. Hyperpolarized NMR Spectroscopy: D-DNP, PHIP, and SABRE Techniques. *Chem. Asian J.* **2018**, *13*, 1857–1871. [CrossRef] [PubMed]